AD0620887

POLYMER STRUCTURES AND PROPERTIES

E. F. Casassa, T. A. Orofino, J. W. Mickey,

T. G. Fox, G. C. Berry, D. J. Plazek, R. E. Kerwin,

H. Nakayasu, V. R. Allen, C. A. J. Hoeve, M. O'Brien

MELLON INSTITUTE

20040224169

AERONAUTICAL SYSTEMS DIVISION

DISCLAIMER NOTICE

THIS DOCUMENT IS BEST
QUALITY AVAILABLE. THE COPY
FURNISHED TO DTIC CONTAINED
A SIGNIFICANT NUMBER OF
PAGES WHICH DO NOT
REPRODUCE LEGIBLY.

POLYMER STRUCTURES AND PROPERTIES

E. F. Casassa, T. A. Orofino, J. W. Mickey,
T. G Fox, G. C. Berry, D. J. Plazek, R. E. Kerwin,
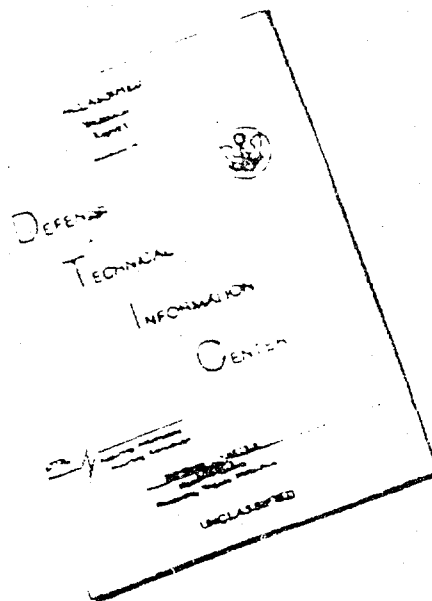H. Nakayasu, V. R. Allen, C. A. J. Hoeve, M. O'Brien

Mellon Institute

AERONAUTICAL SYSTEMS DIVISION
UNITED STATES AIR FORCE
WRIGHT-PATTERSON AIR FORCE BASE, OHIO

FOREWORD

This report was prepared by Mellon Institute under USAF Contract
No. AF 33(616)-6968. This contract was initiated under Project No. 0(7-7340),
"Polymer Structures and Properties," Task No. 73404. The work was adminis-
tered under the direction of the Directorate of Materials and Processes,
Deputy for Technology, Aeronautical Systems Division.

This report covers work conducted from February 1, 1960 to
April 30, 1961.

ABSTRACT

Investigations relating to dilute solutions of polymers have comprised: a theoretical treatment of Rayleigh scattering to include both intramolecular and intermolecular optical interference effects; the temperature dependence of the second virial coefficient for polystyrene in cyclohexane; the intrinsic viscosity-molecular weight relation for poly-(vinyl acetate) in butanone; and design and construction of a precision light scattering photometer.

The melt viscosity-molecular weight relation at 218° for monodisperse polystyrene prepared anionically was found to be identical with that for ordinary fractions.
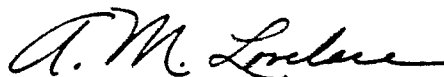
Poly-(vinyl acetate), prepared by an emulsion polymerization in the presence of a protein, yielded an insoluble component containing bound protein.

Preliminary stress-strain measurements on cross-linked swollen polyethylene gave only equivocal evidence for specific solvent effects on the unperturbed random-flight dimensions of the polymer chains.

PUBLICATION REVIEW

This report has been reviewed and is approved.

FOR THE COMMANDER:

A. M. LOVELACE
Chief, Polymer Branch
Nonmetallic Materials Laboratory
Directorate of Materials & Processes

TABLE OF CONTENTS

PART I DILUTE SOLUTION STUDIES

Page

TABLE OF CONTENTS - continued

PART III   ELASTICITY OF POLYMERIC NETWORKS

LIST OF FIGURES

LIST OF TABLES

PART I - DILUTE SOLUTION STUDIES

I. Theory of Rayleigh Scattering from Solutions of Polymers: Effect of Intermolecular Correlations — Edward F. Casassa

A. Introduction

The problem of the dependence of Rayleigh scattering from dilute polymer solutions upon solute concentration and scattering angle has been solved exactly only for special cases of limited applicability or more generally only for approximate molecular models. The difficulties encountered do not pertain to the electromagnetic calculation per se: that is, the customary formulation[1,2] involving the classical electromagnetic theory for scattering centers embedded in a medium of slightly different dielectric constant appears to be altogether adequate now that a long-standing controversy concerning the local electric field acting on a scatterer has been resolved.[3] However, the intramolecular and intermolecular optical interference effects which determine the form of the angular scattering envelope depend on the configurational statistics of the dissolved polymer molecule; and hence all the formidable difficulties encountered in the statistical theory of real polymer chains with excluded volume must appear also in the light scattering problem. In calculating the scattering from a system with the aid of statistical mechanics one evidently develops in effect an equation of state in virial form or, more precisely, a series expression which reduces to the purely thermodynamic virial expansion when the interference effects vanish.

The most complete treatment of scattering from polymer solutions was initiated by Zimm[4] who utilized the molecular distribution functions of McMillan and Mayer[5] to obtain a theory valid to the approximation that in accounting for intermolecular interactions only configurations with single contacts between pairs of solute molecules need be considered. In more recent work, Albrecht[6] has extended Zimm's method to include bimolecular clusters with two intermolecular contacts. Although some valuable generalizations can be inferred from the results carried to this approximation, further progress in the exact treatment is obstructed by difficulties which appear nearly insuperable, even for machine computations; and thus much interest attaches to approximate molecular models for which calculation is feasible. One such model was devised by Flory and Krigbaum,[7,8] who represented a polymer molecule by a Gaussian distribution of chain segments spherically symmetrical about the molecular center of mass, and thermodynamic interaction between two molecules as the interpenetration of two such "soft" spheres. Flory and Bueche[9] then used this model in studying the light scattering problem.

1

Our principal aim in the present contribution is the determination of the angle and concentration dependence of scattering for another smoothed-density molecular model[10-12] which appears a priori in some respects more satisfactory than that of Flory and Krigbaum. We shall find it useful first, however, to express the Rayleigh scattering in complete generality for a multicomponent solute and then to make approximations as required in order to obtain explicit results. The formalism employed here is, as far as possible, uniform with that in Paper I[11] and Paper II[12] of this sequence, in which the statistical thermodynamics of our model is discussed in greater detail.

B. Theory for Linear Macromolecules

We consider a solute molecule to be composed of a linear sequence of segments, all identical, of arbitrary size within limits imposed by two conditions: that each segment must be small enough to act as a point source of radiation (i.e., there must be no internal interference effect for scattering from an isolated segment) but must be chosen so that interaction between two segments of different molecules does not involve neighboring segments. The polymer chain may therefore be imagined approximately as a series of beads strung on wire segments connected by universal joints.

The system under study is confined to a macroscopic volume V containing N_1, N_2, $\cdots N_\alpha \cdots N_C$ molecules of each solute species 1, 2, $\cdots \alpha$, $\cdots$ C. Each molecule of type α contains n_α segments of type α; hence there are $N_\alpha n_\alpha = m_\alpha$ segments of type α in V. The instantaneous configuration of the system may be specified by a set of vectors $\underset{\sim}{r}_{\alpha i}$ indicating the position of segment i of kind α relative to some point of reference. We proceed in standard fashion[13] to determine the intensity of scattering at a distance R large compared to the $r_{\alpha i}$. We let $\underset{\sim}{s} = k_0 \underset{\sim}{k}$ and $k = k_0 = 2\pi/\lambda'$ where the vectors $\underset{\sim}{k}_0$, k lie in the direction of incident and scattered rays respectively and are both perpendicular to the electric vector of a polarized incident beam, and λ' is the wavelength of light in the medium. The electric vector at R due to scattering from a particular segment is

$$(A_\alpha/R)\exp(i\delta_0 + i\underset{\sim}{s}\cdot\underset{\sim}{r}_{\alpha i})$$

where δ_0 is the phase of the incident wave at the reference point. The amplitude A_α depends on the field of the incident radiation and the excess polarizability of segments of species α in the solvent. For simplicity, any contribution to scattering from the solvent is ignored. Except as subscript and index, the symbol i as usual signifies $(-1)^{1/2}$. The total electric vector $\mathcal{E}_s$ at R is obviously the sum of all the electric vectors due to all scattering elements of all species. The energy density of scattering $I(\theta)$ with respect to the incident beam is given by

$$I(\theta) = \frac{1}{4\pi}|\mathcal{E}_s|^2 = \frac{1}{4\pi R^2}\sum_\alpha^C \sum_\beta^C A_\alpha A_\beta \sum_i^{m_\alpha} \sum_j^{m_\beta} \exp[i\underset{\sim}{s}\cdot(\underset{\sim}{r}_{\alpha i} - \underset{\sim}{r}_{\beta j})] \quad (1)$$

2

where the summations with respect to i and j run over all molecules of each of the C components.

By assuming throughout that the number of segments per chain is large so that $1/n \ll 1$, we can achieve some simplification. Thus we can replace sums in Eq. (1) by integrals, writing

$$I(\theta) = \frac{1}{4\pi R^2 V^2} \sum_{\alpha}^{C} \sum_{\beta}^{C} \int \int A_\alpha A_\beta W(\underset{\sim}{r}_\alpha, \underset{\sim}{r}_\beta) \exp[i\underset{\sim}{s} \cdot (\underset{\sim}{r}_\alpha - \underset{\sim}{r}_\beta)] d\underset{\sim}{r}_\alpha d\underset{\sim}{r}_\beta$$

in which $W(\underset{\sim}{r}_\alpha, \underset{\sim}{r}_\beta)$ is a distribution function for segment coordinates. As the integral depends only on relative coordinates of segment pairs, i.e. on $\underset{\sim}{r}_{\alpha i} - \underset{\sim}{r}_{\beta j}$, we may perform one integration immediately obtaining merely a factor V:

$$I(\theta) = \frac{1}{4\pi R^2 V} \sum_{\alpha}^{C} \sum_{\beta}^{C} \int A_\alpha A_\beta W(\underset{\sim}{r}_{\alpha\beta}) \exp(i\underset{\sim}{s} \cdot \underset{\sim}{r}_{\alpha\beta}) d\underset{\sim}{r}_{\alpha\beta} \qquad (2)$$

Here $W(\underset{\sim}{r}_{\alpha\beta})$ is normalized so that $W(\underset{\sim}{r}_{\alpha\beta}) d\underset{\sim}{r}_{\alpha\beta}/V$ is the number of terms in the double sum over segments, Eq. (1), for which $\underset{\sim}{r}_{\alpha i} - \underset{\sim}{r}_{\beta j}$ lies within the differential increment $d\underset{\sim}{r}$. Equation (2) may be regarded as the basic expression for the scattered intensity due to a multicomponent solute. For a single solute it is equivalent to Zimm's[4] Eq. (1).

When $\alpha = \beta$, the intersegmental distances in Eq. (2) are of two kinds, those between segments within a single molecule and those between segments of different molecules. It is useful, therefore, to split the distribution function W into two parts,[4]

$$W(\underset{\sim}{r}_{\alpha\alpha}) = W_{11}(\underset{\sim}{r}_{\alpha\alpha}) + W_{12}(\underset{\sim}{r}_{\alpha\alpha}),$$

W_{11} referring to the intramolecular pairs, W_{12} to the intermolecular ones. Then Eq. (2) becomes

$$I(\theta) = \frac{1}{4\pi R^2 V} \left\{ \sum_{\alpha}^{C} A_\alpha^2 \Phi_1 + \sum_{\alpha}^{C} \sum_{\beta}^{C} A_\alpha A_\beta \Phi_2 \right\} \qquad (3)$$

3

$$\Phi_1 = \int W_{11}(\underset{\sim}{r}_{\alpha\alpha})\exp(i\underset{\sim}{s}\cdot\underset{\sim}{r}_{\alpha\alpha})d\underset{\sim}{r}_{\alpha\alpha}$$

$$\Phi_2 = \int W_{12}(\underset{\sim}{r}_{\alpha\beta})\exp(i\underset{\sim}{s}\cdot\underset{\sim}{r}_{\alpha\beta})d\underset{\sim}{r}_{\alpha\beta}$$

Following Zimm[4,14] we now introduce the molecular distribution functions[5] for the solute $F_1(1)$, $F_1(2)$, and

$$g_2(1,2) = F_2(1,2) - F_1(1)F_1(2)$$

defined by the probabilities $F_1(1)d(1)d(1)/V$ that an isolated molecule 1 has its 3n spatial coordinates in a certain range $d(1)$ and $F_2(1,2)d(1)d(2)/V^2$ that the coordinates of two molecules fall within the increment $d(1)d(2)$. The functions W_{11}, W_{12} are easily related to F_1, F_2. The probability density for the separation $\underset{\sim}{r}_{i_1 j_1}$ between two segments i_1 and j_1 of molecule 1 is

$$P(\underset{\sim}{r}_{i_1 j_1}) = \frac{1}{V}\left[\int F_1(1)d(1 - \underset{\sim}{r}_{i_1 j_1})\right]$$

$d(1 - \underset{\sim}{r}_{i_1 j_1})$ indicating integration over all coordinates except the relative coordinates of i_1 and j_1. Since all molecules of a given species are equivalent, we may write for each species

$$W_{11}(\underset{\sim}{r}_{\alpha\alpha}) = N_\alpha \sum_{a_1,j_1} P(\underset{\sim}{r}_{i_1 j_1}),$$

the double index indicating summation over all segment pairs i_1, j_1. For the first term on the right-hand side of Eq. (3) we require the integral

$$\Phi_1 = N_\beta \sum_{i_1,j_1}\int P(\underset{\sim}{r}_{i_1 j_1})\exp(i\underset{\sim}{s}\cdot\underset{\sim}{r}_{i_1 j_1})d\underset{\sim}{r}_{i_1 j_1} = N_\alpha n_\alpha^2 P_\alpha(\theta), \qquad (4)$$

the last equality defining $P(\theta)$, the angular distribution function for scattered intensity when intermolecular segment interactions vanish, i.e. at infinite dilution.

4

The function $F_2(1,2)$ has now to be introduced into the integral Φ_2 of Eq. (3). From the definitions above it is evident that

$$P(r_{q_1 q_2}) = \frac{1}{V^2} \int F_2(1,2) d(1) d(2 - r_{q_1 q_2})$$

and

$$W_{12}(r_{\alpha\beta}) = N_\alpha N_\beta \sum_{q_1, q_2} P(r_{q_1 q_2}),$$

q_1, q_2 designating segments of molecules 1 and 2 of types α and β. To proceed, we factor $F_2(1,2)$ in the way prescribed by Zimm[4]

$$F_2(1,2) = F_1(1) F_1(2) \prod_{i_1, i_2} [1 - \chi(i_1, i_2)]$$

and expand the product. Since the short-range interaction functions χ are zero except when the segments in question are in contact, they may properly be represented by three-dimensional Dirac delta functions.[15] Combining these expressions we have:

$$\Phi_2 = \frac{N_\alpha N_\beta}{V^2} \sum_{q_1, q_2} \left\{ \int F_1(1) F_1(2) \left[1 - \sum_{i_1, i_2} \chi(i_1, i_2) \right. \right.$$

$$+ \sum_{(i_1, i_2, j_1, j_2)} \sum \chi(i_1, i_2) \chi(j_1, j_2) + \cdots \right]$$

$$\times d(1) d(2 - r_{q_1 q_2}) \exp(is \cdot r_{q_1 q_2}) \left. \right\} dr_{q_1 q_2}. \qquad (5)$$

The first term of Φ_2

$$\frac{N_\alpha n_\alpha N_\beta n_\beta}{V} \int \exp(is \cdot r) dr$$

5

relates to the surface scattering from the volume V. It will be omitted in all that follows since it is negligible at experimentally accessible scattering angles.

Again invoking the short range nature of the χ functions we can set $r_{q_1 q_2} = r_{i_2 q_2} - r_{i_1 q_1}$ and factor the second term of Eq. (5) to obtain

$$\frac{N_\alpha N_\beta}{V} \sum_{i_1, i_2, q_1, q_2} \int \chi(i_1, i_2) dr_{i_1 i_2} \int P(r_{i_1 q_1}) \exp(is \cdot r_{i_1 q_1}) dr_{i_1 q_1}$$

$$\times \int P(r_{i_2 q_2}) \exp(is \cdot r_{i_2 q_2}) dr_{i_2 q_2} = \frac{N_\alpha N_\beta}{V} n_\alpha^2 n_\beta^2 X_{\alpha\beta} P_\alpha(\theta) P_\beta(\theta) \qquad (6)$$

The integral of $\chi(i_1, i_2)$, denoted by $X_{\alpha\beta}$ (β in Papers I and II), is taken to be the same for all segment pairs of each type $\alpha - \beta$.

C. The Single Contact Approximation

So far, the treatment has been rigorous with respect to the properties of the string-of-beads molecular model and represents simply a generalization of Zimm's theory to more than one solute component. In fact, since the probability densities remain unspecified no characteristic of the model except the short range nature of interactions has yet been used. Albrecht's[6] work comprises the evaluation of the third term in Eq. (5) for a single solute component. It is only in this term that probabilities of intermolecular contacts dependent on chain statistics first appear. By combining Eqs. (4) and (6) in Eq. (3), we obtain the scattering from the system:

$$4\pi R^2 V I(\theta) = \sum_\alpha^C A_\alpha^2 N_\alpha n_\alpha^2 P_\alpha(\theta) - \frac{1}{V} \sum_\alpha^C \sum_\beta^C A_\alpha A_\beta N_\alpha n_\alpha N_\beta n_\beta X_{\alpha\beta} P_\alpha(\theta) P_\beta(\theta) + \cdots . \qquad (7)$$

Expressing concentrations c in the customary units of mass/volume, and writing the amplitudes A_α, A_β in terms of the refractive increments $\xi_\alpha = \partial_\eta / \partial c_\alpha$ etc., with η the refractive index of the solution, we obtain an expression of the more familiar form

$$\frac{K}{R(\theta)} = \frac{1}{\sum_\alpha M_\alpha P_\alpha(\theta) \xi_\alpha^2 c_\alpha} + 2A_2(\theta)$$

6

where M_α is the molecular weight of component α and $R(\theta)$ is the reduced intensity $I(\theta)R^2/I_0$, I_0 being the energy density of the incident beam.

If we now assume that no intermolecular contacts involving more than one pair of segments need be considered, we can terminate the series (7) after two terms. Then in this "single contact" approximation (indicated by a superscribed prime) we write

$$A_2(\theta) = A_2'(\theta) \cong \frac{\sum_\alpha \sum_\beta B_{\alpha\beta}' M_\alpha P_\alpha(\theta) \xi_\alpha w_\alpha M_\beta P_\beta(\theta) \xi_\beta w_\beta}{\left(\sum_\alpha M_\alpha P_\alpha(\theta) \xi_\alpha w_\alpha \right)^2}, \qquad (8)$$

where

$$B_{\alpha\beta}' = \frac{N_0 n_\alpha n_\beta X_{\alpha\beta}}{2 M_\alpha M_\beta},$$

w_α, w_β are weight fractions of components in the solute, and N_0 is Avogadro's number. Furthermore since

$$B_{\alpha\beta}' \approx B_{\alpha\beta} \equiv -\frac{N_0}{2 V M_\alpha M_\beta} \int g_2(1,2) d(1) d(2),$$

$A_2'(\theta)$ for a single solute component reduces simply to $B_{\alpha\alpha}'$ for any angle θ. Similarly, whenever all the $P(\theta)$ are unity for a multicomponent solute (if $\theta = 0$ or if the scattering molecules are much smaller than the wavelength of light) the form of Eq. (8) is of general validity independent of a particular molecular model; i.e. from both the molecular theory and the statistical fluctuation theory[16-18] one finds the second virial coefficient $A_2 \equiv A_2(0)$ to be given by

$$A_2 = \sum_\alpha \sum_\beta B_{\alpha\beta} M_\alpha w_\alpha M_\beta w_\beta / \left(\sum_\alpha M_\alpha w_\alpha \right)^2.$$

Blum and Morales[19] proposed Eq. (8) as a generalization of Zimm's expression although they gave no derivation. Still earlier Stockmayer and Stanley[20] had suggested the same form.

It is interesting to observe that while the single contact approximation cannot be adequate for coiling chain molecules to which Zimm applied it, it should be exact for systems of stiff rod-shaped

particles.[14] Hence for a distribution of rod species or a mixture of rods and small molecules (with $P(\theta)$ unity) Eq. (8) gives $A_2(\theta)$ without approximation. In certain rather simple cases, therefore, it should be possible to determine the interaction coefficients $B_{\alpha\beta}$ from the dependence of $A_2(\theta)$ on θ, in measurements on a single composition of a mixed solute. This has been accomplished in at least the one instance[21] of solutions of mixtures of the plasma protein fibrinogen and a rod-like polymeric form.

D. An Approximate Theory for Multiple Contacts

In devising a theory in which all orders of intermolecular contacts are included we are obliged to resort to some approximation which renders tractable the higher members of the series of integrals in Eq. (5). We therefore adopt the simplification, elaborated in Papers I and II that probabilities of intermolecular contacts may be expressed as products of probabilities for single contacts. Explicitly, we assume that

$$P(O_{j_1 j_2}, O_{k_1 k_2}, \cdots O_{m_1 m_2})_{i_1 i_2} = P(O_{j_1 j_2})_{i_1 i_2} P(O_{k_1 k_2})_{i_1 i_2} \cdots P(O_{m_1 m_2})_{i_1 i_2},$$

$P(O_{j_1 j_2})_{i_1 i_2}$, for example, denoting the conditional probability of a contact between segments j_1, j_2 given the "initial" intermolecular contact between segments i_1 and i_2. With the consistent additional assumption that the separation $r_{q_1 q_2}$ depends only on the initial contact, Eq. (5) is replaced by

$$\Phi_2 = -\frac{N_\alpha N_\beta}{V} X_{\alpha\beta} \sum_{i_1, i_2, q_1, q_2} \sum \left[1 - X_{\alpha\beta} \sum_{j_1, j_2} P(O_{j_1 j_2})_{i_1 i_2} \right.$$
$$\left. + X_{\alpha\beta}^2 \sum_{j_1, j_2, k_1, k_2} \sum P(O_{j_1 j_2})_{i_1 i_2} P(O_{k_1 k_2})_{i_1 i_2} + \cdots \right]$$
$$\times \int P(r_{i_1 q_1}) \exp(i s \cdot r_{i_1 q_1}) dr_{i_1 q_2} \int P(r_{i_2 q_2}) \exp(i s \cdot r_{i_2 q_2}) dr_{i_2 q_2}$$

8

As we pointed out earlier the series in square brackets can be summed to give

$$\Phi_2 = -\frac{N_\alpha N_\beta}{V} X_{\alpha\beta} \sum_{i_1,i_2} \frac{1 - \exp\left[X_{\alpha\beta} \sum_{j_1,j_2} P(0_{j_1 j_2})_{i_1 i_2}\right]}{X_{\alpha\beta} \sum_{j_1,j_2} P(0_{j_1 j_2})_{i_1 i_2}}$$

$$\times \sum_{q_1,q_2} \int P(\underset{\sim}{r}_{i_1 q_1}) \exp(i\underset{\sim}{s} \cdot \underset{\sim}{r}_{i_1 q_1}) d\underset{\sim}{r}_{i_1 q_1} \int P(\underset{\sim}{r}_{i_2 q_2}) \exp(i\underset{\sim}{s} \cdot \underset{\sim}{r}_{i_2 q_2}) d\underset{\sim}{r}_{i_2 q_2} \quad (9)$$

At this point it is necessary to introduce a specific form for the probabilities in Eq. (9). We take them to be given by random-flight statistics although it is not strictly correct to do so when chains exhibit an intramolecular excluded volume effect. (If this is the case, $X_{\alpha\alpha}$ does not vanish and the distribution function F_1 does not correspond to a random flight.[12]) Assuming therefore that

$$P(\underset{\sim}{r}_{i_1 q_1}) = [(2\pi b_\alpha^2/3)|q_1 - i_1|]^{-3/2} \exp(-3r_{i_1 q_1}^2/|q_1 - i_1|2b^2) \quad (10)$$

we obtain

$$\int P(\underset{\sim}{r}_{i_1 q_1}) \exp(i\underset{\sim}{s} \cdot \underset{\sim}{r}_{i_1 q_1}) d\underset{\sim}{r}_{i_1 q_1} = 2\pi \int_0^\infty \int_0^\pi P(\underset{\sim}{r}_{i_1 q_1}) r^2 \cos(sr \cos\theta) \sin\theta \, d\theta dr$$

$$= \exp(-|q_1 - i_1|s^2 b_\alpha^2/6)$$

where b^2 is the mean square segment length or mean square separation between beads of the chain (assumed now to obey a Gaussian distribution). We substitute this result into Eq. (10), introduce the random-flight values[11] of the contact probabilities $P(0_{j_1 j_2})_{i_1 i_2}$, etc., and replace sums by integrals. The integrations over q_1 and q_2 are readily performed leaving finally an intractable double integration over i_1 and i_2.

Since it would be a cumbrous affair to obtain numerical results for a multicomponent system from the approximate Φ_2 derived by this procedure, we shall consider further only the simplest, but difficult

9

enough, case of a homogeneous solute, for which $\alpha = \beta$. Thus, suppressing the greek subscripts and using the reduced variables $x = i_1/n$, $y = i_2/n$, we obtain from Eq. (9)

$$\Phi_2^* = - N^2 n^4 X \int_0^1 \int_0^1 \phi(\psi, w) f(u,x) f(u,y) dx dy \tag{11}$$

in which

$$\phi(\psi, w) = \frac{1 - \exp(-\psi w)}{\psi w} ,$$

$$w = 2x^{1/2} + 2y^{1/2} + 2(1-x)^{1/2} + 2(1-y)^{1/2} - (x+y)^{1/2}$$
$$- (1-x+y)^{1/2} - (1+x-y)^{1/2} - (2-x-y)^{1/2}, \tag{12}$$

$$f(u,x) = u^{-1}(2 - e^{-ux} - e^{-u(1-x)}),$$

$$f(u,y) = u^{-1}(2 - e^{-uy} - e^{-u(1-y)}),$$

$$\psi = 4Xn^{1/2}(3/2\pi b^2)^{3/2},$$

$$u = \frac{1}{6} nb^2 s^2 = \langle r^2 \rangle \left(\frac{4\pi}{\lambda} \sin \frac{\theta}{2}\right)^2,$$

$\langle r^2 \rangle = \frac{1}{6} nb^2$ being the mean square molecular radius <u>for the random flight chain</u>. We shall use the star to designate quantities consistent with the assumptions leading to Eq. (11).

Recalling that $A_2(\theta)$ approaches the second virial coefficient $A_2 \equiv A_2(0)$ as θ approaches 0, we may define a new angular scattering function

$$P_2(\theta) = A_2(\theta)/A_2(0)$$
$$= \frac{\sum \int g(1,2) \exp(i\underset{\sim}{s} \cdot \underset{\sim}{r}_{q_1 q_2}) d(1) d(2)}{n^2 \int g(1,2) d(1) d(2)}$$

10

for a cluster of two molecules, analogous to $P(\theta)$ for a single molecule.
Then the general expression for scattering from a homogeneous solute may
be written

$$R(\theta) = Kc[MP(\theta) - 2A_2M^2P_2(\theta)c + \cdots]$$

or

$$\frac{Kc}{R(\theta)} = \frac{1}{MP(\theta)} + 2A_2Q(\theta)c + \cdots \qquad (13)$$

where

$$Q(\theta) = P_2(\theta)/P^2(\theta)$$

The function $Q(\theta)$ is thus unity, by definition, at zero angle, and
ordinarily decreases with increasing angle. Apart from its direct
occurrence in the reciprocal scattering expression, $Q(\theta)$ is convenient
for tabulation since, as a measure of deviations from the single contact
approximation, it may be expected to vary less rapidly with θ than does
$P_2(\theta)$. As we have already assumed random-flight statistics in developing
the approximate expression, Eq. (11), it is consistent to use the random-
flight model again in introducing $P(\theta)$, i.e. to let

$$P(\theta) = \frac{2}{u^2}[u + e^{-u} - 1] \qquad (14)$$

in

$$Q^*(\theta) = \frac{-\Phi_2^*}{n^4X}\left(P^2(\theta)\int_0^1\int_0^1\frac{1 - \exp(-\psi w)}{\psi w}\ dxdy\right)^{-1} \qquad (15)$$

An exact analytic evaluation of $Q^*(\theta)$ appears impossible; but
even without resorting to numerical integration, we can investigate the
behavior of the function in certain limiting cases and in approximation.
If thermodynamic interactions are weak (that is, if β, and thus ψ and

A_2, are small) we can profitably use the series form of $\phi(w,\psi)$

$$Q^*(u) = \frac{\int\int_0^1\int_0^1 f(x,u)f(y,u)(1 - \frac{1}{2}\psi w + \cdots)dxdy}{P^2(u)\int\int_0^1\int_0^1 (1 - \frac{1}{2}\psi w + \cdots)dxdy}$$

(16)

$$= 1 - \frac{1}{2}\psi \int\int_0^1\int_0^1 [P^{-2}(u)f(x,u)f(y,u) - 1]w\ dxdy + 0(\psi^2).$$

The integral

$$w_0 = \int\int_0^1\int_0^1 w\,dxdy = \frac{16}{15}(7 - 4\sqrt{2}) = 1.43269,$$

has already appeared in an important role in Paper I. The integration of

$$w_u = P^{-2}(u)\int\int_0^1\int_0^1 f(x,u)f(y,u)w\ dxdy,$$

(17)

though a tedious proposition, poses no fundamental difficulty. The result may be expressed in the form:

$$\frac{u^4 w_u P^2(u)}{4} = 2P(u)\left[\frac{4}{3}u^3 - u^2(1 - e^{-u}) - \frac{\sqrt{\pi}}{2}u^{3/2}\text{erf}(u^{1/2}) + u^{3/2}e^{-u}\mathcal{E}(u^{1/2})\right]$$

$$+ 6 - \frac{11}{2}\sqrt{2} + \frac{16}{3}\sqrt{2}\,u - \frac{32}{15}u^2(2\sqrt{2} - 1)$$

$$+ e^{-u}\left[14 - 2\sqrt{2} - \frac{16}{3}\sqrt{2}\,u\right] - e^{-2u}\left(\frac{3}{2}\sqrt{2} + 2\right)$$

$$+ \frac{\sqrt{\pi}}{2}u^{-1/2}\text{erf}(u^{1/2})[-7 + 2u + e^{-u} - 3e^u]$$

$$+ \frac{\sqrt{\pi}}{2}u^{-1/2}\text{erf}[(2u)^{1/2}]\left[\frac{3}{2} - 2u + 3e^u\right]$$

$$+ u^{-1/2}e^{-2u}\mathcal{E}[u^{1/2}][-7 - 3e^u - 2u + e^{-u}]$$

$$+ u^{-1/2}e^{-2u}\mathcal{E}[(2u)^{1/2}]\left[\frac{11}{2} + 2u - e^{-u}\right]$$

(18)

Tables[22,23] are available for both the error function

$$\operatorname{erf}(x) = \frac{2}{\sqrt{x}} \int_0^x e^{-t^2} dt$$

and the integral

$$\mathcal{E}(x) = \int_0^x e^{t^2} dt.$$

The limiting behavior of $Q^*(\theta)$ for the case in which interactions are weak and particle size is small as well, may be obtained by expansion of $P^{-2}(\theta)$, $f(x,u)$, and $f(y,u)$, in Eq. (16) in powers of u and integration of the first two terms with respect to x and y:

$$Q^*(u) = 1 - \frac{1}{2} \psi \int_0^1 \int_0^1 \left\{ \left[1 + \frac{2}{3} u \right] \right.$$

$$\times \left[1 - \frac{u}{2}(1 - 2x + 2x^2) + \cdots \right]\left[1 - \frac{u}{2}(1 - 2y + 2y^2) + \cdots \right] - 1 \right\} w \, dxdy + \cdots$$

$$= 1 + \frac{1}{2} \psi u \int \int \left(\frac{1}{3} - 2x + 2x^2 \right) w \, dxdy + \cdots$$

$$= 1 - 0.00880 \psi u + \cdots \tag{19}$$

In Paper I we derived an approximate form for the integral of $\phi(\psi,w)$, replacing the integral by its integrand with an appropriate choice of constant $w = w_0$. Fortunately we can proceed in similar fashion to approximate the more complicated integral Φ_2^* although the calculations are far more involved and the result is not as satisfyingly simple. First we expand $\phi(\psi,w)$ in a Taylor's series about a point w',

$$\phi(\psi,w) = \phi_0 + \left. \frac{\partial \phi}{\partial w} \right|_{w'} (w - w') + \cdots,$$

13

and then, after multiplying by $f(x)f(y)$, integrate the series term by term with respect to x and y to obtain

$$-\frac{\Phi_2^*}{N^2 n^4 X} = \phi_0(w')P^2(u) + \frac{\partial \phi}{\partial w}\bigg|_{w'} \int_0^1\int_0^1 (w - w')f(x)f(y)dxdy + \cdots$$

As in the earlier work we neglect the higher terms and cause the second to vanish by a proper choice of w'. That is, we let

$$\int_0^1\int_0^1 wf(x)f(y)dxdy = w'P^2(u);$$

hence w' is identical with w_u of Eq. (18). Then Φ_2^* is given by

$$-\Phi_2^*/N^2 n^4 X P^2(\theta) \approx \phi_0(w_u) = [1 - \exp(-\psi w_u)]/\psi w_u;$$

and finally using this, together with the same approximation for the particular case u = 1,

$$\iint \phi(\psi,w)dxdy \approx [1 - \exp(-\psi w_0)]/\psi w_0,$$

in Eq. (15) gives for an approximation to $Q^*(\theta)$

$$Q^{**}(\theta) = \frac{w_0[1 - \exp(-\psi w_u)]}{w_u[1 - \exp(-\psi w_0)]} \tag{20}$$

E. Discussion

The function w_u, which depends only on the value of u, is equal to w_0 at u = 0 and increases slowly as u increases. Therefore as either ψ or u increases positively (with neither zero), $Q^*(\theta)$, at least initially, decreases gradually from unity; that is, it decreases as thermodynamic interactions become stronger or as the scattering molecules become larger.

14

That this behavior is correct qualitatively, is shown by comparison with the (almost) exact treatment of Albrecht.[6] Quantitatively, though, our theory predicts only a very small effect; for $Q^{**}(\theta)$ can scarcely be more than a few per cent less than unity for physically realizable values of u and ψ. Albrecht's theoretical development gives the first two terms of a power series

$$Q(\theta) = 1 - 0.074u\psi + \cdots \tag{21}$$

which is to be compared with our Eq. (19) above. The wide discrepancy in the coefficients of the linear terms does not of course prove anything about the behavior of the closed form, Eq. (20), at large values of w_u, but it does suggest that this series may well be seriously inadequate.

The only other theory available for comparison is that of Flory and Bueche[9] based on the Flory-Krigbaum molecular model. Their series expansion of $Q(\theta)$ gives

$$Q(\theta) = 1 - 0.038u\psi + \cdots \tag{22}$$

and from numerical calculations for large values of u and ψ they find that $Q(\theta)$ may fall to about 0.5 for values of these parameters that are quite reasonable physically. It seems surprising at first sight that for small values of $u\psi$ the new theory shows much poorer agreement with Eq. (21) than does the Flory-Bueche expression, since in two respects the model we have used appears superior. Inasmuch as it preserves the correct random-flight value for the separation of segment pairs within a molecule, it automatically yields the correct random-flight $P(\theta)$. The averaging of the segment density distribution inherent in the Flory-Krigbaum model leads to a considerably different function.[24,25] In view of this, Flory and Bueche retained the $P(\theta)$ of Eq. (14) in their theory of $Q(\theta)$ and used their model only in accounting for the intermolecular interference effects. The second and more significant consideration is that our model gives correctly the simultaneous probability of two intermolecular distances (e.g. one segment-segment contact and one segment-segment separation) whereas the Flory-Bueche treatment is approximate in the specification of more than one such distance. Consequently, although the coefficient of the second term in the series for $Q(\theta)$ depends on probabilities for simultaneous occurrence of three distances, it does not seem obvious why Eq. (19) should be more inaccurate than Eq. (22).

II. Dimensions of Polymers--Specific Solvent Effects — T. A. Orofino, J. W. Mickey and T. G Fox

A. Introduction

A number of years ago, Flory[28] and co-workers advanced the theory that the intrinsic viscosity of a polymer solution $[\eta]$ may be expressed by the relationship

$$[\eta] = KM^{1/2}\alpha^3 \tag{23}$$

where M is the polymer molecular weight and α is a factor by which the linear dimensions of the polymer coil are expanded due to long-range polymer-solvent interactions. The constant K is a molecular weight independent quantity defined

$$K = \Phi(\overline{r_0^2}/M)^{3/2} \tag{24}$$

where $\overline{r_0^2}$ is the root mean square end-to-end distance (proportional to M) of the polymer chain in a solvent for which α is unity, and Φ is a universal constant.

For any given polymer-solvent pair there exists a thermodynamically significant temperature, θ, at which α is unity. This temperature may be determined experimentally, as, for example, from an observation of the temperature[29,30] at which the second virial coefficient A_2 in the expression for the reduced osmotic pressure π/c

$$\pi/c = (\pi/c) \cdot [1 + MA_2 c + \ldots] \tag{25}$$

where c is polymer concentration, vanishes. (At temperatures a few degrees below θ, the polymer solution separates into two phases.) Values of θ have been recorded for many systems.[31,32] In accordance with Eq. (23) the constant K may be evaluated from the ratio of $[\eta]$ and $M^{1/2}$ in a θ-solvent mixture, and, again, a number of values[31] for various polymers have been so determined.

16

On the basis of early measurements[28,33] it was believed that K would to a first approximation be independent of the solvent chosen for any given polymer, although in general dependent upon temperature. The effects of the two variables, i.e. solvent and θ-temperature, are not easily separated and for this reason the constancy of K with solvent type has not been unequivocally established to date for the systems studied. Moreover, there is experimental evidence[33,34] to support the notion that, indeed, variations of K with solvent type occur.

We may therefore conclude that the dimension of an isolated polymer coil, as reflected by such measurable quantities as the intrinsic viscosity and light scattering radius of gyration, in a θ-solvent solution where the net segment-solvent interaction is nil, may in general be presumed to depend upon two factors: (a) the temperature at which the particular polymer-solvent pair is a θ-mixture and (b) the chemical and physical nature of the solvent molecule. The latter, in relation to the structural characteristics of the polymer repeating unit, may impose certain conformational restrictions upon relatively short sections of the polymer chain. We are interested in studying this effect, whose elucidation necessarily involves control or elimination of factor (a) as a variable. On this account, we have endeavored to select a number of solvent pairs for a particular polymer, the members of each pair of which exhibit approximately the same θ-temperature with the polymer chosen, but which differ considerably in chemical type or structure. Thus, for any selected solvent pair, differences in the θ-solvent dimensions of the dissolved polymer, which it is our object to determine, may be meaningfully attributed to the specific short range polymer-solvent interaction, the more general, and obscuring, effect of temperature having been circumvented by selection of θ-temperatures in approximate juxtaposition.

In our current program we have selected polystyrene-solvent systems for study; the method of the dependence of the second virial coefficient on temperature has been chosen for the definition of θ-temperatures. In the next section, experimental results obtained to date are presented and discussed.

In Section C a draft of a manuscript entitled "The Molecular Weight Dependence of the Intrinsic Viscosity in Polymer Solutions. A Comparison of Theory and Experiment" is presented. Although somewhat more general in scope, the results of this investigation are pertinent to the present project.

B. Experimental. Virial Coefficient-Temperature Studies on Polystyrene-Solvent Systems

1. Selection of polymer molecular weight. In selecting a single polystyrene sample of suitable molecular weight for our investigations, the following considerations were taken into account: The polymer sample should be stable and relatively homogeneous, to minimize possible complications of molecular weight polydispersity on the physical properties

of interest, and should be available in sufficient quantity for all measurements. The molecular weight should be high enough to (a) permit accurate determinations of solution viscosities and (b) present no diffi-culties in diffusion through osmotic membranes. It should be sufficiently low so that (a) shear corrections to the intrinsic viscosities are inconsequential (b) the polymer solutions do not exhibit phase separation until five or more degrees below the θ-temperature and (c) dissymmetry corrections in light scattering measurements are small.

With the above criteria in mind, we decided upon an optimum molecular weight of $3.5\text{-}4.5 \times 10^5$. A thirty gram sample of anionically polymerized polystyrene meeting this specification was generously supplied to us by co-workers in our laboratories.

2. Phase studies and selection of solvents. In the selection of suitable solvents for our investigations, the objective was to obtain two or more solvent pairs, members of each pair of which exhibited approxi-mately the same θ-temperature with polystyrene, and which preferably differed considerably in structure. As there is no way to predict the solubility characteristics with any assurance of accuracy, a large number of solvents was investigated by the following method: A small amount of a readily available polystyrene sample was added to the solvent under consideration and the solubility, or lack of it, observed over a wide range of temperature. Our preliminary observations are recorded in Table I, where in the last column the approximate precipitation temperatures noted (which presumably are somewhat below the θ-points for the systems) are listed.

On the basis of the data summarized in Table I, four solvents were selected for more detailed investigation. For each of these, reversible precipitation temperatures of dilute solutions of a high molecular weight polystyrene sample were determined in a water bath controlled to $\pm0.01°C$. The precipitation temperatures observed may be presumed to correspond, within a few degrees, to the respective θ-points of the systems. Estimated values of the latter are listed in Table II together with other pertinent information. Listed also in Table II are values of $\delta - \delta_{ps}$, the Hildebrand solubility parameter differences between the solvents and polystyrene ($\delta_{ps} = 9.2$). These differences may be regarded as semi-quantitative measures of the degree to which members of a given θ-solvent pair are dissimilar in structure and polarity; it is desirable for our purposes that values for a given pair exhibit opposite algebraic signs, as is the case for the two pairs cited.

The estimated θ-temperatures, boiling points and refractive indices of the four solvents listed in Table II are such that it is feasible to employ them as suitable media for polystyrene in osmotic pressure, light scattering and viscometric measurements. Our work in the past and in the immediate future has been and will be confined to these solvents.

3. Osmotic pressure studies. As mentioned earlier, it is our aim to establish accurate values of the θ-temperatures for a number of

Table I

Preliminary Solubility Studies

Polystyrene-Solvent Systems

Solvent	Boiling Point (°C)	Approx. Precipitation Point (°C)
cyclohexane	81	33
nitroethane	115	68
methyl cyclohexane	101	68
n-hexadecane	288	190
cyclohexanol	160	86
2-ethyl hexanol	183	150
n-octanol	194	170
1-dodecanol	257	180
n-heptaldehyde	155	50
methylisobutyl ketone	118	-5
diisopropyl ketone	124	5
diisobutyl ketone	168	80
amyl acetate	141	8
diethyl malonate	199	27
acetoacetic ester	180	100
dimethyl malonate	180	150
decalin	190	10

Solvents for which ppt. point with polystyrene is below -20°C

nitrobenzene, decane, 1-nitropropane, bromobenzene, cyclohexyl bromide, 2-bromoctane; benzyl alcohol; ethyl ether; methyl n-propyl ketone, acetophenone, methyl n-amyl ketone, methyl n-hexyl ketone; tricresyl phosphate, ethyl octanoate, n-propyl-n-butyrate, sec. butyl acetate, di-n-butyl sebacate, ethyl isobutyl malonate, diethyl bromo malonate, diethyl phthalate, ethyl α,β-dibromopropionate, n-heptyl acetate, n-hexyl acetate, dimethyl phthalate; dimethyl formamide, benzonitrile, acrylnitrile, N,N,-diethyl formadide; di-n-butylaniline; tetralin.

Solvents in which polystyrene is insoluble below boiling point

n-hexane; isoamyl alcohol, n-amyl alcohol, sec-butanol, 2-heptanol, n-butyl carbinol; ethyl lactate, butyl cellosolve, ethyl formate, isopropyl acetate, acetonitrile.

Table II

Precipitation Data for Polystyrene-Solvent Pairs

Solvent	B.P.	ρ_{25}(g/cc)	n_{25}^D	$\delta - \delta_{ps}$	Approx. θ-temp.,°C
cyclohexane	81	0.779	1.4262	-1.0	34
diethylmalonate	199	1.055	1.4143	+0.3	32
methyl cyclohexane	101	0.769	1.4231	-1.4	71
nitroethane	115	1.047	1.3901	+1.94	71

polystyrene-solvent systems by interpolation of the temperature at which the second virial coefficient A_2 for the system is zero. The light scattering method is the most convenient procedure for evaluation of A_2 and will be extensively utilized in most of our work. It is desirable, however, to establish for one (or more) systems the value of θ by an independent means. We have completed a study of the osmotic second virial coefficient-temperature relationship for polystyrene in cyclohexane, the results of which are herein reported.

The osmometer used in our work was an all brass Fuoss-Mead block instrument with a membrane-capillary tube cross-section ratio of 4360. The membranes were wet regenerated cellulose, 300 gauge, obtained from American Viscose Corporation. Temperature control for the osmometer was maintained by means of a water bath, regulated by a sensitive thyratron relay, enclosed in an insulated cabinet fitted with an air thermostat, heating element and blower. With this apparatus, temperatures in the range 30-45°C, measured with Beckman thermometers, could be maintained within ±0.002 for extended periods and within less than ±0.001 for a few hours. Reading of the capillary tube levels was accomplished by means of a cathetometer scaled directly to 0.001 cm.

A typical membrane permeability plot for one of the membranes used in our study is shown in Fig. 1. The half-time computed from the slope is 56 minutes.

The procedure employed in the osmotic pressure measurements was as follows: A solution of polystyrene in redistilled cyclohexane was carefully prepared and allowed to stand overnight at a temperature (44°C) well above the precipitation point. Taking care to avoid cooling, the solution was used to rinse, and eventually to fill, the osmometer already at constant temperature (44°C) in the water bath. Preheated, long hypodermic needles and syringes were found useful in these operations. After elimination of any bubbles, the osmotic pressure of the solution at the filling temperature (the highest temperature employed

20
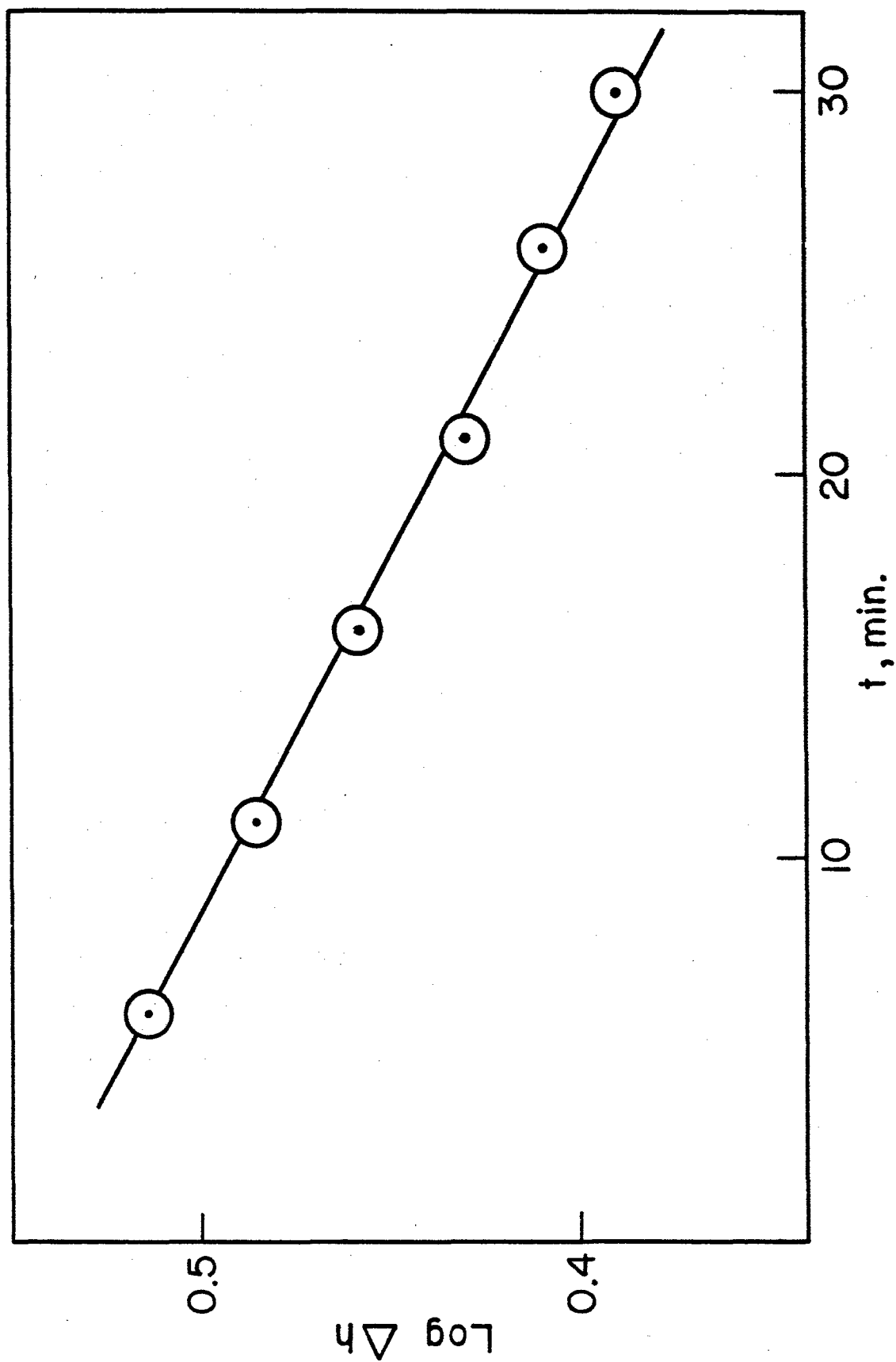
Figure 1 Membrane Permeability. Plot of Log Δh versus Time for Cyclohexane at 44°C, no. 300 Gel Cellophane.

in the series of measurements) was determined by allowing the levels to equilibrate from two directions - an initial setting of the difference in solution and solvent levels Δh greater than the equilibrium value Δh_{EQ} and a setting of Δh less than Δh_{EQ}. The stable values obtained in the two determinations usually differed by less than 1-2%; the mean value was taken as the equilibrium difference in height.

Upon completion of measurements at the highest temperature, 44°C, bath temperature was reduced to 40° and the osmotic pressure redetermined. Subsequently, measurement at 36, 32 and 30°C was carried out, at the end of which portions of the solution and solvent were withdrawn from the osmometer and analyzed by a dry weight determination of polymer. The osmometer was then rinsed and filled with the next solution and fresh solvent.

The series of equilibrium Δh values obtained for a given solution was converted to osmotic pressure units (g/cm^2) by multiplication of each by the density appropriate to the temperature of measurement and the polymer concentration. For this purpose, the following relationships, established experimentally, were used

$$\rho(t,c) = \rho(t,o) + (3.22)10^{-3}c$$

$$\rho(t,o) = 0.764 + (1.06)10^{-3}(34-t) \tag{26}$$

where $\rho(t,c)$ is the density of a polystyrene-cyclohexane solution of concentration c g/100 cc. at temperature t°C.

The osmotic pressure values π were divided by the appropriate solution concentrations to yield the ratio π/c, which values are listed in Table III. The concentrations appropriate to each measurement were arrived at as follows: from the dry weight concentration established at the end of a temperature series, together with data for the progressive decrease of the sum of the heights of the capillary levels throughout the run, it was possible to correct each concentration for the loss of solvent which had occurred from the beginning of a temperature series to the end of a measurement at a given temperature. These corrections were usually of the order of 1% or less. The concentration values, corrected for evaporation, were then expressed in units appropriate to the particular temperature of measurement.

The final osmotic data were plotted in accordance with the square root relationship

$$(\pi/c)^{1/2} = [RT/\overline{M}_n]^{1/2}[1 + (A_2\overline{M}_n/2)c] \tag{27}$$

Table III

Osmotic Pressure Data Polystyrene - Cyclohexane

C, g/100cc	t, °C	Δh observed, cm	π/C
0.499	44.03	0.491	0.743
0.504	40.26	0.423	0.638
0.509	36.01	0.440	0.660
0.514	31.93	0.424	0.634
0.516	29.92	0.411	0.613
1.007	44.03	1.018	0.765
1.015	40.26	0.956	0.717
1.026	36.01	0.902	0.672
1.034	31.93	0.810	0.602
1.039	29.92	0.744	0.552
1.513	44.03	1.801	0.904
1.528	40.26	1.611	0.804
1.543	36.01	1.390	0.691
1.599	31.93	1.188	0.588
1.570	29.92	1.032	0.508
2.035	44.03	2.596	0.970
2.055	40.26	2.272	0.850
2.079	36.01	1.866	0.689
2.114	31.93	1.503	0.549
2.126	29.92	1.230	0.448

where R is the gas constant, T is the absolute temperature and $\overline{M}_n$ is the number average molecular weight. According to Eq. (27), a plot of $(\pi/c)^{1/2}$ versus c should yield a straight line whose slope is $(R T \overline{M}_n)^{1/2} A_2/2$. Our data are shown in Fig. 2. Values of the second virial coefficient, deduced from the slopes of the lines in Fig. 2, are listed as a function of temperature in Table IV. The values listed for t were obtained by calibration of the Beckman thermometer, used to monitor bath temperature, against an accurate resistance thermometer.

In Fig. 3, values of A_2 are plotted versus temperature. The interpolated temperature, corresponding to a zero value of A_2, is 34.6°C. Thus, we find for the theta temperature of the system the value θ = 307.8°K, with a probably uncertainty of $\pm$ 0.2°, based upon accountable experimental error. The result agrees favorably with the value θ = 307.6°K deduced by Krigbaum and Flory[35] from measurements on a number of polystyrene fractions in cyclohexane.
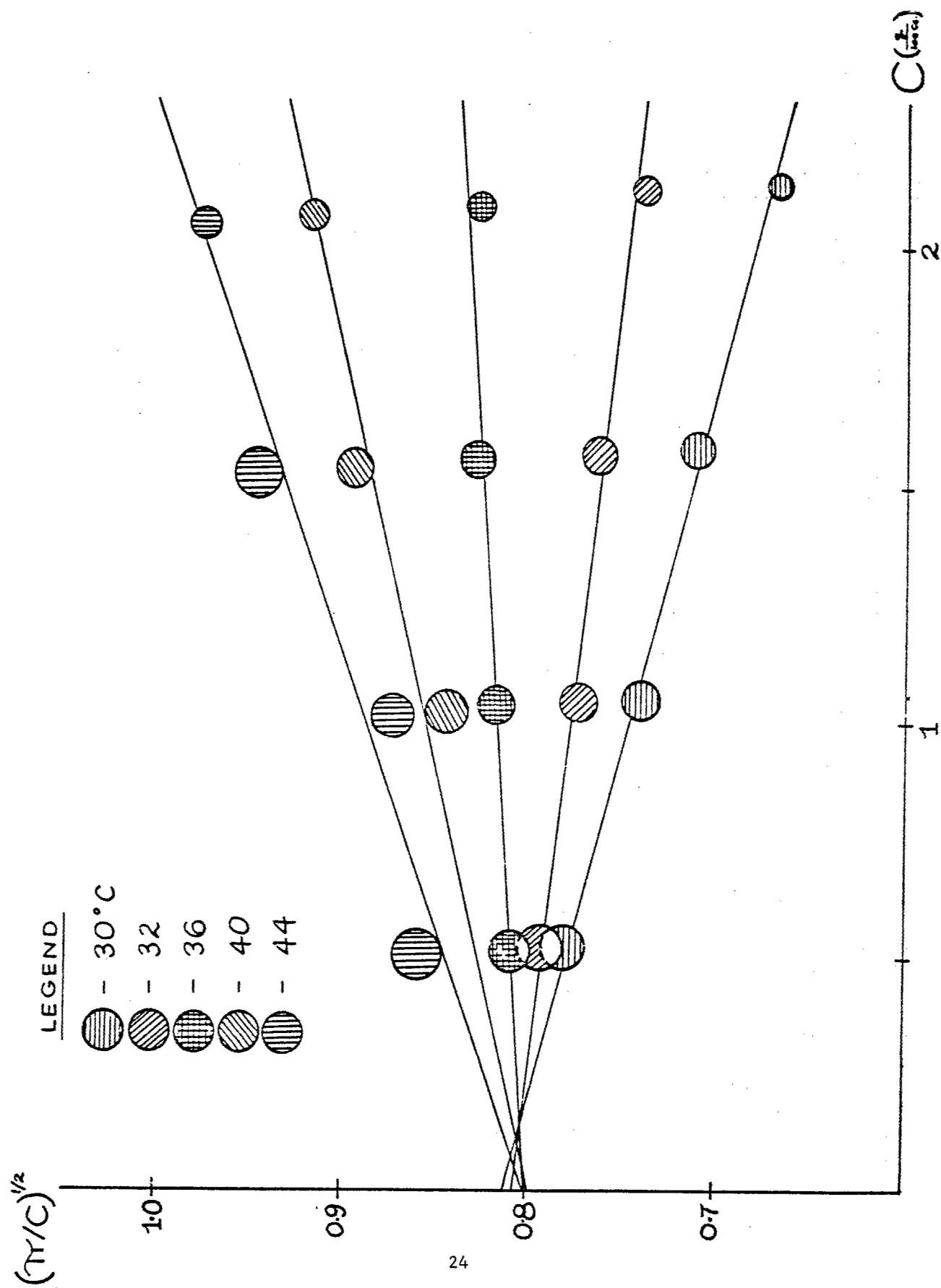
Figure 2 Plot of $(\pi/c)^{1/2}$ vs. c, Polystyrene-Cyclohexane

24

Table IV

Virial Coefficient-Temperature Results Polystyrene-Cyclohexane

$$(\overline{M}_n = 4.04 \times 10^5)$$

$t°C$	$10^4 A_2$
44.03	0.543
40.26	0.350
36.01	0.093
31.93	-0.195
29.92	-0.420

4. _Light scattering studies_. We have recently begun light scattering measurements, by means of which we plan to determine accurate Θ temperatures for each of the four solvents listed in Table II. As in the preceeding osmotic pressure studies, it is our intention to compute the Θ-temperatures by interpolation of the virial coefficient-temperature relationships. The light scattering virial equation analogous to Eq. (25) for osmotic pressure is

$$c/\tau° = (c/\tau)_o[1 + 2A_2Mc + \ldots] \tag{28}$$

where $\tau°$ is the excess turbidity, extrapolated to zero angle. Thus, determination of the scattering intensity as a function of angle, concentration and temperature for a given polystyrene-solvent system permits evaluation of A_2 as a function of temperature, from which Θ may be deduced.

The light scattering instrument at our disposal is a Brice-Phoenix unit which we are presently calibrating and adapting to our particular needs.

We have designed and constructed a thermostat by means of which close temperature control of the light scattering cell may be maintained. In the operating position, the cell rests on a hollow base through which water from a large constant temperature reservoir is recirculated via heavily insulated conduits. A heavily insulated, double-wall jacket slips over the cell and makes contact with the hollow base. Bath water is also directed through this jacket in an efficient manner by the placement of
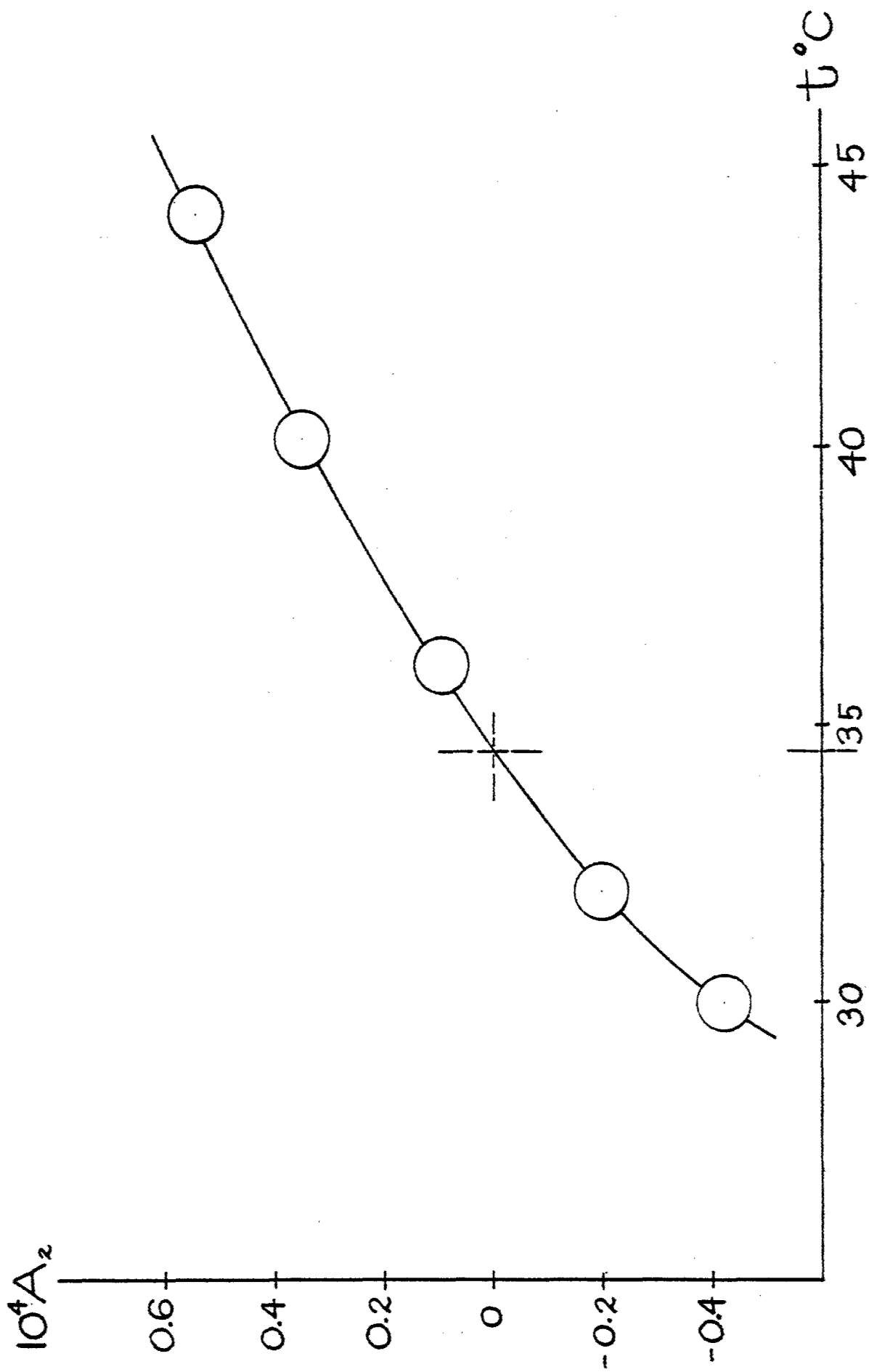
Figure 3 Plot of A_2 vs. Temperature, Polystyrene-Cyclohexane

26

suitable baffles. We are presently in the process of determining the relationship between bath and cell temperatures, as a function of the former, when the aforementioned assembly is in operation.

Calibration of the instrument has been completed and light scattering measurements will be carried out in the near future.

C. Theoretical. The Molecular Weight Dependence of the Intrinsic Viscosity in Polymer Solutions. A Comparison of Theory and Experiment*

1. Introduction. From a large amount of experimental data collected over the years, one may ascertain certain general characteristics of the molecular weight dependence of the intrinsic viscosity of linear polymers. It is the purpose of this communication to investigate the extent to which theoretical relationships currently available are able to account for and, to some degree, elaborate upon the more important of these features observed.

Over a limited, although often quite useful, range of polymer molecular weights M, the intrinsic viscosities $[\eta]$ of a given polymer--solvent system at a specified temperature may be adequately represented by a semi-empirical relationship of the Mark-Howink form

$$[\eta] = K'M^a \tag{29}$$

where K' and $\underline{a}$ are constants characteristic of the particular system investigated. Values of these parameters have been determined for a large number of polymer-solvent pairs in the range of molecular weights normally of interest for characterization purposes, about $10^5 - 10^6$.

The parameter $\underline{a}$ in most cases assumes values between 0.5 and 0.8 and, in magnitude, is qualitatively associated with the solvent power of the medium. The constant K' is usually in the range $10^{-3} - 10^{-4}$ and for a given polymer in a series of solvents (or in a given solvent at various temperatures) tends to decrease with increasing $\underline{a}$[36,37].

For some polymer-solvent pairs, investigated over wide ranges of molecular weights, two relationships of the form (29),with different values of the constants, have been used to describe the systems; one set of parameters is applicable to the region of low molecular weight, (less than about 3×10^4), the other, with a larger value of $\underline{a}$, to the region of moderate to high molecular weight. Systems[38] have been studied in which $\underline{a}$ for the low molecular weight region was found to be 0.5, a value usually associated with θ-solvent systems over the entire molecular weight range (cf. seq.).

---

*This section represents in part a manuscript which is to be submitted for publication.

2. _Theoretical_ $[\eta]$-_M_ relationships. According to the Flory-Fox relationship[39], the intrinsic viscosity of a linear polymer is given by the expression

$$[\eta] = \Phi(\overline{r_0^2}/M)^{3/2}M^{1/2}\alpha^3 = KM^{1/2}\alpha^3 \qquad (30)$$

where $\overline{r_0^2}$ proportional to M, is the unperturbed root mean square end-to-end separation of chain ends in a θ-solvent mixture, Φ is a constant (about 2.2×10^{21} for most systems, with $[\eta]$ in deciliters/g.) and α is an expansion factor by which the linear dimensions of the molecular coil are assumed to be increased by segment-solvent interactions. The latter quantity may be operationally defined

$$\alpha = ([\eta]/[\eta]_\theta)^{1/3} \qquad (31)$$

where $[\eta]_\theta$ is the intrinsic viscosity of the specified polymer of given molecular weight, at a specified temperature, in a θ-solvent mixture. According to the theory[40] of _intra_ molecular interactions, the parameter α may be expressed by the relationship

$$\alpha^5 - \alpha^3 = 2C_m\psi_1(1 - \theta/T)M^{1/2} = GM^{1/2} \qquad (32)$$

where C_m is a constant previously defined[41], ψ_1 and θ are interaction parameters characteristic of the polymer-solvent pair and T is the absolute temperature. Higher terms are neglected[42]. When the right hand side of the above equation becomes zero, as it does, for example, at the unique temperature $T = \theta$ for a given polymer-solvent pair, α becomes unity, $[\eta]$, in accordance with Eq. (31), reduces to $[\eta]_\theta$ and the intrinsic viscosity-molecular weight relationship of Eq. (30) becomes

$$[\eta]_\theta = KM^{1/2} \; ; \quad K = \Phi(\overline{r_0^2}/M)^{3/2} \qquad (33)$$

The constant K is independent of polymer molecular weight. It may be expected to vary somewhat with temperature through its dependence on the unperturbed root mean square end-to-end distance, and, taking into account possible effects on the latter arising from short range specific solvent interactions, may in general depend to some degree upon the nature of the medium in which the polymer is dissolved. Evidence for the latter effort has been noted in the case of cellulose derivatives.[43]

Values[39,41] of K for a number of different polymers have been derived from θ-solvent intrinsic viscosity measurements in accordance with the first of the equations (33).

28

An alternate, indirect method for the determination of K values from viscosity data in good solvents was suggested a number of years ago[39]. A variant of this procedure has been developed recently by Kawai and Naito[37]. In the next section, the details of the original treatment are examined and are applied to data on a number of polymer-solvent systems.

3. _Derivation of K from data on good solvents_. Equations (8) and (10) of the preceding section may be combined, with elimination of α, to yield the relationship[39]

$$([\eta]^2/M)^{1/3} = K^{2/3} + K^{5/3}G(M/[\eta]) \tag{34}$$

Thus, according to theory, a plot of $([\eta]^2/M)^{1/3}$ versus $M/[\eta]$ for any polymer-solvent system at a given temperature should produce a straight line with intercept $K^{2/3}$ and slope $K^{5/3}G$. Graphs for the systems polyisobutylene[36], polystyrene[44] and polymethylmethacrylate[45] in various solvents are shown in Figs. 4, 5, and 6 respectively. The data appear to describe linear relationships in all cases, although in some there is considerable scatter. In the polyisobutylene and polystryene systems, common intercepts, within experimental error, are obtained. The respective values of K derived from these intercepts are 9.2 and 7.7 x 10⁻⁴, in reasonably good agreement in each case with those values (at the same temperature) deduced from θ-solvent viscometric data[39], 10.6 and 8.0 x 10⁻⁴. With the exception of the curves for chloroform and dichloroethane, the data on polymethylmethacrylate also yield a common intercept, corresponding to a K value of 4.4 x 10⁻⁴, which stands in good agreement with the value[46] 4.8 x 10⁻⁴ deduced from θ-solvent measurements. Possible explanations for the apparent anomolies observed in the case of the two aforementioned solvents are 1. the existence of specific solvent effects which could conceivably alter the K values appropriate to these systems, 2. failure to take into account higher terms in Eq. (32) the effect of which may be significant in these cases[*], and 3. other deficiencies in theory.

Everything considered, the procedure described for the determination of K values from good solvent data does appear to afford a useful means of polymer characterization when direct evaluation of K from θ-solvent measurements is impracticable or inconvenient. Moreover, the method described, when applied with objective reservation, may serve as a useful guide in the detection and evaluation of specific solvent effects.

---

[*]The equivalent version of Eq. (34) with retention of the second order interaction term[7] in Eq. (32) is of the form

$$([\eta]^2/M)^{1/3} = K^{2/3} + K^{5/3}G(M/[\eta]) + K^{5/3}H(M^{1/2}/[\eta]^2)$$

where H is a molecular weight independent quantity proportional to the secondary interaction parameter $(1/3 - X_2)$. The additional term could conceivably make a significant contribution at low values of $M/[\eta]$, in line with the deviations observed in the two solvents cited.
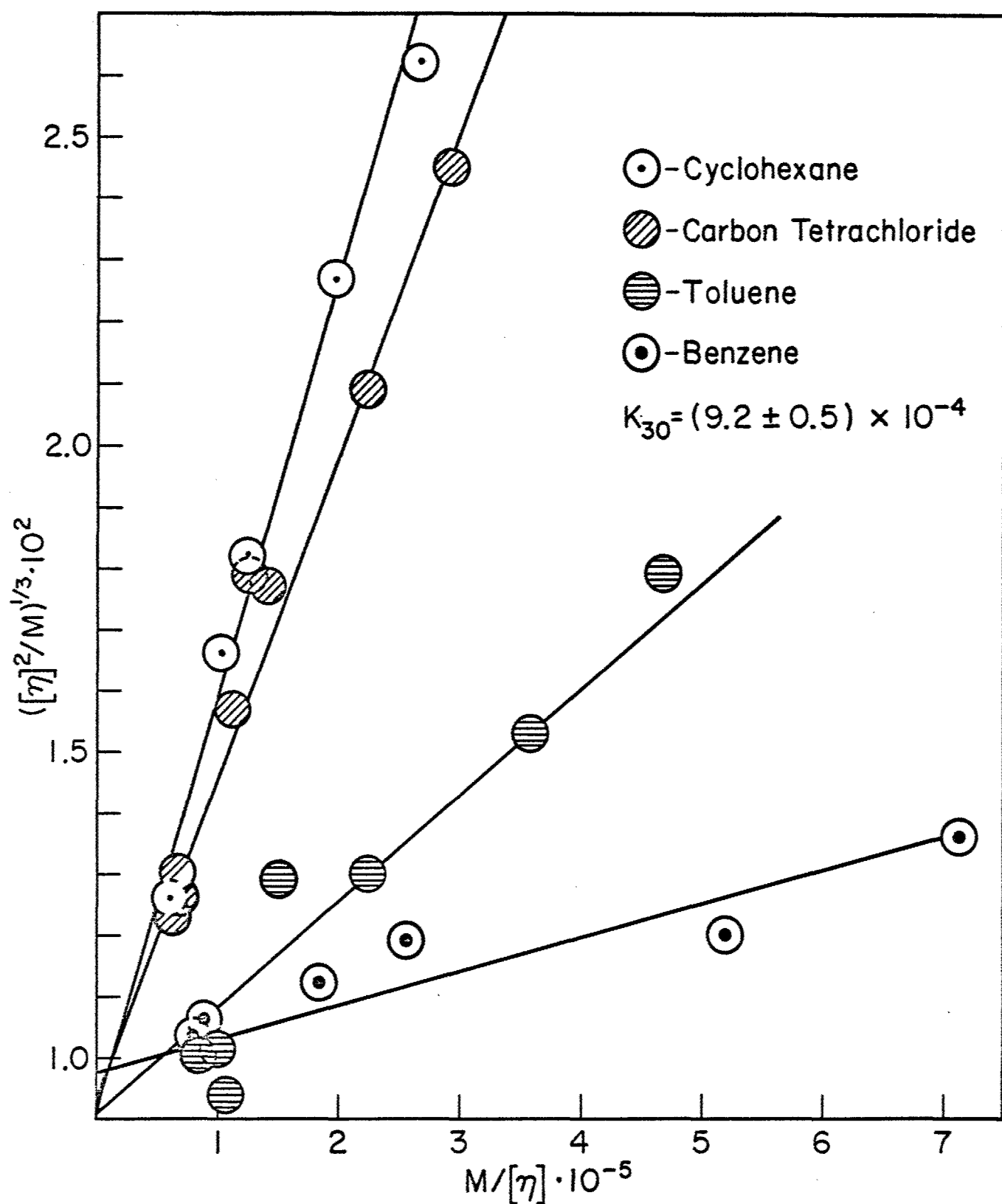
Figure 4. $([\eta]^2/M)^{1/3}$ versus $M/[\eta]$ for Polyisobutylene at 30°C (Ref. 36)

30
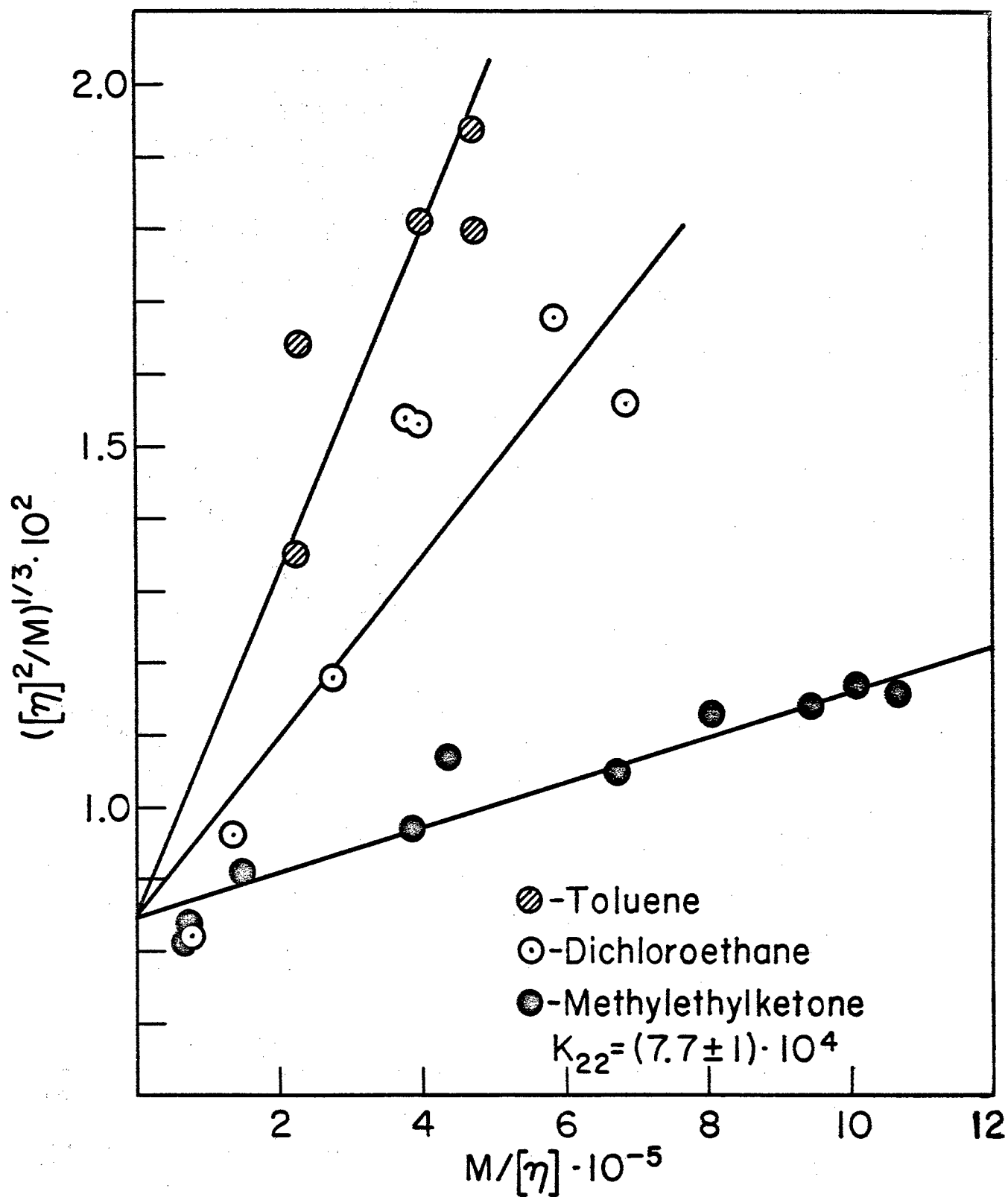
Figure 5 $([\eta]^2/M)^{1/3}$ versus $M/[\eta]$ for Polystyrene at 22°C (Ref. 44)

31
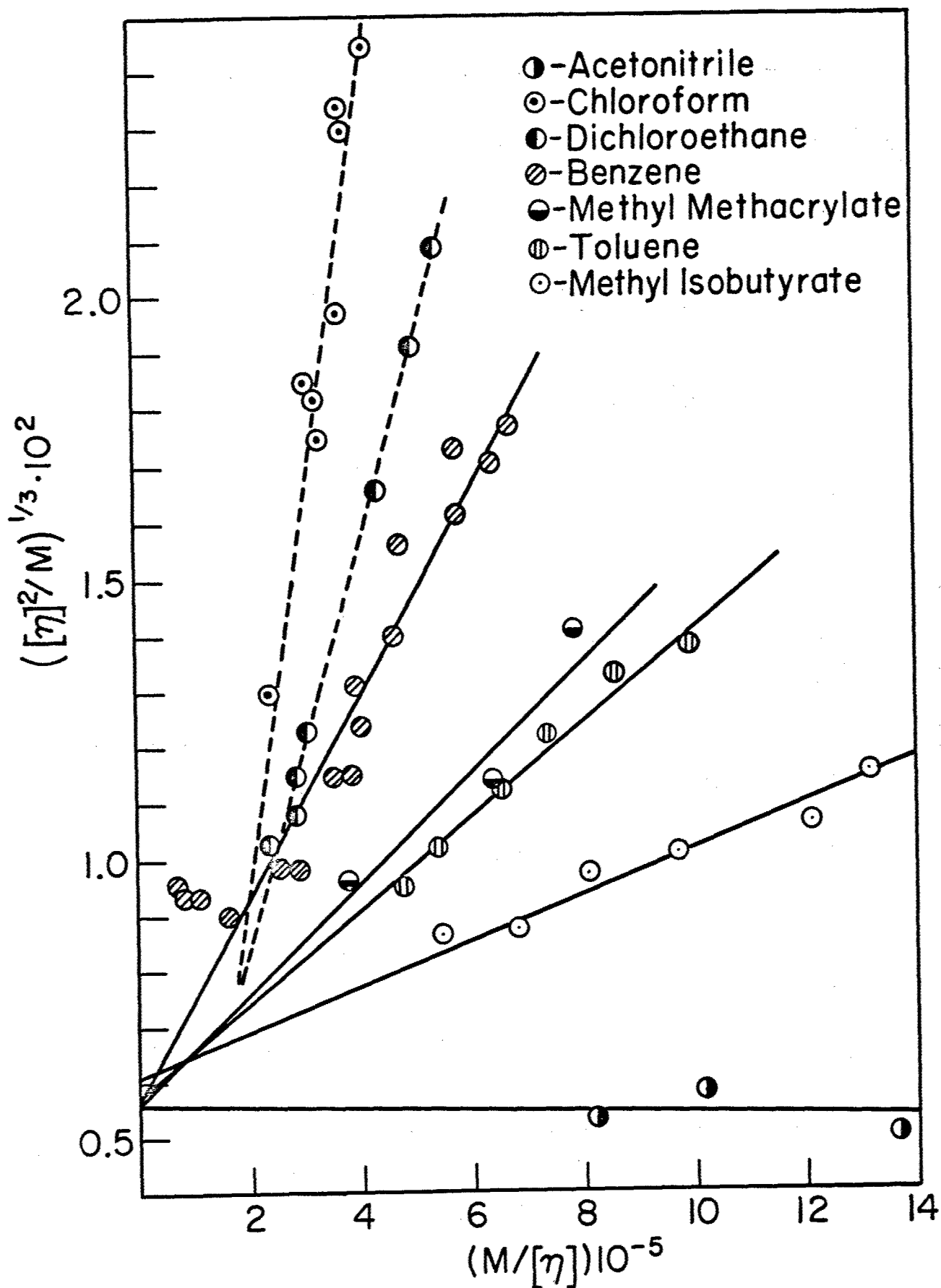
Figure 6 $([\eta]^2/M)^{1/3}$ versus $M/[\eta]$ for Poly-(methyl methacrylate)

32

4. The $[\eta]$-M relationship at high molecular weight.

a. Correlation of the Mark-Howink equation with theory. Combination of Eq. (30), for the intrinsic viscosity as a function of M and α, with Eq. (32), in which α is expressed as an implicit function of M, permits a prediction of the general molecular weight dependence of $[\eta]$ for a given system. The relationship so obtained does not strictly correspond to the semi-empirical Eq. (29) observed experimentally, but rather, if cast in this form, requires both K' and a to vary continuously with molecular weight. Thus, whereas a plot of log $[\eta]$ versus log M in accordance with Eq. (29) yields a straight line of slope a, a similar plot derived from the theoretical relations of eqs. (30) and (32) for any arbitrary values of the molecular weight independent quantities K and G (the latter not equal to zero) produces a curve, the first derivative of which increases monotonically throughout the range of M. Plots of log $[\eta]$ versus log M so constructed for various values of G in the range of solvent interaction normally encountered are shown in Fig. 7. A value 10^{-3} for K (Eq. (30) was arbitrarily assigned for computation purposes; the choice affects only the overall vertical position of the parametric curves.

Close inspection of the theoretical log $[\eta]$ versus log M curves of Fig. 7 shows that over a range of several decades in M, in the vicinity of 10^5, a linear relationship for practical purposes exists[36,41]. It is unlikely that the curvature in this region, if accepted in strict accordance with theory, would be detected from experimental viscometric data obtained over a moderate range of molecular weights. In good solvents (large values of G), the theoretical log $[\eta]$ versus log M curves could be approximated by single lines, e.g., the tangent lines at M equal to 10^5, over the range $10^4 - 10^7$ with a maximum error probably undetectable by ordinary experimental techniques. We may therefore conclude that the theoretical relationships embodied in the Eqs. (30) and (32), the validity of which admittedly has not been demonstrated by the negative argument just presented, are at least not at variance with the semi-empirical relationship of Eq. (29) in the (usual) cases where the latter is found to be applicable over a restricted range of polymer molecular weight.

Careful viscosity measurements extended to the low molecular weight region (but still above molecular weights for which theory may be expected to be valid) do, in fact, substantiate the curvature predicted, particularly in the case of poor solvents[36,38].

If the compatibility of the Mark-Howink Eq. (29) and the theoretical relationships of Eqs. (30) and (32) are accepted, one may attempt some additional correlations between theory and experiment. For this purpose, we shall assume that the log $[\eta]$-log M curves of Fig. 4 may be satisfactorily approximated over a few neighboring decades in molecular weight by the corresponding tangent lines at M equal to $10^{5.5}$.* The latter are assumed to correspond to the experimentally determined relationships of the form of Eq. (29).

---

*A convenient, single value which might be expected to provide an equivalent linear representation over the range of molecular weights 5 x 10^4 to 2 x 10^6 (log M = 5.5 $\pm$ 0.8).
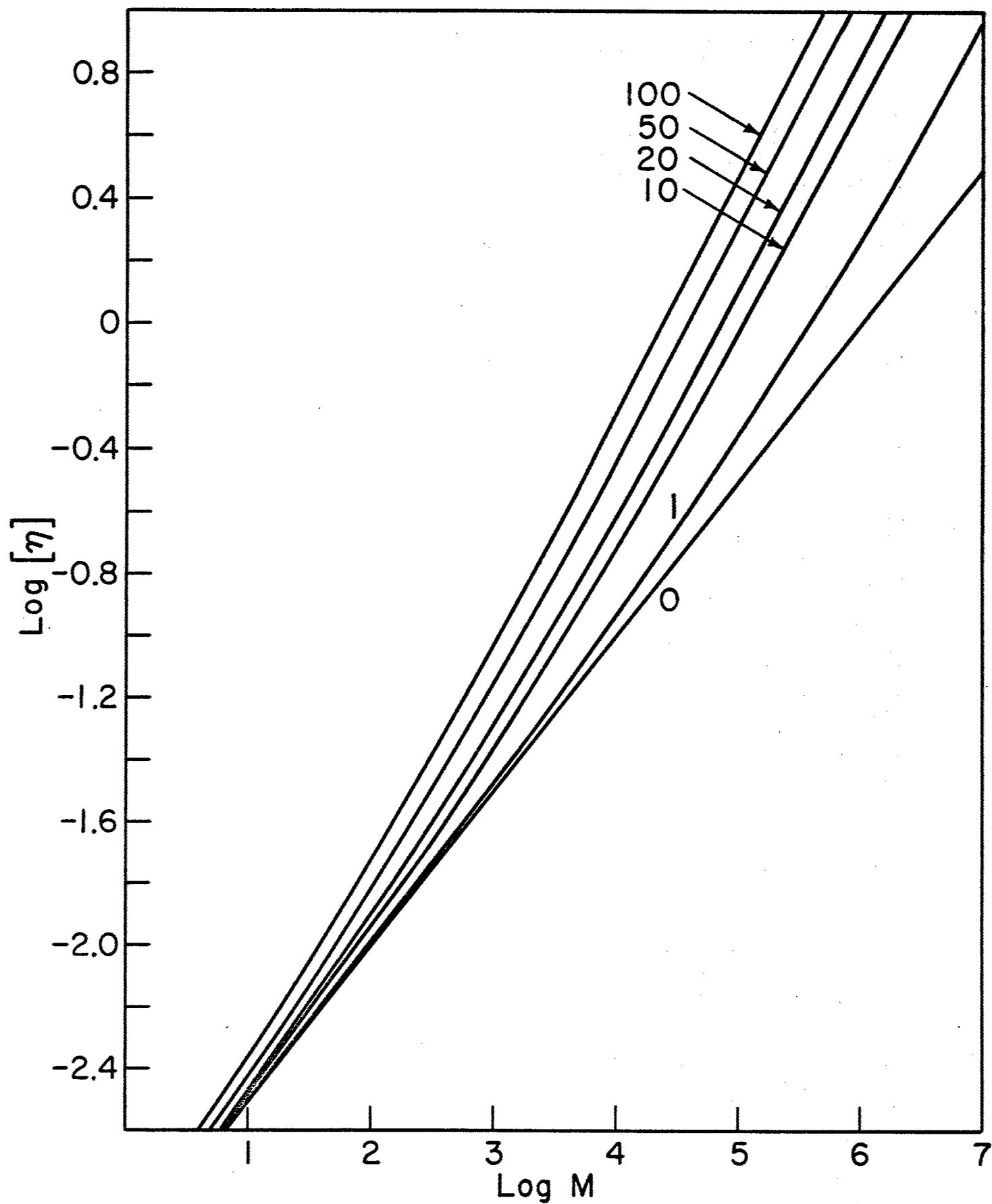
Figure 7 Theoretical Log [η], Log M Plots for Various G × 10³

34

In Table V, values of $\underline{a}$ and the ratio K'/K are listed for various (arbitrary) G appropriate to the range of solvent power usually encountered. The parameter $\underline{a}$ was computed with the aid of the general theoretical relation

$$a = d \ln [\eta]/d \ln M = 1/2 + 3(\alpha^2 - 1)/2(5\alpha^2 - 3) \qquad (35)$$

derivable by differentiation of Eqs. (30) and (32). Taking M equal to $10^{5 \cdot 5}$, α for various G was computed from Eq. (32); these, inserted into the above equation, yielded the desired values of $\underline{a}$. Combination of Eqs. (29) and (30) yields for the logarithm of the ratio $\overline{K}'/K$

$$\log (K'/K) = (1/2 - a) \log M + 3 \log \alpha \qquad (36)$$

by means of which entries in the last column of Table V were computed taking, again, M equal to $10^{5 \cdot 5}$.

Table V

Viscosity-Molecular Weight Parameters Derived from Theory

(for M = 3.16 x 10^5)

10^3 G	α	a	K'/K
0	1.00	0.5000	1.000
1	1.16	0.6413	0.264
5	1.41	0.7141	0.187
10	1.57	0.7354	0.196
20	1.75	0.7416	0.224
30	1.88	0.7591	0.250
50	2.06	0.7669	0.296
100	2.33	0.7752	0.387

In Figs. 8 and 9, plots of $\underline{a}$ and K'/K versus G and a plot of K'/K versus $\underline{a}$, respectively, are given. The latter curve retains no parameters of the theoretical relationships employed in its construction, other than K whose value for each of a number of polymers, ignoring possible specific solvent effects (see preceding section) may be regarded as a fairly well known quantity. We have accordingly included in Fig. 9 for comparison some experimental values available from the literature.

From the plots of Figs. 7, 8 and 9 a number of interesting features, borne out for the most part by experimental data, are evident. In the theoretical log $[\eta]$ versus log M plots of Fig. 7, for example, we note that the spacing of the parametric curves is not in linear proportion to the values of the interaction quantity G (see Eq. (32)) to which they refer. The effect is more pronounced in the plot of $\underline{a}$ versus G in Fig. 8, which in addition to exhibiting the increase in $\underline{a}$ with solvent power of the medium experimentally observed, predicts a rapid initial increase of the viscosity-molecular weight exponent, followed by a gradual asymptotic approach to the limiting value required by theory, 0.8, with increasing G. If the G value characteristic of some arbitrarily selected polymer-solvent pair is regarded as a random quantity, uniformly distributed within observable limits, it is very likely that the corresponding $\underline{a}$ value for the system will fall within narrowly defined limits (about 0.72-0.77). Whatever the basic origin of this effect, it is interesting to note that the predictions of theory in this instance are supported by experimental evidence, i.e., the preponderance of reported $\underline{a}$ values in the region described, and, perhaps more significantly, the paucity of observed values in the range $0.5 < a < 0.7$.

We note finally in Fig. 8 that theory predicts a decrease in K' with increasing $\underline{a}$ over most of the range of polymer-solvent interaction encountered, and that qualitatively, at least, the effect is in accord with experimental observations.

b. Calculation of the constants K' and a. In their recent publication, Kawai and Naito suggest a "one point" method for the estimation of the Mark-Houwink viscosity-molecular weight relationship appropriate to a particular polymer-solvent pair of interest. The calculation requires a knowledge of the molecular weight of a single sample (preferably of minimal heterogeneity and lying about in the middle of the molecular weight range of interest) and the intrinsic viscosity of this sample in the solvent chosen, together with extensive $[\eta]$-M data for the same polymer dissolved in some other solvent. In accordance with the relationships presented earlier, we shall describe a similar, and perhaps more direct, procedure for carrying out this calculation.

If a number of values of $[\eta]$ and M are known for some polymer-solvent pairs, the constant K (Eq. (33)) for the polymer at the corresponding temperature may be evaluated by the graphical procedure described in an earlier section. Ignoring possible specific effects, the value of K so established is, in accordance with theory, also applicable to the same polymer dissolved in other media. Thus, insertion of this K value, together with a single set of $[\eta]$-M values for the solvent of interest, in Eq. (30) permits evaluation of the expansion parameter α appropriate to the new system.
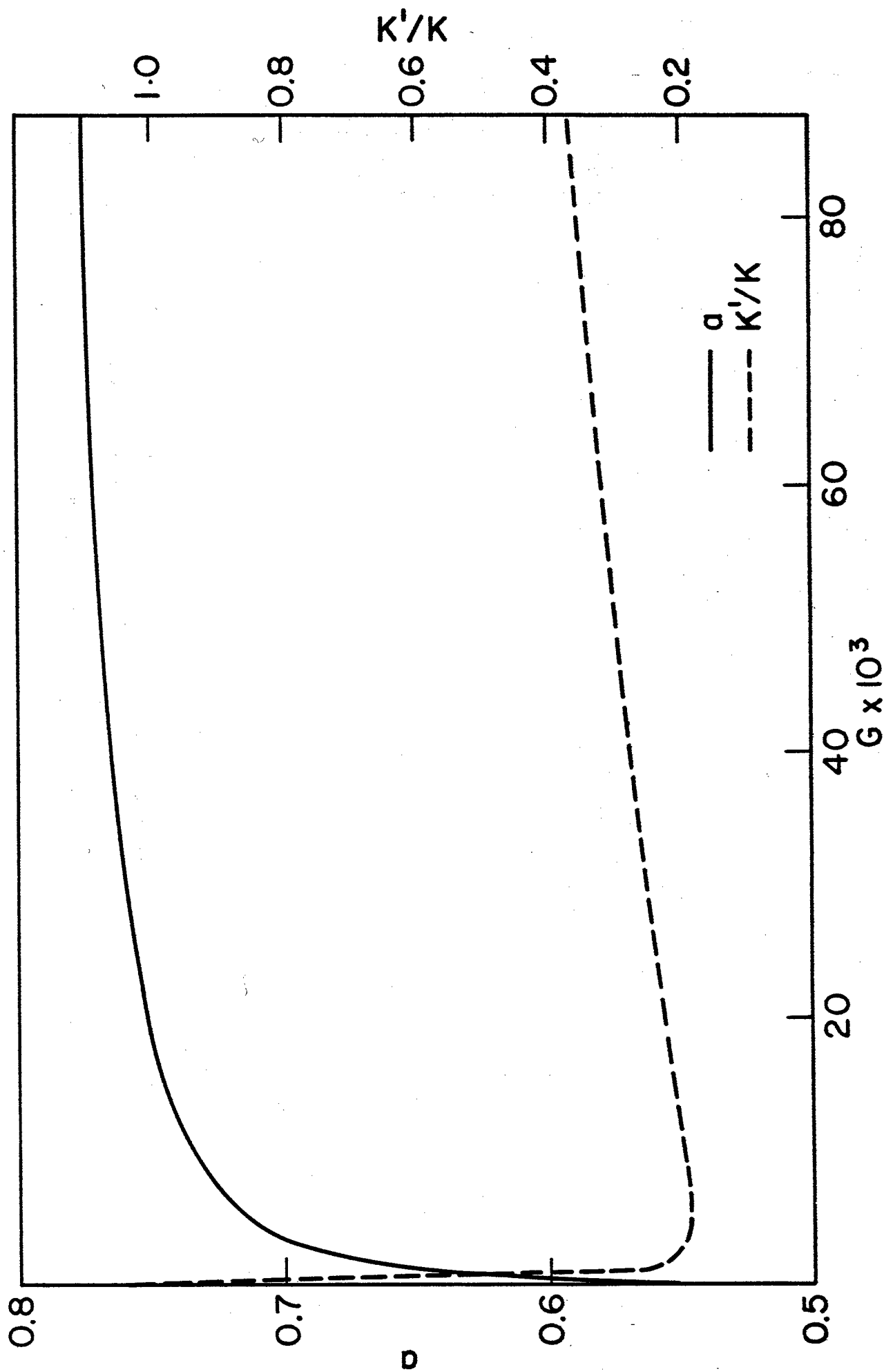
Figure 8   Plots of a and K'/K versus G (M = $10^{5.5}$)

37
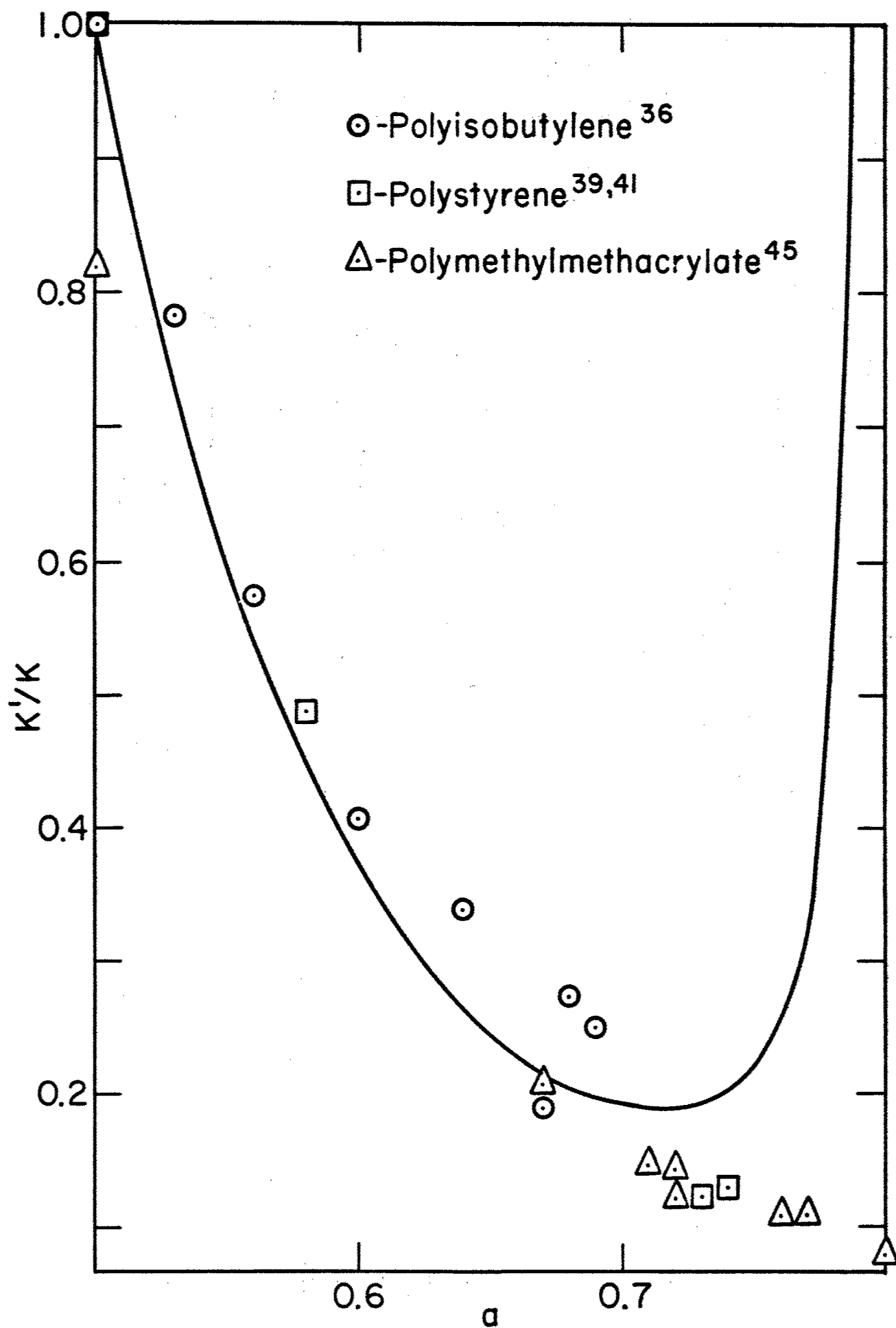
Figure 9 Plot of K'/K versus a, Theoretical Curve for $M = 3.16 \times 10^5$

38

From α, the slope of the tangent line to the theoretical $[\eta]$-M curve, which we have interpreted as the Mark-Howink exponent $\underline{a}$, may be computed in accordance with Eq. (35). The companion constant K' is obtainable from Eq. (36), utilizing previously determined values of K, a, α and M derived from data on the single sample studied.

The viscosity-molecular weight relationship calculated in the manner described should provide a satisfactory representation over a range of molecular weights not differing greatly from that of the sample used in its construction. The validity of the values deduced for K' and $\underline{a}$, rests primarily upon the validity of the single set of $[\eta]$-M data utilized; the general theoretical relationships assumed serve only as a means of introducing a perturbation for variations in M from the assigned value. The use of average values of the viscosity constants (the logarithmic mean in the case of K') derived from data on two or more fractions would, of course, increase the reliability of the relationship.

The viscosity-molecular weight relationship for a given polymer-solvent pair may also be estimated by another "one point" method which does not require viscometric data on a reference system. According to the theory[41,42] of intermolecular interactions advanced by Flory and co-workers, the expansion factor α is related to the second virial coefficient A_2 which appears in the series expansion of the reduced osmotic pressure π/c.

$$\pi/c = RT[1/M + A_2 c + \ . \ . \ .] \tag{37}$$

where c is polymer concentration and R is the gas constant, in accordance with the expression

$$\ln[1 + (\pi^{1/2}/2)(\alpha^2 - 1)] = (27\Phi/2^{5/2}\pi N)(A_2 M/[\eta]) \tag{38}$$

Here, Φ is the viscosity constant appearing in Eq.(30) and N is Avogadro's number. Thus, a single set of the quantities M, $[\eta]$ and A_2 for a given polymer-solvent pair suffices to establish the associated value of α appearing in Eq. (38). Once α is known, K may be computed from Eq. (30) and the constants K' and $\underline{a}$ may be evaluated in the manner described in the preceding "one point" method. It should be noted, however, that in the present procedure, theory plays a somewhat more dominant role in assigning the Mark-Howink constants.

5. The $[\eta]$-M relationship at low molecular weight. In the preceding sections we have demonstrated the general compatibility of the theoretical relationships (30) and (32) with the semi-empirical Mark-Howink equation, applicable to high molecular weight polymers over a restricted range in M. We may conclude that the apparent linearity of log $[\eta]$-log M plots experimentally observed in this region arises from the insensitivity of the derivative d ln α^3/d ln M, an effect which seems to be adequately accounted for by the theory presented.

Some[45,47,48] polymer-solvent systems have been investigated in which viscometric measurements extended to the low molecular weight region indicate the need for two equations of the Mark-Howink form in order to satisfactorily represent the data. One of the relationships applies to the high molecular weight region, in accordance with the customary representation, the other, of lesser slope, to the region of low molecular weights, usually less than about 30-50,000. On a logarithmic plot, the two lines intersect, forming an apparent "break point" in the $[\eta]$-M plots. Close inspection of the data obtained for such systems shows that the log $[\eta]$-log M relationship may in fact be equally well described by a smooth curve. Thus, by this interpretation, the representation by two intersecting lines would appear to be merely a convenient means of expressing the data within experimental error.

According to the theoretical relationships presented here, the slope of the ln $[\eta]$- ln M curve should decrease monotonically with decreasing M, and, regardless of G, should attain at sufficiently low molecular weight a value experimentally indistinguishable from the characteristic 0.5 found for θ-solvent mixtures over the entire range of M. This conclusion has been reached by Rossi[38] et al, in whose publication an experimental verification is presented for polystyrene-toluene solutions.

The degree to which the theoretical curves fit experimental data over a range of M in which d ln $[\eta]$/d ln M approaches one-half has been examined by Fox and Flory for polyisobutylene systems[38]. The agreement in these cases is rather good.

D. Summary and Conclusions

In this report we have outlined and discussed the progress to date on an experimental program designed to further our understanding of the specific effects of solvents on the θ-point dimensions of polymer chains. Accurate θ-temperatures for the system selected in our initial work should be established in the near future, at which time an extensive investigation of the molecular dimensions of polystyrene in these θ-solvents will be undertaken. We have in mind extending our general methods to other polymer-solvent systems at a later date.

Many aspects of the problem of the specific effect of solvents on chain dimensions are also amenable to theoretical treatment. In this connection, we have included in our report a draft of a manuscript which, in more general terms, deals with the viscometric behavior of polymer solutions, and which presents a re-interpretation of current polymer theory in light of the possible influence of specific solvent effects.

We are also presently engaged in another theoretical investigation on the temperature dependence of the intrinsic viscosity, and hence molecular dimensions, in the vicinity of the θ-temperature.

III. Light Scattering Photometer — G. C. Berry, E. F. Casassa, D. J. Plazek

A. Introduction

A precision light scattering photometer has been designed and constructed. The instrument is primarily intended to provide accurate measurements of the relative scattering from polymer solutions as a function of angle and temperature. The design is such, however, that the instrument can also be used to measure absolute scattering. The optical design is similar in principle to that described by McIntyre and Doderer[49], and the mechanical arrangement includes many features described by Katz[50]. A highly collimated monochromatic beam is split and then focused in a light scattering cell and on a monitoring photomultiplier. The scattered light is detected by a second photomultiplier which "sees" the scattering volume in the cell through a suitable optical system. The ratio of the two photocurrents generated in this manner is measured in a bridge circuit. This method tends to eliminate the effect of lamp intensity fluctuations on the measured response due to scattered light. The following report is a description of the mechanical, optical and electronic design of the photometer.

B. Apparatus

1. <u>General description</u>. Fig. 10 is a schematic drawing of the instrument and associated equipment. Since the details of the construction are available in a set of mechanical drawings, it is sufficient here to point out the major components in the instrument. These consist of separate housings for a lamp; for a set of monochromatic filters; for a mechanical beam chopper; for a set of neutral filters, beam splitter, and monitoring photomultiplier; and for the detector photomultiplier. The last unit mounted on a goniometer permits accurate determination of scattering as a function of angle. The sample cell is placed at the center of the goniometer either on an open pedestal or in an enclosed thermostat. The mechanical construction is such that all of the optical parts may be individually adjusted, as required for the optical alignment. The entire unit is sturdily constructed to eliminate difficulties from vibration or unintentional mechanical shocks.

A model NBS Brinkman-Haake thermostat is used as the water bath and pump to supply the thermostating liquid to the cell thermostat. This liquid is circulated between the double walls of the thermostat and thus controls the temperature of a liquid bath surrounding the sample.

2. <u>Optical design</u>. Fig. 11 is a schematic diagram of the optical system of the instrument. The light source is a mercury vapor lamp, with the arc aligned perpendicular to the optical axis. Two such lamps are considered below. The source is located approximately at the focal point of lens L_1 (the characteristics of the optical parts are given in Table VI).

41
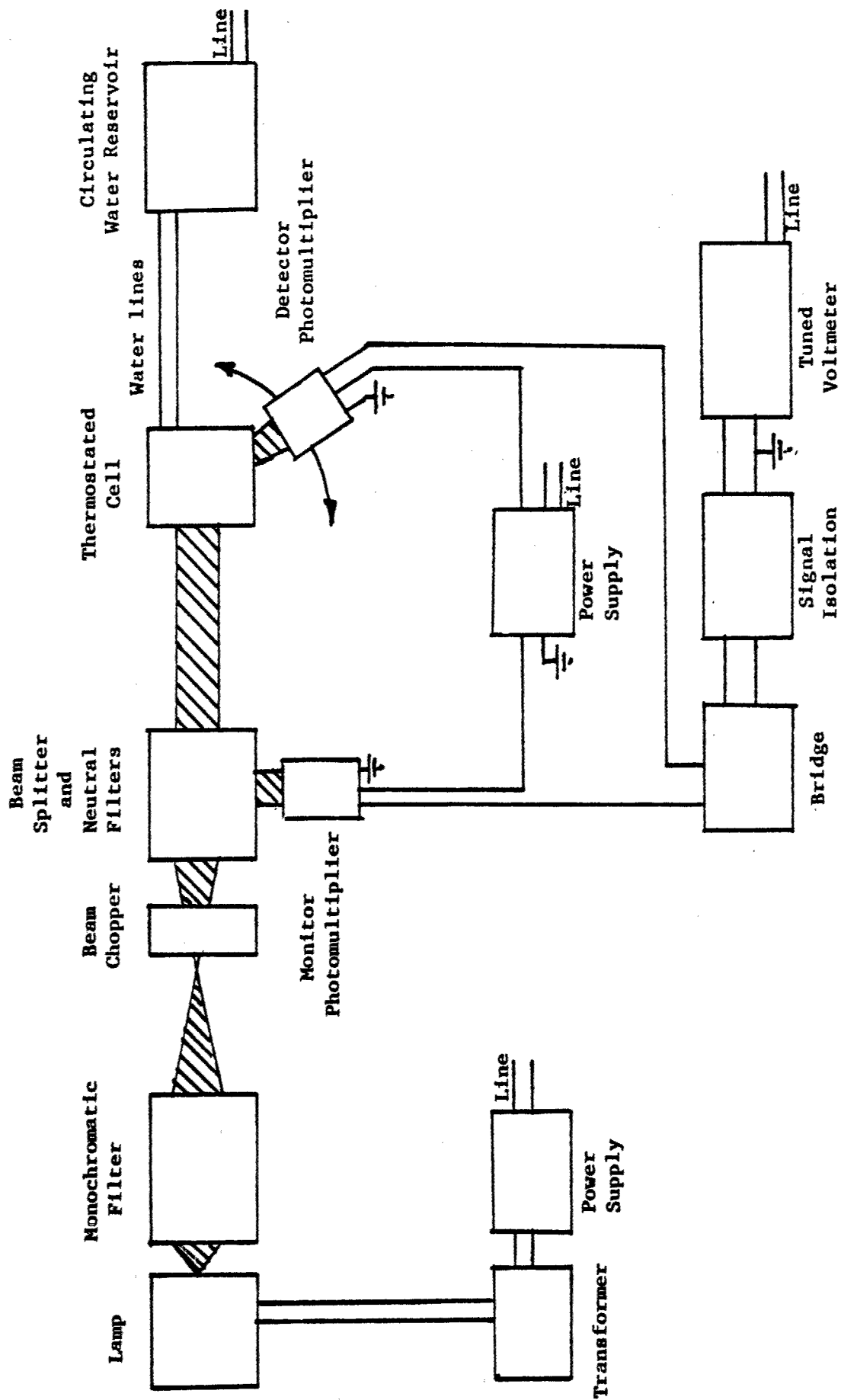
Figure 10 Instrument and Associated Equipment
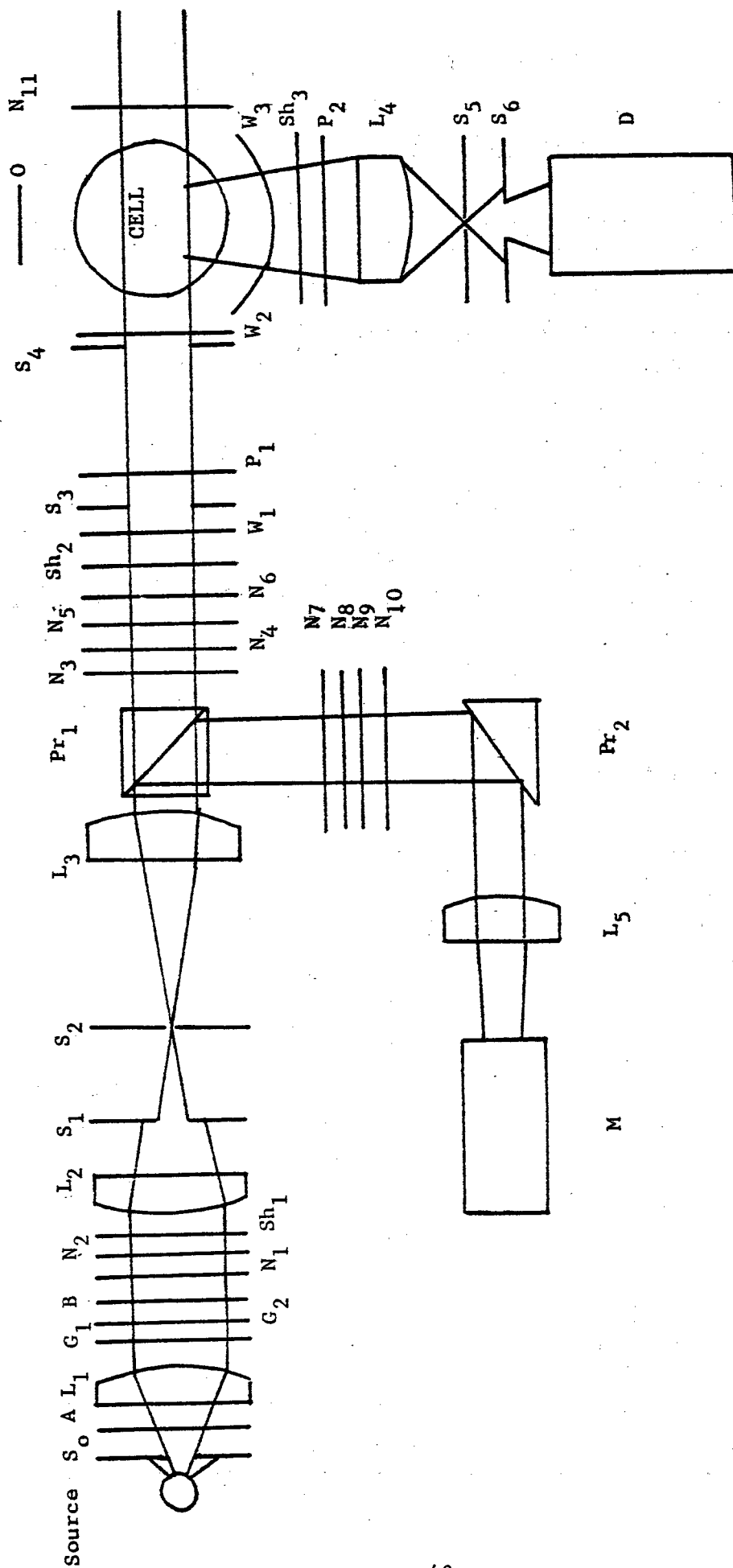
Figure 11 Optical System

43

Table VI

Optical Parts of the Photometer

Part	Description
L_1, L_2	35 mm projection lens, 7 in f.l.; Anastigmat F/3.6 coated lens
L_3	44 mm dia; 189 mm f.l.; coated achromatic lens
L_4	18 mm dia; 39 mm f.l.; coated achromatic lens
L_5	29 mm dia; 40 mm f.l.; lens
A	2 3/8" dia. heat absorbing glass
G_1	Corning glass filters 3484, 5120
G_2	Corning glass filters 3484, 4303, 5120
B	Corning glass filters 3309, 5113
N_1	2" dia. Series VII metallic neutral filter (Tiffen Optical Co.), trans 1/8
N_2	2" dia. Series VII metallic neutral filter (Tiffen Optical Co.), trans 1/32
N_3	Neutral filters, Phoenix Co., trans 1/2
N_4	Neutral filters, Phoenix Co., trans 1/4
N_5	Neutral filters, Phoenix Co., trans 1/8
N_6	Neutral filters, Phoenix Co., trans 1/16
N_7	Schott neutral filters, (Fish-Schurman Co.), NG 4; trans 1/10
N_8	Schott neutral filters, (Fish-Schurman Co.), NG 4; trans 1/10
N_9	Schott neutral filters, (Fish-Schurman Co.), NG 5; trans 1/3
N_{10}	Schott neutral filters, (Fish-Schurman Co.), NG 11; trans 1/2
N_{11}	Neutral filter, trans about 1/20
Sh_4	Prontor II shutter
P_1, P_2	1 1/2" dia., 3.5 mm thick polarizers, Polaroid HN22C, SpC, FGE Glass
M, D	DuMont K1780 photomultiplier tubes
W_1	32 mm dia.
W_2	Cut from 100 mm ID pyrex tube
Pr_1	Silvered right angle prism; 34 mm width, 45 mm hypotenuse, 32 mm side
Pr_2	1 1/4" glass cube (n_0 = 1.508) fabricated from two 45° right angle prisms with cement of refractive index about 1.495 (Tiffen Optical Co.)
Source	200/250 volts, 250 watt ME/D box lamp
Source	H100-A4 General Electric mercury vapor lamp

Lens L_1 receives light through a large slit S_0 and a heat absorbing filter A. The essentially parallel light from L_1 passes through one of the three monochromatic filters G_1, G_2 or B. N_1 and N_2 are removable neutral filters; Sh_1 is a sliding shutter. Lens L_2 is identical to L_1, and may be moved independently of L_1. The position of L_2 is adjusted so that the aperture S_2 is in the focal plane of L_2 by focusing an image of the source at S_2. The position of S_1 is adjusted so that its image is focused in the cell. Lens L_3 is adjusted so that S_2 is in its focal plane. This arrangement gives a highly collimated beam of light from the exit of L_3.

The beam splitting prism is a glass tube constructed from two triangular prisms cemented along the diagonal faces. The refractive index of the cement is close to that of the glass so that the primary beam suffers only negligible polarization and attenuation at the interface. The opposite sides of the cube are ground parallel and polished.

The lens L_5 is chosen to make the optical path length from L_3 to the monitor photomultiplier M nearly identical to that from L_3 to the cell. Thus, a uniformly irradiant image of S_1 is focused both in the cell and on M. A second prism, Pr_2 merely turns the monitor beam downward through 90° into M to maintain compact dimensions in the unit. Other components in the main filter box include the removable neutral filters for the primary beam, N_3 to N_6, and for the monitor beam, N_7 to N_{10}. Sh_2 is a sliding shutter and W_1 is a plane glass window to keep dust out of the housing. S_3 and S_4 are stray light slits, made slightly larger than the primary beam at their respective positions.

The cell is normally enclosed in a thermostat with a clear glass W_2 and a neutral filter N_{11} as plane entrance and exit windows respectively for the primary beam. The neutral filter (of about 5 percent transmission) serves to reduce back reflection of the incident beam into the cell from the glass-air interface by a factor of 400. Without this attenuation the back reflection of about 5% of the incident beam would produce scattering in the sense opposite from the incident beam sufficient to falsify seriously angular dependence measurements on very large molecules[52]. The scattering volume is viewed through a curved window W_3, ground and polished on the outside surface. The light scattering cell may be cylindrical in shape, such as that used in the Brice-Phoenix photometer, or conical, a form which helps to reduce reflections[53]. In the latter case, the thermostat liquid in which the cell is immersed must have a refractive index rather close to that of the scattering liquid if undesirable refractions are to be avoided. The detector optics follow a design given by Kushner[54]. Slits S_5 and S_6 are placed in the focal and image planes, respectively, of lens L_4. The detector photomultiplier, D, views the light passing slit S_6. Sh_3 is a camera shutter and 0 is an opal glass diffuser which is in the line of view only when the detector is viewing the primary beam directly.

The removable polarizers, P_1 and P_2, are mounted so as to be easily rotated precisely through 90°. They have a resolving power of 10 seconds of arc.

3. <u>Optical alignment</u>. It is clear from Fig. 11 that the positions of the optical parts are interrelated, that is, a movement of one component usually requires an adjustment of other parts also. The optical alignment was accomplished by successive trials, the adjustments being made by visual observation of the primary beam and its reflections at critical points. Thus, the beam from L_2 and the beam reflected back through L_3 from the plane surface of Pr_1 or W_1 were focused on S_2. The position of S_1 is adjusted so that its image is focused in the cell. The thin lens formula is useful in determining the approximate distances required,

$$1/d_1 + 1/d_2 = 1/f \tag{39}$$

where d_1 and d_2 are the distances from the lens to the object and image respectively, and f is the focal length of the lens.

The divergence of the primary beam is conveniently characterized by the angle ϕ indicated below.
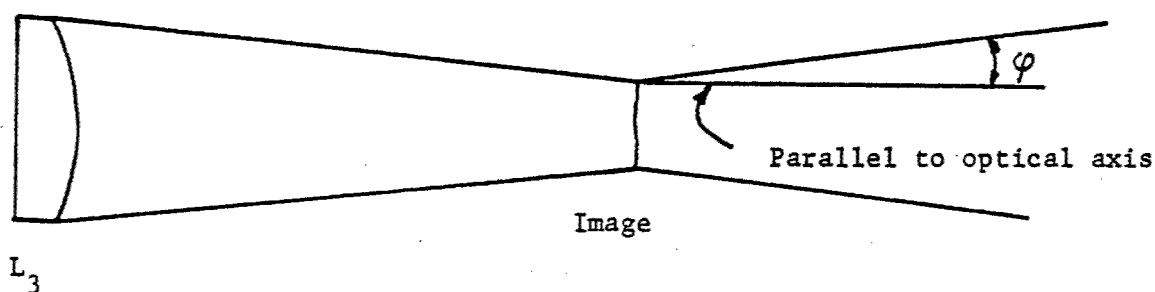
The magnitude of ϕ may be varied by changing the size of slit S_2 or of the source, one of which will be controlling. Some typical figures are given below for two mercury lamps of different arc size

Source	Size of S_2	ϕ vertical	ϕ horizontal
ME/D	∞	27'	6'
ME/D	2 x 6 mm	24'	6'
ME/D	1 x 3 mm	24'	3'
HA 4	∞	2° 10'	--
HA 4	3 x 9	1° 20'	--
HA 4	3 x 6	38'	--

The size of S_2 has a minor effect on the degree of collimation when the ME/D lamp is the source because of the small size of this arc. Conversely, the slit size becomes noticeably important when the arc is larger as in the case of the HA 4 lamp.

46

The monitor system is similarly aligned by visual means. The prism Pr_2 is placed so that light falls on the central part of M, and then L_5 and M are adjusted until the image of S_1 is focused on M.

The alignment of the detecting system involves two adjustments after the photomultiplier housing has been placed on the optical axis of the primary beam. S_5 is placed in the focal plane of L_4 by visually focusing a beam of parallel light on S_5. Placement of S_6 in the image plane of L_4 requires a scattering source located in the position of the cell. Thus, the image of an opal diffuser at the cell position was focused on S_6 by movement of the system $L_4 : S_5$, with the distance between the latter two elements fixed. The distances from the cell to L_4 and from L_4 to S_5 and S_6 can be estimated by Eq. (39) and the lens focal length, but visual adjustment is necessary unless the nodal points of L_4 are determined and used to define the distances in Eq. (39), since L_4 is not thin compared to d_2 and f. The observation may be made by viewing the image on a thin paper screen in the plane of the slit.

For a given lens and scattering volume, the angular resolution of the detecting system is determined by slit S_5 or the lens diameter, one of which will be controlling. Fig. 12 shows the angle ψ, defined as the limiting plane angle of acceptance. No ray incident on L_4 making an angle with the axis of the receiver greater than ψ can pass through S_5.

The angle ψ may be estimated by assuming a uniform scattering volume, and refraction at the air-glass interface of the thermostat. There results

$$\tan \psi = \begin{cases} \ell/2f & \text{if} \quad \ell < f(D + y)/d_1 \\ (D + y)/2d_1 & \text{if} \quad \ell > f(D + y)/d_1 \end{cases} \qquad (40)$$
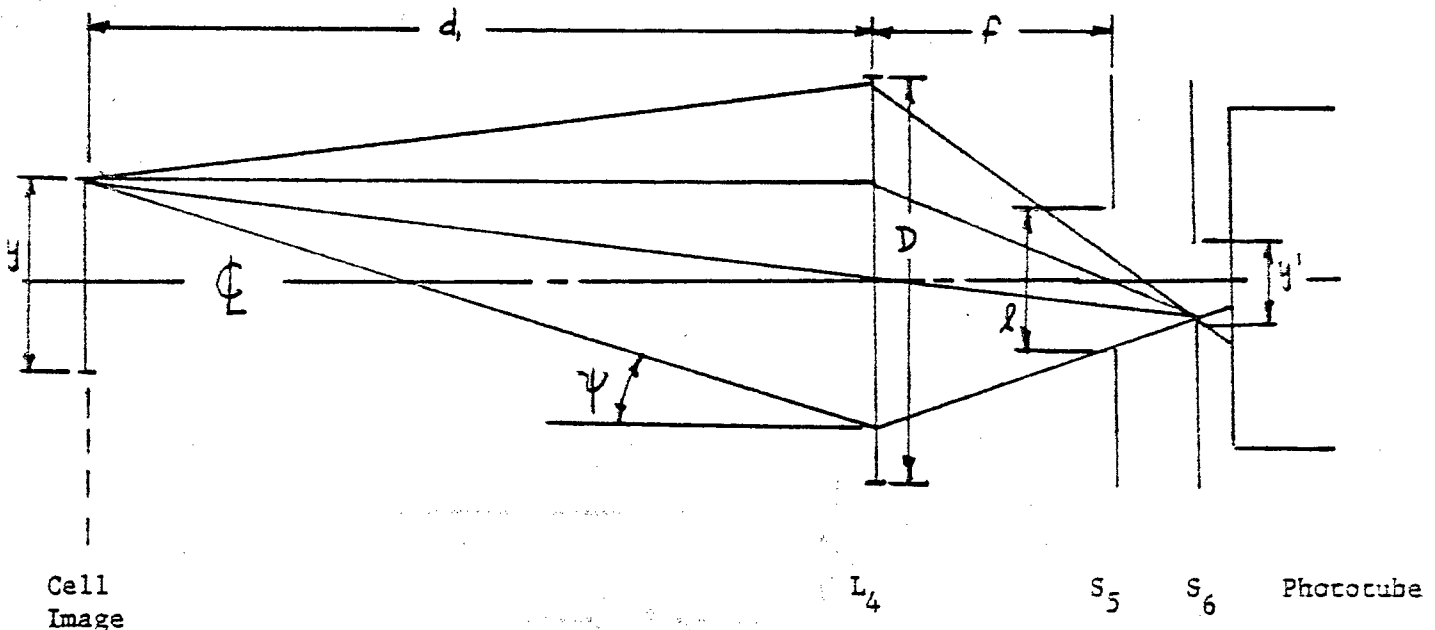
Figure 12   Detector Optics

47

Refraction can be accounted for approximately by replacing ψ with $\psi' = \psi/n$, where n is the liquid refractive index. The distance y is fixed by the dimensions of S_6 or the scattering volume in the cell. Since it is desirable not to have the detector photomultiplier see past the edges of the beam, S_6 is made to be the controlling element. In particular y', the size of S_6, is given approximately by

$$y' = nyf/(d_1 - f) \qquad (41)$$

It is important to note in Eq. (40) that if ℓ is small enough, the angle of acceptance becomes independent of the size of the scattering volume.

These detector optics and the highly collimated primary beam make it possible to use the photometer as an absolute instrument if desired. Kushner[54] has shown that the scattering volume defined by these optics is easily calculated from the geometric parameters of the system. This, combined with the observations of Hermans and Levinson[55] concerning the refraction corrections applicable when the detector does not see past the edges of the scattering volume, allows a direct correlation between the Rayleigh scattering factor and the ratio of the instrument response to the light scattered at 90° and to a section of the primary beam attenuated by a dense filter of accurately known transmittance.

The height of the scattering volume is limited by the entrance window to the thermostat. The width and depth of the scattering volume, that is, its dimensions parallel and perpendicular to the axis of the primary beam in a horizontal plane, are limited by two criteria. The volume must be small enough so that the detector will not see scattering and reflections from the entrance and exit positions on the cell wall at any angle of observation and so that deviations from uniform irradiance in the scattering volume are negligible. At present the apparatus includes a 1 x 3 mm slit at S_5 and a 1.8 x 1.8 mm slit at S_6 with S_6 209 mm from the center of the cell. These dimensions are critical since a change in one without a change in others could result in the detector photomultiplier seeing past the edges of the scattering volume or in an increased angular acceptance. This arrangement sets the angular acceptance, ψ', at about 2.7° in the vertical and 1° in the horizontal directions. These angles would both be 3° in the absence of slit S_5.

4. _Electrical design._ The photomultiplier circuit is shown schematically in Fig. 13. The dynode resistors (not shown) are sealed into the tube base by the manufacturer. Resistors R_5 prevent formation of a space charge about the anode. Resistor R_6 allows the monitoring photomultiplier tube to be operated at a lower voltage than the detector tube to reduce its noise contribution. This can be done since obtaining sufficient light at the monitor tube is never a problem. The DC power supply (John Fluke, Mfg. Co., Model 405) provides voltages adjustable continuously from 600 to 3000 volts, regulated to within 0.1% maximum deviation for a 20% change in line voltage, with less than 0.005% drift per hour.

M

D

Power
Supply

−E   −E

R6

R5   R5

Anode   Anode

Sw1   Sw2

① Sw3
②

CH   R1   R2   RH   C1

+ 200 V   Tube No. 5963

②   ①

R3   R3

R4   R4

Tuned
Voltmeter

T
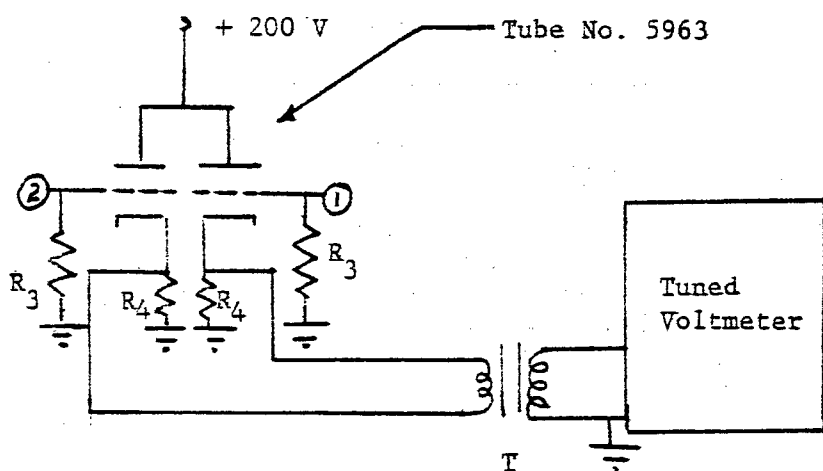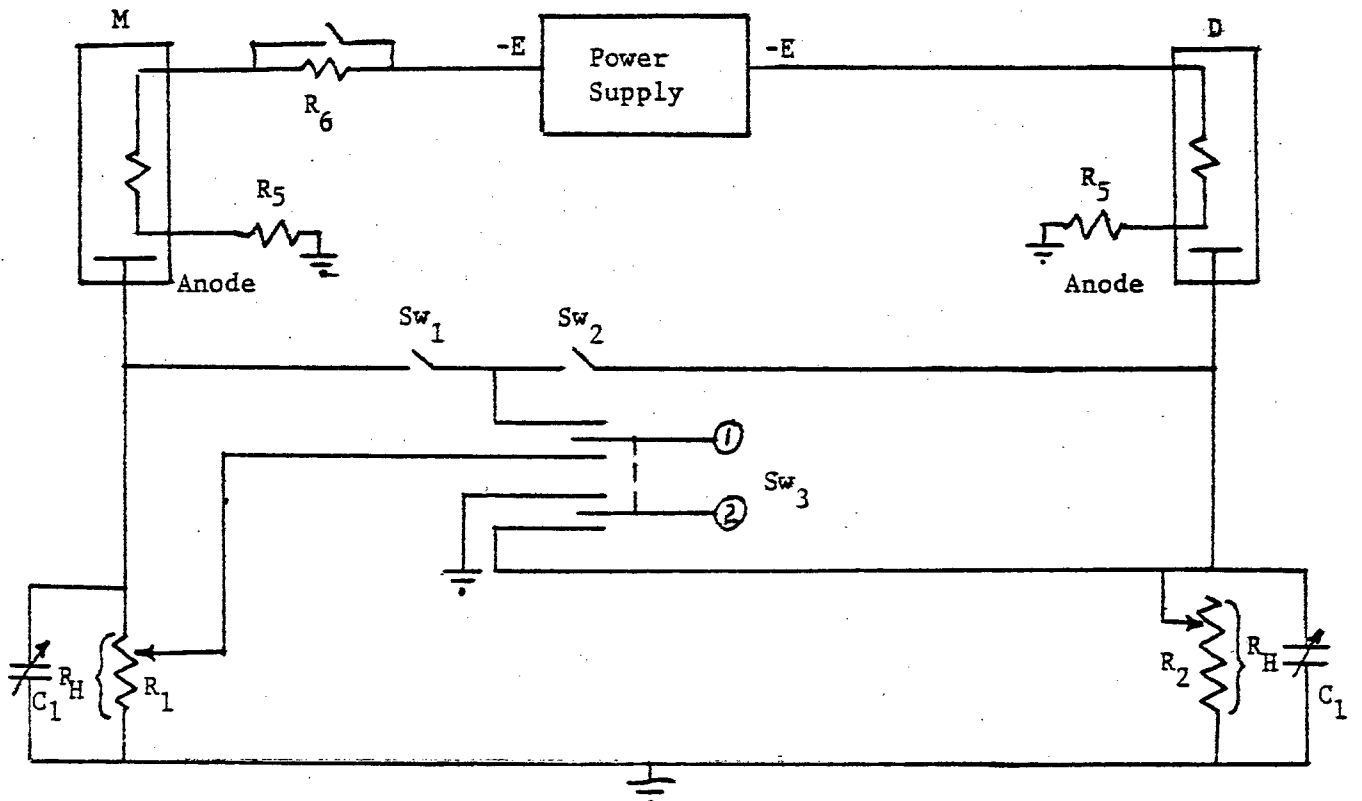
RH = 100 K

R3 = 10 M

R4 = 22 K

R5 = 100 K

R6 = 3.5 M

C1 = 18 to 200μμf

Sw1, Sw2   JBT#ST52K

Sw3, JBT#ST52P

M, D, duMont K1780

T, Triad No. G-22

Figure 13   Electronic Circuit

49

The anode photocurrents are sent to ground potential through two resistors, R_H and R_2 (normally, $R_2 = R_H$). The resistors are 10-turn model 7601 Beckman "Helipots." These potentiometers are linear to within 0.015% for readings greater than 20% of full scale, and to within 0.025% for readings greater than 5% of full scale.

The switching arrangement shown allows one to observe the voltage impressed on either R_H or R_2, or the difference between the voltages impressed on R_1 and R_2. The variable capacitors C_1 are used to shift the relative phase of the voltages in the bridge to that necessary for exact cancellation (180°). Although the photocurrents are produced in exactly this relationship, reactances in the circuit are sufficient to require compensation. The details of this adjustment are discussed below.

The signal from the bridge (points 1 and 2, Fig. 13) is sent to the grids of an impedance matching dual cathode-follower tube, type 5963. The plate voltage for this tube may be supplied by any regulated power supply, or by batteries. The signal from the cathode follower goes to the primary winding of an isolation step-up transformer (4:1) so that the differential signal is transformed into a single ended signal. This signal is then measured on a voltmeter tuned to the chopper frequency. A Hewlett-Packard model 302-A wave analyzer serves this purpose.

The wave analyzer utilizes the heterodyne principle. The incoming signal is mixed with a signal from an internal oscillator to give a signal of a fixed difference (or heterodyne) frequency to which a selective amplifier is tuned. The selective amplifier includes a crystal filter circuit of very narrow bandpass characteristic: the response attenuated by 3db at $\pm$ 3 cycles and by 80db at $\pm$ 70 cycles. The light beam is chopped mechanically so that the desired signal has a frequency of 450 cps. The 450 cps frequency is chosen so that the 60 cps pickup or its harmonics will be effectively attenuated. There is no observable signal from this source when the voltmeter is tuned to 450 cps. The signal also has a strong component at 120 cps (and harmonics) since the lamp is operated from a 60 cps power supply. An alternative to this would be to operate the lamp from a DC power supply, chopping the beam at 450 cps. This should increase the RMS signal measured on the tuned voltmeter. The lamp is presently being operated from an AC supply because the high current regulated supply required for DC operation is not readily available.

5. <u>Electronic performance</u>. The purpose of the bridge circuit is to reduce so far as possible the effect of lamp intensity fluctuations on measurement of the response due to scattering and to allow more accurate determinations of the relative photocurrent than might be possible from direct reading of a single phototube signal on a meter. If both photo tubes respond identically to fluctuations in the intensity or position of the arc, the ultimate resolution of the bridge is governed by the noise generated in the photomultipliers and by the resolution of the tuned voltmeter. The photomultiplier noise far exceeds that generated elsewhere in the circuit (amplifier noise, Johnson noise, 60 cps pickup, etc.) and can be estimated by the relationship[56]

$$(S/N)^2 = i_p{}^2/2e\Delta f(i_t + i_p) \tag{42}$$

where S/N is the signal to noise ratio, i_p and i_t are the photo current and thermonic emission at the cathode, respectively, e is the electronic charge, and Δf the bandwidth of the measuring instrument. There are two contributions to the noise given by Eq. (42): the thermonic emission and the shot noise arising from the statistical nature of the photo emission process. Eq. (42) predicts that the S/N ratio will vary with the square root of i_p for large photocurrents (intense light flux), and with i_p for very small photocurrents.

The percentage error in the bridge balance can be obtained from

$$\frac{R_1}{R_2} = \frac{I_D}{I_M} \left\{ 1 \pm \frac{\delta V}{v_D} \right\} \tag{43}$$

where I_D and I_M are the detector and monitor photocurrents, respectively, and v_D is the voltage impressed on R_2, of the order of 1 mv. The uncertainty in the signal at the null balance of the bridge is given by δV. If the noise from the phototubes were sufficiently small, δV would be determined by the resolution of the measuring instrument, of the order of 1 μ volt for the tuned voltmeter. In fact, if the phototube impressed some constant voltage across R_H and R_2, the voltmeter resolution would still determine δV. There are, however, low-frequency fluctuations in the noise level which are partially damped out by the meter, but which still make it difficult to determine the exact null point. Fig. illustrates this problem schematically. The voltage across the bridge is plotted as a function of the resistor ratio R_2/R_2. The desired null balance occurs when $R_1/R_2 = I_D/I_M$. The amplitude fluctuations in the noise level, however, allow one to come only within δV of the desired balance.
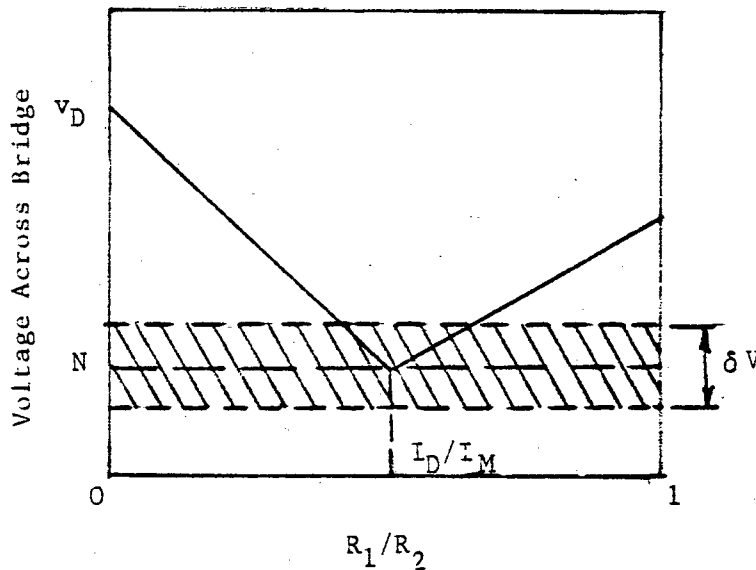
Figure 14   Effect of Noise on Null Sensitivity

The S/N ratio is useful, however, in the initial evaluation of different photomultipliers since the stability of the noise signal may be expected to be proportional to S/N. Eq. (42) indicates steps one can take to improve this ratio. The band pass of the instrument should be as narrow as possible and the thermonic emission should be as small as possible relative to the photoemission at the cathode. To meet the former requirement the tuned voltmeter is used. The latter factor depends on the characteristics of the cathode surface and conditions of use (temperature and light level). Eq. (42) indicates that S/N should be independent of E, the tube voltage, since the cathode currents, i_p and i_t, are presumably insensitive to E. In fact, though, a slight increase in S/N is observed as E decreases. Thus, one can decrease E to the point where the resolution or noise level in the voltmeter becomes a factor in gaining the optimum sensitivity.

Magnetic shielding is helpful in maintaining a high S/N ratio, since a loss of electrons by magnetically induced deflection between the cathode and first dynode will reduce S/N. It is possible to reduce i_t by cooling the phototube, but this has not been done as yet, due to the inconvenience of the operation. Such a procedure would only be of value when viewing weakly scatter systems, where i_p is less than the room temperature value of i_t.

6. <u>Choice of the photomultiplier tube.</u> Two photomultiplier tubes were examined, the RCA 1P21 and the duMont K1780. The K1780 has a cathode sensitivity of about 60 μ amp/lumen compared to about 40 μ amp/lumen for the 1P21. The K1780 also has greater thermonic emission than the 1P21, however. The relative importance of the thermonic emission varies with the incident light intensity, since i_t remains fixed and i_p increases as the light intensity increases. Conversely, as the light intensity decreases, i_t will become the dominant term in the denominator of Eq.   . The minimum light level that can be observed is fixed by the sensitivity of the cathode surface and the level of the thermonic emission, so long as the voltmeter is capable of measuring the signal produced by the thermonic emission. The 1P21 and the K1780 may be compared on this basis. Some representative response characteristics for the light level corresponding to observation of scattering through 90° from benzene are shown below.

Tube	E	v_D	N_D	n_D	v_D/N_D	v_D/n_D
1P21	1000 V	6.6 mV	0.10 mV	0.035 mV	66	220
1P21	800	1.8	0.020	0.010	90	180
1P21	600	0.24	0.004	0.001$_5$	60	160
K1780	1400	3.0	0.040	0.015	80	200
K1780	1100	0.48	0.005	0.002	100	240
K1780	900	0.11	0.001	-----	110	---

The response is expressed as the voltage impressed across R_H, v_D being the RMS contribution from the photocurrent, and N_D and n_D the total tube noise and the thermonic component, respectively. The ratio v_D/n_D is approximately independent of E, as epxected, and indicates that the weakest light level for which the photomultiplier will give a usable signal is about the same for both tubes. The lower limit of detection, fixed by the cathode sensitivity and the thermonic emission, is about 200 times less than the scattering observed from benzene at 90° with the ME/D lamp as the source and both phototubes at room temperature. In addition, the low frequency fluctuations in the phototube noise are less severe with the K1780. Thus, the present apparatus employs the K1780 for both monitor and detector.

7. Choice of the light source. Two mercury vapor lamps were examined: the 250 watt Mazda (Metropolitan Vickers) ME/D and the 100 watt HA4 (General Electric). The former source produces a primary beam about 12 times more intense than the latter if the comparison is made for beams collimated such that θ is about 30' in the vertical direction. Unfortunately, however, the ME/D also exhibits much greater fluctuations in the arc position and intensity than does the HA4, and apparently has a relatively short lifetime (average lifetime given as 500 hr. in lamp specifications). Some of the loss in intensity incurred when using the HA4 can be recovered by sacrifice in beam collimation. Thus, the beam intensity can be increased by a factor of two if ϕ is allowed to change from 38' to 2°10' in the vertical direction. The Me/D is used in the present apparatus since it will allow measurements of scattering from materials which give only one hundredth the scatter from benzene at 90°. If the use of the instrument is to be confined to strongly scattering polymer solutions, however, it appears the HA4 would be a more suitable choice in view of its longer lifetime and better stability.

8. Performance. Several aspects of the performance have already been discussed, including the divergence of the primary beam, the angular acceptance of the detector, and the phototube behavior. In this section some measurements of a null balance and its behavior will be considered.

The bridge circuit effectively removes the effects of long term drifts in the lamp intensity, but the effect of rapid fluctuations in the intensity and position of the arc are uncertain. This effect has been minimized by keeping the optical path lengths from L_3 to the cell and to the monitor phototube as nearly alike as possible, but complete compensation has probably not been accomplished. Further study is necessary to clarify this point. In any case, the effect is now small enough so that it constitutes no severe problem in attaining an accurate null point. Another source of error is the effect of temperature on the beam splitter, Pr_1. The amount of light reflected to the monitor may vary by as much as 5% per 1°C shift in the prism temperature. This is apparently due to the closeness of the refractive indices of the glass and cement. A slight shift in either caused by the change in temperature is sufficient to cause a marked change in the amount of light reflected from the interface, since this depends on the square of the difference of the refractive indices. This drift is unfortunate but is no real problem since room temperature variations are negligible during any single series of measurements, and the ratio of the intensities determined at any two angles is independent of this effect.

53

The table below indicates the reproducibility of the null balance readings. These readings were determined with E = 1100 volts for the magnetically shielded detector photomultiplier, and with the ME/D lamp as the light source.

Source	Photocurrent	Root-mean-square deviation from mean reading
Benzene 90° scatter	0.0050μ amp	0.3%
Attenuated benzene scatter	0.00060	1 %
Attenuated benzene scatter	0.00012	3 %
Attenuated benzene scatter	0.00007	8 %

These figures indicate satisfactory performance of the bridge circuit.

The bridge circuit includes two variable capacitors which have impedance much greater than the helipots. As mentioned above, these are necessary to balance the out-of-phase portion of the signal. A complete network analysis of the bridge has not been done, but the results for some cases included in Appendix II, are useful at this point. It is shown there that if the out-of-phase imbalance is caused by some capacitive shunt to ground, then it may be corrected by suitable adjustment capacitors shunted across the phototubes. The calculation indicates that this setting should be independent of the ratio R_1/R_2, i.e. of the helipot setting. Another limiting case occurs when only inductance in the helipots is of importance. This result indicates that such an effect ought to be corrected for automatically, since the correction requires the ratio of the two inductances to vary as the ratio R_1/R_2 and this should be close to the actual situation in the helipots.

In practice, one adjusts the capacitors so that the minimum voltage at null balance is equal to that impressed on the bridge by the phototube noise (this can be determined at 500 cps where the main signal is greatly attenuated and the signal left is due to the phototube noise). This adjustment increases the sharpness of the null, although it has a negligible effect on the exact position of the null. The capacitor adjustment is not independent of the helipot setting, however, suggesting that there must be sources of the phase imbalance other than those included in the simplified network analyses we have worked out. The observation that the value of R_1/R_2 is only negligibly affected by the capacitor adjustment is taken as an indication that the resistor ratio is truly the ratio of the photocurrents, at least within the experimental error of determining R_1/R_2.

C. Conclusion

The light scattering photometer described is capable of determining the relative scattering to within 0.3% from materials ranging in scattering power from benzene to strongly scattering polymer solutions. In addition, depolarization measurements and the scattering from much more weakly scattering liquids may be determined with some loss in precision. The scattering volume is illuminated by a highly collimated beam of light, and the detector has a low angular acceptance, making the instrument useful where high angular resolution is necessary. The temperature of the scattering volume may be held constant over a wide range.

D. Future Work

The completion of the light scattering photometer brings the immediate project to a conclusion, but since the instrument was constructed with certain studies in mind, a brief note of some anticipated investigations is pertinent. In general terms, the future work will be concerned with measurements on the thermodynamic and configurational properties of polymers in solution for comparison with theoretical predictions. In particular, the effect of molecular weight, temperature, and molecular weight distribution on the second virial coefficient and on the molecular configuration will be studied. These investigations will be made on polymers of various structures, i.e., flexible linear and branched chains, stereoregular molecules, and stiff chains. It is expected that these data will also be useful in suggesting possible directions for new developments.

IV. Viscosity - Molecular Weight Relationship for Poly-(Vinyl Acetate) — R. E. Kerwin and H. Nakayasu

A. Introduction

The intrinsic viscosity - molecular weight relationship for linear Poly-(vinyl acetate) in methyl ethyl ketone has been studied by a number of investigators[57-60]. All of these studies deal principally with polymers of molecular weight higher than 100,000 with a few measurements of lower molecular weight material covered in references 59 and 60. In connection with other work undertaken in this laboratory, it has become necessary to know which, if any, of these published relationships remain valid in the region of lower molecular weights. Accordingly, we have carried out viscosity and light scattering measurements on this system using polymer fractions of molecular weight from 6,000 to 30,000.

B. Experimental

The polymer labeled PD-2 in Table VII is a linear, low conversion (14.8%), low molecular weight poly-(vinyl acetate) prepared in bulk at 30°C by photo-polymerization of vinyl acetate with α,α'-azodiisobutyronitrile photosensitizer (.289 moles/liter) and acetaldehyde chain transfer agent (.233 moles/mole of monomer; chain transfer constant C = 0.02). This material was fractionated at 30° from a 2% solution in benzene using ligroin (solvent naphtha) as the non-solvent[61]. Polymer RKI was prepared similarly except that chloroform was used as chain transfer agent (1.15 moles/mole of monomer; C = 0.015) and the polymerization proceeded to 36% conversion. This polymer was fractionated at 28°C from a 4.4% solution in toluene using n-hexene as non-solvent. The high chain transfer constants of these two chain transfer agents insured low molecular weight products.

The methyl ethyl ketone used as solvent in the viscosity and light scattering measurements was purchased as reagent grade and further purified by drying over "Drierite", distilling, and storing in dark bottles at 0°C.

The light scattering measurements were made at 25°C with a Brice-Phoenix light scattering photometer and a cylindrical cell with flat entrance and exit windows. The apparatus was calibrated with respect to a 0.75% solution of "Cornell Polystyrene" in methyl ethyl ketone for which the absolute excess scattering at right angles (Rayleigh's ratio) for unpolarized 5416A° light was taken[62] as 632×10^{-6}. Measurements were made on the solvent and four concentrations of each fraction and at at least 7 angles including 45°, 90° and 135°. These concentrations ranged from 0.7% to 2.0% for the highest molecular weight solutions and from 3.0% to 9.8% for the lowest molecular weight solutions. Fraction PD-2-12A was measured in a small semi-octagonal cell since only 1.5 grams were available. All results were treated according to the method of Zimm[63] to determine the weight average molecular weight, $\overline{M}_w$. Fig. 15, the Zimm plot for fraction PD-2-12A, serves as an illustration. The refractive index increment used in these calculations was 0.080 cc/g, the value reported by Shultz[57] and by Matsumoto and Ohyanagi[60]. The concentrations of all solutions were determined by weighing freeze-dried polymer directly into volumetric flasks and diluting to volume at known temperature. The glassware used to contain or transfer the solutions for light scattering was rinsed in acetone distilled to remove all traces of dust. The solutions were rendered dust-free by centrifuging for one hour at 14,000 RPM in a "Servall" SS-1 centrifuge.

Viscosity measurements were carried out with a Cannon-Ubbelohde semi-micro viscometer, model A 258. No kinetic energy correction was applied to the data since the maximum correction factor, calculated from the dimensions of the viscometer and the solvent flow time, amounted to only 0.03%.

For polymer PD-2 four concentrations were measured for each fraction, each being prepared separately to avoid dilution error in the viscometer. The ranges of concentration employed were 1 to 3 g/100 cc. for the highest [η] and 1 to 10 g/100 cc. for the lowest. Solutions were
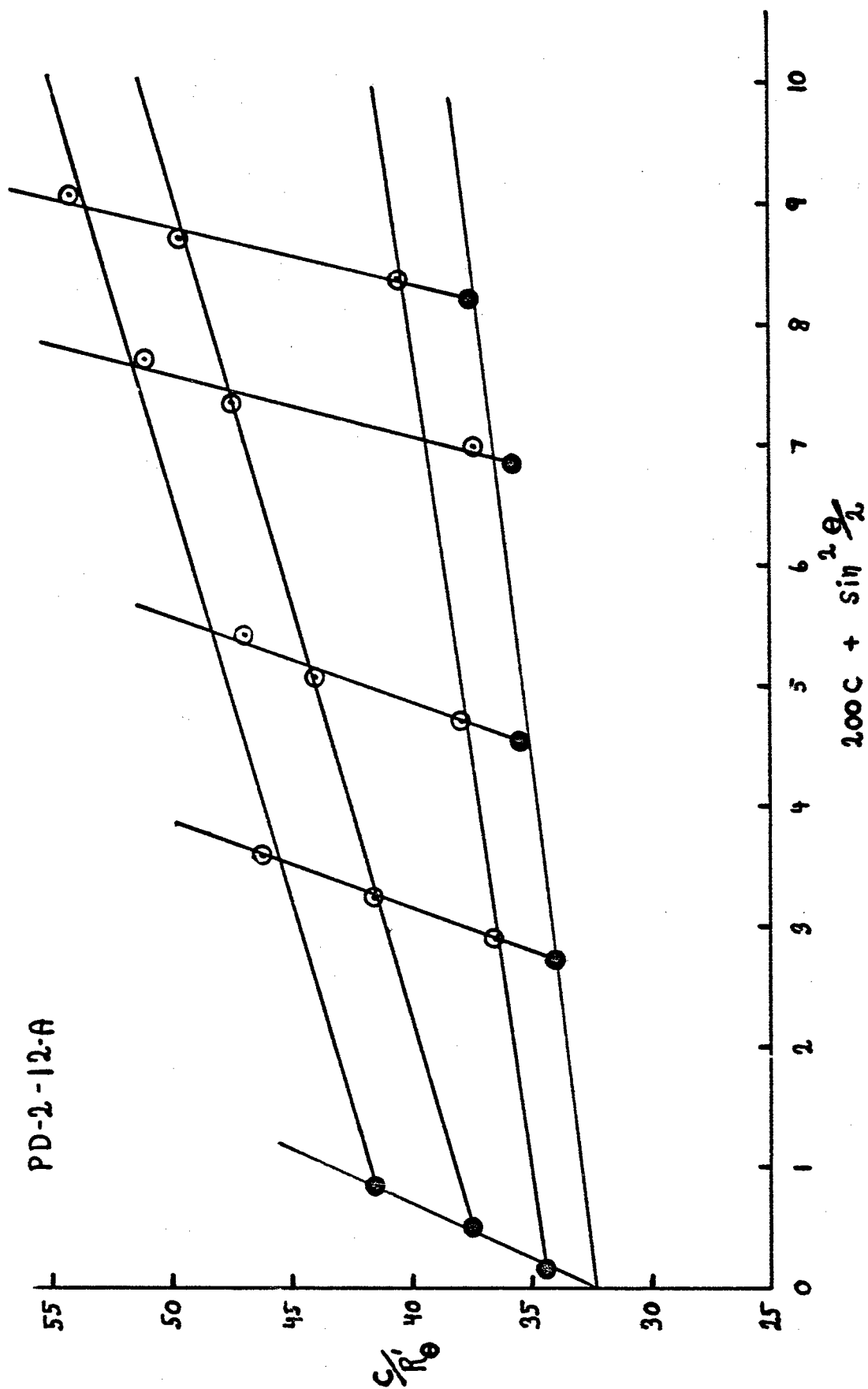
Figure 15 Zimm Plot, Poly-(vinyl acetate), Fraction PD-2-12A, in Butanone

57

prepared on a weight/weight basis and concentrations were converted to the weight/volume basis by using the specific gravity of solvent at the temperature of measurement. For polymer RK-1 the solutions were prepared on a weight/volume basis, as was always the case for light scattering.

The intrinsic viscosities were determined by plotting the data according to the empirical relationships of Huggins:[64]

$$\eta_{sp}/C = [\eta] + k_1[\eta]^2 C$$

$$(\ln \eta_{rel.})/C = [\eta] - k_2 [\eta]^2 C$$

$$k_1 + k_2 = 1/2$$

i.e. $[\eta]$ for each fraction was determined from the common intercepts of linear η_{sp}/C vs. C and $(\ln \eta_{rel.})/C$ vs. C plots. All experimental points fit these lines within 2% and all specific viscosities fell within the range 0.1 - 0.9. Within the same 2% experimental error it was found empirically that $[\eta]$ 25°C = $[\eta]$ 35°C for this system.

C. Results and Discussion

The intrinsic viscosities and light scattering molecular weights determined in this work are listed in Table VII. The light scattering dissymmetry ratios and the viscometric Huggins' constants, k_1, are also listed.*

Table VII

Fraction	$[\eta]$ cm³/g	k_1	$\overline{M}_W$	R'45°/R'135°
PD-2-2A	19.3	.45	28,430	1.01
PD-2-3A	16.0	.50	22,170	1.05
PD-2-5A	12.6	.54	15,500	1.01
PD-2-6A	11.3	.68	13,690	1.07
PD-2-8B	9.75	.57	9,940	.98
PD-2-9A	9.08	.53	9,730	1.38
PD-2-12A	6.72	.73	6,050	1.14
RK-1-6	9.10	.55	9,710	1.03
RK-1-11	5.96	.75	6,550	1.18

*Four measurements on poly-(vinyl acetate) prepared by other procedures resulted in anomalously high dissymmetry ratios and have been omitted.

58

These data are plotted with those from references 57-60 on the usual double logarithmic coordinates in Fig. 16. The published viscosity-molecular weight relations obtained in the earlier work are listed below and the pertinent data are collected in Appendix III.

Shultz[57] $\text{Log } [\eta] = -1.871 + 0.71 \text{ Log } \bar{M}_w$

Elias and Patat[60] $\text{Log } [\eta] = -1.377 + 0.62 \text{ Log } \bar{M}_w$

Matsumoto and Ohyanagi[61] $\text{Log } [\eta] = -1.9706 + 0.71 \text{ Log } \bar{M}_w$

The straight lines determined by the first two equations are shown in Fig. 14. The line corresponding to the equation of Matsumoto and Ohyanagi lies slightly below all of the existing data including their own. A good fit to their data is given by a line of the same slope but with $K = 1.135 \times 10^{-2}$ instead of $K = 1.07 \times 10^{-2}$.

Shultz's equation was derived as the best fit to his data and those of Howard which together cover the molecular weight range from 246,000 to 3,460,000. From the graph it may be readily seen that except for the point for RK-1-11 the results of this present work agree within 2% with the low molecular weight extrapolation of Shultz's line.

It is evident from the figure that the line corresponding to the equation of Elias and Patat deviates by about 25% from the very low molecular weight data of this work and by about 15% from the very high molecular weight data of Shultz. In addition to their light scattering data, which is presented in Fig. 16, Elias and Patat considered sedimentation-diffusion molecular weight measurements for the range $17,000 \leq M_{s,D} \leq 1,200,000$ in deriving their equation. Of their eight experimental points for $\bar{M}_w$ from light scattering the lowest six agree well with Shultz's line. Of the remaining two, one, the point for $\bar{M}_w = 1.2 \times 10^6$, may be considered doubtful as the polymer was poorly fractionated, $\bar{M}_w/\bar{M}_n$ being listed by the authors as 3.00. Light scattering and sedimentation-diffusion molecular weights determined on duplicate samples by Elias and Patat are in agreement within experimental error; hence it is the points at lower molecular weight, for which only sedimentation-diffusion data are available, which cause their divergence from other studies.

The data of Matsumoto and Ohyanagi fall 12% below Shultz's line and generally below all previous data. There are two possible sources of this disparity, their use of whole polymer and their polymer preparative procedure. The authors themselves consider the fact that their polymer is not fractionated and arrive at the conclusion that the measured viscosity for their heterogeneous polymer ($\bar{M}_w/\bar{M}_n = 2.00$) should be 5% lower than $[\eta]$ for a homogeneous fraction of the same $\bar{M}_w$. (cf. Table VII and discussion, reference 60. It may be that their method of preparation of poly-(vinyl acetate), involving as it does two precipitations in water and finally boiling in water, brings about a significant amount of hydrolysis. This would lead to the presence of species other than poly-(vinyl acetate) in their solutions.
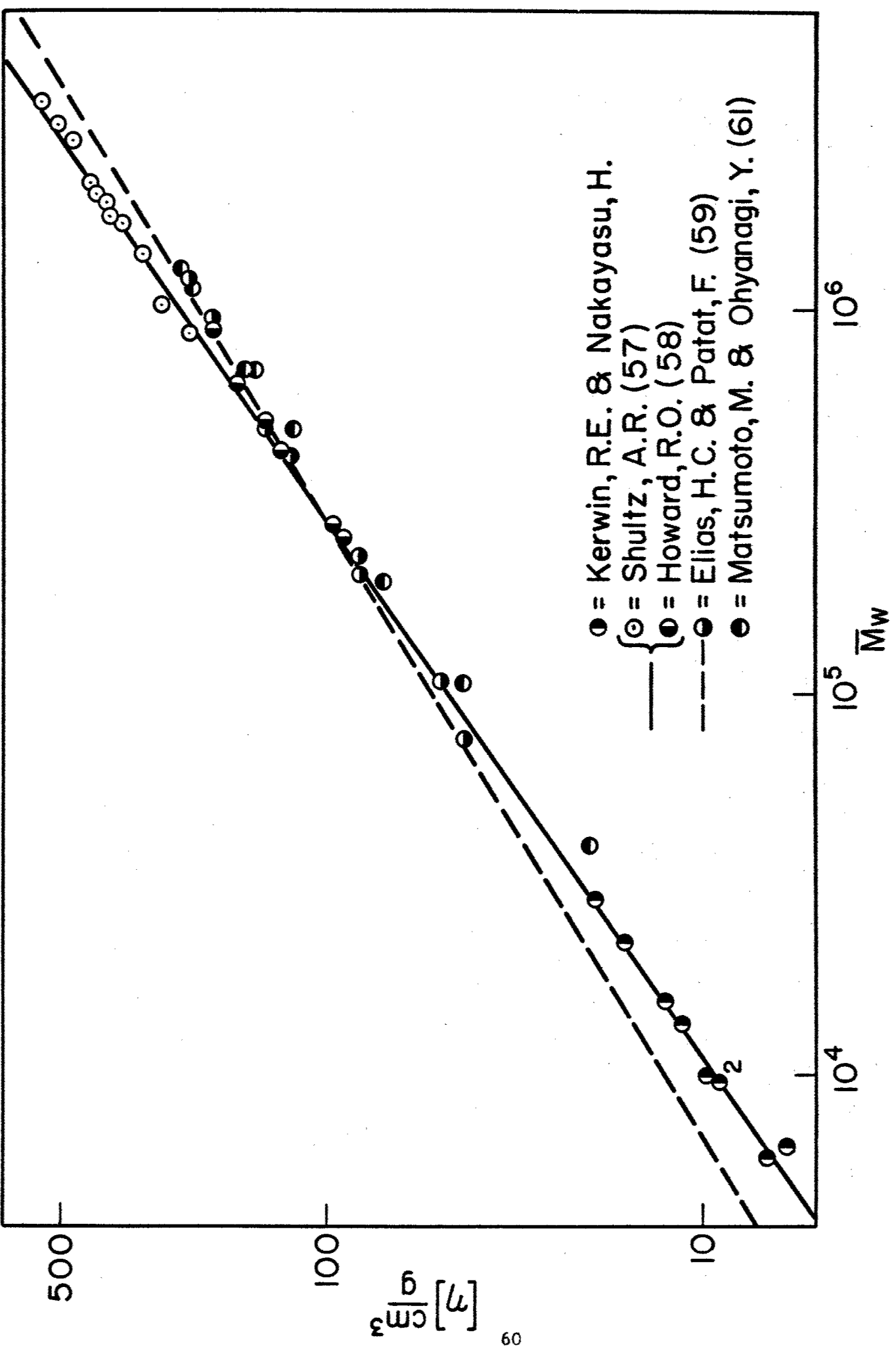
Figure 16 Intrinsic Viscosity, Poly-(vinyl acetate) in Butanone

60

We note, parenthetically, that the data of Long[65] for the viscosity-molecular weight relationship for poly-(vinyl acetate) in <u>benzene</u> fit Shultz's equation cited here well within experimental error. This data has also been included in Appendix III for ease of reference.

D. Conclusion

Taking into account all the recorded light scattering data, with due consideration for the relative merits of the data, as discussed above, we conclude that the viscosity-molecular weight relationship for linear poly-(vinyl acetate) in methyl ethyl ketone at 25°C valid for molecular weights ranging from 6×10^3 to 4×10^6 is given by Shultz's equation:

$$\log [\eta] = -1.871 + 0.71 \log \bar{M}_w$$

or

$$[\eta] = 1.346 \times 10^{-2} \bar{M}_w^{0.71} cm^3/g.$$

Further experiments of similar nature are being carried out on poly-(vinyl acetates) of still lower molecular weight.

Appendix I

Evaluation of w_u — Some details concerning the determination
of w_u are noted here. In performing the integrations indicated in Eq. (39),
we consider in turn each of the eight double integrals obtained in multi-
plying the successive terms of w, as defined in Eq. (34), by $f(x,u)f(y,u)$.
The first four integrals turn out to be identical and expressible in terms
of the forms

$$\int_0^1 x^{1/2} e^{-ux} dx$$

and

$$\int_0^1 x^{1/2} e^{ux} dx,$$

which upon integration by parts yield expressions containing the irreducible
integrals $erf(u^{1/2})$ and $\epsilon(u^{1/2})$.

The last four double integrals in w_u are more difficult to
evaluate but happily are also identical, all being equivalent to

$$\int_0^1 \int_0^1 (x + y)^{1/2} f(x,u) f(y,u) dx dy$$

After substitution of a new variable $v = x + y$ and multiplication of the
factors in this integral, the evaluation of the resulting nine double
integrals proceeds as before to yield results again in terms of error
functions and ϵ.

The final result, Eq. (40), was checked by expansion of
$w_u u^4 P^2 (u)$ in series. When terms in like powers of u were collected, the
obvious requirements were met that coefficients of the terms in u^0
through u^3 vanish and that the coefficient of the u^4 term be w_0.

The integral ϵ (x) — This function was apparently first tabulated
by Dawson[26] in the interval $0 \le x \le 2$; and the compilation was later
corrected and extended $x = 4$ for intervals of 0.01 by Terrill and Sweeney.[23]
More recently tables have been published[27] of the related function

$$e^{-x^2} \int_0^x \exp(t^2) dt$$

which is more convenient for interpolation. The asymptotic series

$$\epsilon(x) \approx \frac{\exp(x^2)}{2x} \left[1 + \frac{1}{2x^2} + \frac{3.1}{(2x^2)^2} + \frac{5.3.1}{(2x^2)^4} + \cdots \right]$$

is useful at high values of x, but physically realizable situations would not ordinarily fall in the range of applicability. The optimum number of terms n (the point at which two successive terms of equal magnitude appear is given by

$$4n = 1 + 2x^2 + (1 - 4x^2 + 4x^4)^{1/2} .$$

For values of x of 2, 3, and 4, the sum of the first four terms of the series is in error by amounts of -0.35, -0.21, and -0.014 per cent, respectively.

Appendix II

The network analysis is based on the following idealization of the bridge circuit.
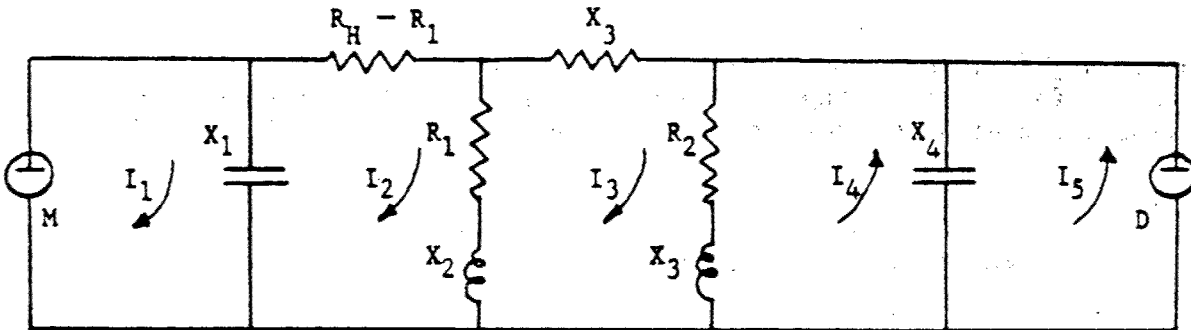
X_3 is immediately assumed to be very large relative to the other impedances since it represents the impedance of the detection system (between points 1 and 2 in figure 13). X_1 and X_4 represent capacitive shunts to ground across the helipots. They could be caused by the capacitance of the lines, switches, etc., or they could be caused by a capacitor placed in the circuit to balance out the effect of the former. X_2 and X_3 represent inductance in the helipot windings. Thus, X_2 will vary with R_1. Applying Kirchoff's law for loops 2, 3, and 4, there results (i is the square root of -1)

$$[R_H + i(X_2 - X_1)]I_2 + (-R_1 - iX_2)I_3 + 0 = I_2 + X_2$$

$$(-R_1 - iX_2)I_2 + [R_1 + R_2 + i(X_2 + X_3)]I_3 + (R_2 + iX_3)I_4 = 0$$

$$0 + (-R_2 - iX_3)I_3 + [-R_2 + i(-X_3 + X_4)]I_4 = I_5 iX_4$$

Solving this system of equations for I_3, one obtains

$$I_3 D \overline{D} = \overline{D} \begin{vmatrix} R_H + i(X_2 - X_1) & -I_1 iX_1 & 0 \\ -R_1 - iX_2 & 0 & R_2 + iX_3 \\ 0 & I_5 iX_4 & -R_2 - i(X_3 - X_4) \end{vmatrix}$$

64

where

$$D = \begin{vmatrix} R_H + i(X_2 - X_1) & -R_1 - iX_2 & 0 \\ -R_1 - iX_2 & R_1 + R_2 + i(X_2 + X_3) & R_2 + iX_3 \\ 0 & -R_2 - iX_3 & -R_2 + i(-X_3 + X_4) \end{vmatrix}$$

and $\overline{D}$ is the complex conjugate of D.

A complete solution for I_3 has not been done, but one can obtain I_3 for some particular cases of interest.

Case I. Let inductances X_2 and X_3 be very small compared to other impedances. The bridge will be balanced when both the real and imaginary parts of I_3 vanish. The imaginary part will vanish when

$$X_4/X_1 = R_2/R_H$$

Substitution of this result into the real part of I_3 shows that the real part will vanish when

$$R_1/R_H = I_5/I_1$$

which is the desired null point.

Case II. Let capacitances X_1 and X_4 be very large compared to the impedances. A similar procedure as outlined in Case I shows the imaginary part will vanish when

$$X_2/X_3 = R_1/R_2$$

and that the real part will vanish when

$$R_1/R_2 = I_5/I_1$$

Appendix III

Intrinsic Viscosity of Poly-(vinyl acetate) in Butanone

Shultz [57]		Howard [58]		Long [65] (in benzene)	
$[\eta]$ cm^3/g	$\overline{M}_w$	$[\eta]$ cm^3/g	$\overline{M}_w$	$[\eta]$ cm^3/g	$\overline{M}_w$
573	3,460,000	200	890,000	560	3,580,000
520	3,020,000	172	640,000	497	2,660,000
473	2,740,000	146	510,000	429	2,280,000
430	2,150,000	132	430,000	371	1,840,000
412	1,990,000	97	280,000	281	1,140,000
389	1,910,000	91	260,000	250	991,000
377	1,740,000			177	654,000
351	1,670,000			137	438,000
310	1,390,000				
276	1,020,000				
231	870,000				

Elias and Patat [59]		Matsumoto and Ohyanagi [60]	
$[\eta]$ cm^3/g	$\overline{M}_w$	$[\eta]$ cm^3/g	$\overline{M}_w$
234	1,200,000	243	1,268,000
201	930,000	237	1,210,000
146	490,000	229	1,136,000
125	420,000	162	695,000
82.5	230,000	159	690,000
83	205,000	122	485,000
50	107,000	70.2	197,000
43	76,000	44.0	106,000
		20.0	40,000

BIBLIOGRAPHY

1. P. Debye, J. Appl. Phys. $\underline{51}$, 18 (1947).

2. B. H. Zimm, R. S. Stein, and P. Doty, Polymer Bull. $\underline{1}$, (1945).

3. M. Fixman, J. Chem. Phys. $\underline{23}$, 2074 (1955).

4. B. H. Zimm, J. Chem. Phys. $\underline{16}$, 1093 (1948).

5. W. G. McMillan and J. E. Mayer, J. Chem. Phys. $\underline{13}$, 276 (1945).

6. A. C. Albrecht, J. Chem. Phys. $\underline{27}$, 1014 (1957).

7. P. J. Flory, J. Chem. Phys. $\underline{17}$, 1347 (1949).

8. P. J. Flory and W. R. Krigbaum, J. Chem. Phys. $\underline{18}$, 1086 (1950).

9. P. J. Flory and A. M. Bueche, J. Polymer Sci. $\underline{27}$, 219 (1957).

10. E. F. Casassa, J. Chem. Phys. $\underline{27}$, 970 (1957).

11. E. F. Casassa and H. Markovitz, J. Chem. Phys. $\underline{29}$, 493 (1958).

12. E. F. Casassa, J. Chem. Phys. $\underline{31}$, 800 (1959).

13. See for example, J. O. Hirschfelder, C. F. Cutiss, and R. B. Bird, Molecular Theory of Gases and Liquids (John Wiley & Sons, Inc., New York, 1957) p. 891 ff.

14. B. H. Zimm, J. Chem. Phys. $\underline{14}$, 164 (1946).

15. M. Fixman, J. Chem. Phys. $\underline{23}$, 1656 (1955).

16. H. C. Brinkman and J. J. Hermans, J. Chem. Phys. $\underline{17}$, 574 (1949).

17. W. H. Stockmayer, J. Chem. Phys. $\underline{18}$, 58 (1950).

18. J. G. Kirkwood and R. J. Goldberg, J. Chem. Phys. $\underline{18}$, 54 (1950).

19. J. J. Blum and M. F. Morales, J. Chem. Phys. $\underline{20}$, 1822 (1952).

20. See H. E. Stanley, Thesis, Massachusetts Institute of Technology (1949).

21. E. F. Casassa and I. H. Billick, J. Am. Chem. Soc. $\underline{78}$, 1377 (1957).

22. Tables of the Error Function and Its Derivatives (U. S. Government Printing Office, Washington, D. C., 1954).

23. H. M. Terrill and L. Sweeny, J. Franklin Inst. 237, 495 (1944); 238, 220 (1944).

24. J. J. Hermans, Rec. Trav. chim. 68, 859 (1949).

25. H. Benoit and M. Goldstein, J. Chem. Phys. 21, 947 (1953).

26. H. G. Dawson, Proc. London Mathematical Soc. 29, 521 (1898).

27. B. Lohmander and S. Rittsten, K. Fysiogr. Salsk. Lund. Forhandl, 28, 45 (1958).

28. P. J. Flory and T. G Fox, Jr., J. Am. Chem. Soc. 73, 1904 (1951).

29. P. J. Flory, J. Chem. Phys. 17, 1347 (1949); P. J. Flory and W. R. Krigbaum, ibid. 18, 1086 (1950).

30. T. A. Orofino and P. J. Flory, J. Chem. Phys. 26, 1067 (1957).

31. P. J. Flory, Principles of Polymer Chemistry, Cornell University Press, Ithaca, New York (1953), Chapter XIV.

32. T. G Fox, to be published.

33. T. G Fox, Jr., and P. J. Flory, J. Am. Chem. Soc. 73, 1909 (1951).

34. P. J. Flory, O. K. Spurr, Jr., and D. K. Carpenter, J. Polymer Sci. 27, 231 (1958).

35. W. R. Krigbaum and P. J. Flory, J. Am. Chem. Soc. 76, 3758 (1954).

36. T. G Fox and P. J. Flory, J. Phys. and Colloid Chem. 53, 197 (1949).

37. T. Kawai and R. Naito, J. Applied Polymer Sci. 3, 232 (1960).

38. C. Rossi, V. Bianchi and E. Bianchi, Makromol. Chem. 41 31 (1960).

39. P. J. Flory and T. G Fox, J. Am. Chem. Soc. 73, 1904 (1951); ibid. 1909 1915.

40. P. J. Flory, J. Chem. Phys. 17, 303 (1949).

41. P. J. Flory, Principles of Polymer Chemistry, Cornell University Press, Ithaca, New York (1953).

42. T. A. Orofino and P. J. Flory, J. Chem. Phys. 26, 1067 (1957).

43. P. J. Flory, O. K. Spurr, Jr., and D. K. Carpenter, J. Polymer Sci. 27, 231 (1958).

44. P. Outer, C. I. Carr and B. H. Zimm, J. Chem. Phys. 18 830 (1950).

45. T. G. Fox, et al. to be published.

46. T. G Fox, et al. to be published.

47. W. R. Krigbaum and P. J. Flory, J. Polymer Sci. 11, 37 (1953).

48. D. C. Pepper, Sci. Proc. Roy. Dublin Soc., 25, 239 (1951).

49. D. McIntyre and M. C. Doderer, J. Res. Nat. Bur. Std., 62 153 (1959).

50. S. Katz, private communication.

52. H. Sheffer and J. Hyde, Can. J. Chem. 30, 817 (1952).

53. E. F. Casassa and S. Katz, J. Polymer Sci. 14, 385 (1954).

54. L. Kushner, J. Opt. Soc. Am. 44, 155 (1954).

55. J. J. Hermans and S. Levinson, J. Opt. Soc. Am. 41, 460 (1951).

56. R. Engstrom, J. Opt. Soc. Am. 37, 420 (1947).

57. A. R. Shultz, J. Am. Chem. Soc. 76, 3422 (1954).

58. R. O. Howard, Ph.D. Thesis, Massachusetts Institute of Technology Cambridge, Massachusetts, 1952.

59. H. G. Elias and F. Patat, Makromol. Chem. $\underline{25}$, 13 (1958).

60. M. Matsumoto and Y. Ohyanagi, J. Polymer Sci. $\underline{46}$, 441 (1960).

61. Technical Report No. 3, Office of Naval Research, Contract Nonr-3693(00), February 29, 1960.

62. C. I. Carr, Jr., and B. H. Zimm, J. Chem. Phys. $\underline{18}$, 1616 (1950).

63. B. H. Zimm, J. Phys. and Colloid Chem. $\underline{52}$, 260 (1948); J. Chem. Phys. $\underline{16}$, 1093, 1099 (1948).

64. M. L. Huggins, J. Am. Chem. Soc., $\underline{64}$, 2716 (1942).

65. V. C. Long, Ph.D. Thesis, University of Michigan, Ann Arbor, Michigan, 1958.

PART II - MOLECULAR MOBILITY AND MECHANICAL BEHAVIOR OF MACROMOLECULES

I. Structural Factors Affecting Flow in Macromolecular Systems — V. R. Allen and T. G Fox

A. Introduction

The ever-increasing demands and advances in technology in recent years have created considerable need for knowledge of the structural factors which influence the nonrecoverable flow of macromolecular systems. Concurrent with this technological progress has been a steady growth in the varieties of available polymeric systems, both organic and inorganic. Thus there are now extensive data available on the viscosities of a variety of polymer systems. From these data empirical laws have been deduced and an approximate quantitative molecular theory has been advanced to interpret the known viscosity behavior. Nevertheless our understanding of the flow mechanism is still incomplete and there exists a need for additional experiments.

One uncertainty relates to the effect of chain-length heterogeneity on the polymer melt viscosity. For well-defined polymer fractions, it has been demonstrated that the melt viscosity, η, of linear polymers and concentrated solutions thereof obey the relation[1,2]

$$\eta = KM_w^{3.4} \tag{44}$$

provided the weight-average molecular weight, M_w, is considerably greater than the molecular weight between chain entanglements. The constant, K, is characteristic of the polymer type and temperature, and independent of the molecular weight. Very recently, the theory[2] for the melt viscosity of high polymers was extended[3] to include the effect of chain-length heterogeneity, in which it was reported that the viscosity should be described by the relation

$$\eta = kM_t^{3.5} \tag{45}$$

The molecular weight average corresponding to M_t lies between the weight and z average[4]. When the chain length polydispersity is very low, i.e. when M_w/M_n is near unity, the value of M_t is essentially the same as M_w. When the polydispersity is greater than two, it is proposed that M_t is better represented by M_z.

71

In apparent contradiction to the theory, it has been reported that the viscosities of whole polymers of known distribution[5,6] and of mixtures of polymer fractions[7] are adequately expressed by Eq. (44). Consequently, it would seem that a need is indicated for additional information relating polymer melt viscosity to chain length in the high molecular weight region with particular emphasis on both the degree of polydispersity and the nature of the distribution.

There exists even greater uncertainty concerning the $[\eta]$-M relation for the low molecular weight region both because of the relative scarcity of data and because of the increased complexity of the relationship. The log-log plots of viscosity versus chain length for various polymers are seldom linear over a broad range of chain length in this low molecular weight region. Further, for these samples of lower average chain length, both the slope and/or shape of the relation seem to be temperature-dependent. Although according to theory[2], the polymer viscosity should be proportional to the first-power of the chain length in this region, it has been recognized[8,9] that variation with molecular weight of local factors become increasingly important with decreasing chain length. This influence of the change in the "free volume" of the polymer with chain length, as expressed by the change in T_g, is also demonstrated by the isothermal viscosity-molecular weight concentration of diluent relationships[10].

Even fewer data are available concerning the effect of chain length heterogeneity in this low molecular weight region. Furthermore, the theory of Bueche[3] does not apply to polydispersity for low molecular-weight polymers. Consequently, a definite need is indicated for additional data in this low molecular weight region in order to allow a better understanding of the factors which affect the viscous flow of short-chain polymers.

This report constitutes a preliminary description of procedures and results in the general investigation of structural factors affecting flow in macromolecular systems. The objectives are to extend the present knowledge of:

(1)   the effect of chain length heterogeneity on viscous flow in both the high and low molecular weight regions.

(2)   the effect of diluents on the η-M relation, and

(3)   the possible effect of chain stereoregularity on both the viscosity and concentration and chain entanglements.

Because of the availability of polystyrene samples having a very low polydispersity, prepared by anionic polymerization methods, and, because of the large amount of data on fractions of this polymer in the literature, it has been decided to use it for the bulk of this investigation.

B. Experimental Procedures

1. **Fractionation and characterization.** Fourteen samples of polystyrene are currently available covering the molecular weight range of 1.17×10^4 and 1.37×10^6. Although the polydispersity of these samples is very low ($M_w/M_n \sim 1.05 - 1.10$), it was decided to fractionate each into about four fractions with the express purpose of removing any very low (and very high) molecular weight material. At present, eight of the polymers have been separated into 3-4 fractions via a one-stage fractionation[11] of a 1% solution in benzene at 30°C with methanol as the nonsolvent.

The intrinsic viscosities in benzene at 30°C have been measured on the whole polymers and on the fractions of five of the polymers. The value of the intrinsic viscosity, $[\eta]$, was taken as the intercept of the linear extrapolation of the inherent viscosity, $\ln \eta_{rel}/C$, and the specific viscosity, η_{sp}/C, to zero concentration. The concentrations were in range of 1.2 - 1.6 g./dl. and two dilutions (C/2, C/4) were made up in the viscometer, which was a Cannon-Ubbelohde No. 75-A133. The kinetic energy correction was assumed negligible.

The molecular weights of these samples were calculated from $[\eta]$ according to the relations

$$\log M_v = (\log [\eta] + 4.013)/0.74^* \quad (M \geq 30{,}000)^{[12]}$$

and

$$\log M_v = (\log [\eta] + 3.380)/0.60 \quad (M < 30{,}000)^{[13]}$$

It was assumed that these samples have sufficiently low polydispersity so that $M_n = M_v = M_w$. Fractionation data, intrinsic viscosities, and calculated molecular weights are given in Table VIII.

2. **Preparation of samples.** Solutions of the polystyrene fractions in benzene were filtered through a medium-grade glass frit in order to remove any extraneous particles. Stabilizer (0.5% phenyl-b-naphthylamine) was added to the solutions and the solvent evaporated under a reduced pressure of nitrogen at 50°C for 24 hours. For bulk studies, these films were cut into small pieces, placed in a 1 x 5 cm tube and melted into a bubble-free mass at 217°C using alternating vacuum and pressure (nitrogen).

In the case of polymer-diluent studies, appropriate amounts of polymer and dibenzyl ether were weighed into 125 cc flasks and 100 cc of chloroform added. This solution was cast into chloroform-extrated, tared aluminum dishes and the chloroform evaporated under reduced pressure of nitrogen of 40°C with a steady flow of nitrogen being maintained. After

---

*This particular relationship was used so that melt viscosity data could be compared with reported[7] values.

Table VIII

Fractionation Data, Intrinsic Viscosities, and Molecular Weights

for Anionically Polymerized Polystyrene

Polymer	Fraction	Grams/Fraction	(%) Fraction	$[\eta]^{(a)}$	$M_W \times 10^{-3}$ (b)
D-1	-	(20)	--	0.400	77.6
	A	4.65	23.2	0.416	80.5
	B	7.06	35.3	0.378	71.0
	C	5.97	29.8	0.358	66.0
	D	1.38	6.9	0.347	63.0
D-3	-	(20)	--	0.608	135
	A	3.92	19.6	0.723	170
	B	8.73	43.6	0.620	141
	C	5.72	28.6	0.566	124
	D	1.05	5.2	0.426	85
D-4	-	(20)	--	0.690	160
	A	2.20	11.0	0.790	193
	B	11.61	58.0	0.690	160
	C	4.90	24.5	0.680	158
	D	0.60	3.0	0.440	88
D-5	-	(20)	--	0.770	188
	A	2.36	11.8	0.860	220
	B	4.12	20.6	0.792	195
	C	9.20	46.0	0.760	182
	D	3.06	15.3	0.713	170
D-6	-	(20)	--	0.860	220
	A	8.15	40.7	0.900	232
	B	5.14	25.7	0.860	220
	C	2.10	10.5	0.858	220
	D	2.15	10.7	0.730	174

(a) Measured in Benzene at 30°C.

(b) $\log M_V = (\log [\eta] + 4.013)/0.74$.

three days, the decrease in rate of the polymer-diluent mixture (0.05% by weight of the diluent per 24 hours) indicated that the chloroform had been removed. [Analytical tests are in progress to determine the exact concentration of ingredients after this drying procedure. Unless these tests indicate otherwise, the above procedure will be followed in preparing the polymer-diluent mixtures.] These concentrated polymer solutions will then be transferred to the 1 x 5 cm tubes and treated as above.

3. Melt viscosity. For the measurement of melt viscosity, an apparatus was constructed which is a model of that described by Fox, Gratch, and Loshaek[14]. A scale model is diagrammed in Fig. 17. Temperature control and flexibility were achieved through the use of different vapor baths containing diethylene glycol (244.5°C), naphthalene (217°C), cyclohexanol (161.5°C), and toluene (110.8°C). (A thermostated oil bath will be used if lower temperatures should be required.)

Eight different sizes of viscometers (thirty-three in all) are available of the capillary type, i.e. straight, uniform-bore. The length of the capillary portion varies from 7.0 to 20 cm with 43 to 30 cm of 8 mm tubing fused to the capillary. There are four successive marks along the capillary with the first mark being one cm from the tip. This arrangement allows three viscosity determinations to be made with a single capillary.

Four viscometers are of the capillary pipette type, having a bulb ca. 12 mm in diameter located at various distances (7.0, 16.0, and 25 cm) from the tip. The reference marks are located on the uniform-bore portions immediately adjacent to the bulb. Thus, only a single viscosity determination is obtained per capillary.

The viscometers were calibrated by H. Nakayasu, formerly of this laboratory, against selected National Bureau of Standards oils and from the bore dimensions[14]. A recalibration and reproducibility check was made on twelve viscometers (three different sizes) using Oronite polybutene 128 (η = 5400 poises at 25.05 $\pm$ 0.05°C). An example of the reproducibility achieved in these measurements is demonstrated by the results obtained on two similar viscometers having calibration constants, as measured by Nakayasu, of ca. 1000 poises/cm.Hg/min. With an applied nitrogen pressure of 3.5-4.0 cm Hg and flow times of 1.0-1.6 minutes, the result of twelve measurements was η = 5392 poises with a maximum deviation of $\pm$ 2.2%. This not only indicates the reproducibility expected in these measurements but also points out the excellent reliability of the constants determined by Nakayasu, which are listed in Table IX for each type of viscometer.

There were slight discrepancies noted in four of the viscometers which were checked. For example, the viscosities measured between marks 1-2 and 3-4 of a certain viscometer were in agreement with the value for the polybutene, but the viscosities measured between marks 2-3 were consistently higher by 4%, using the constants determined by Nakayasu. Until such time as these viscometers can be checked against several standard oils, they will not be used.
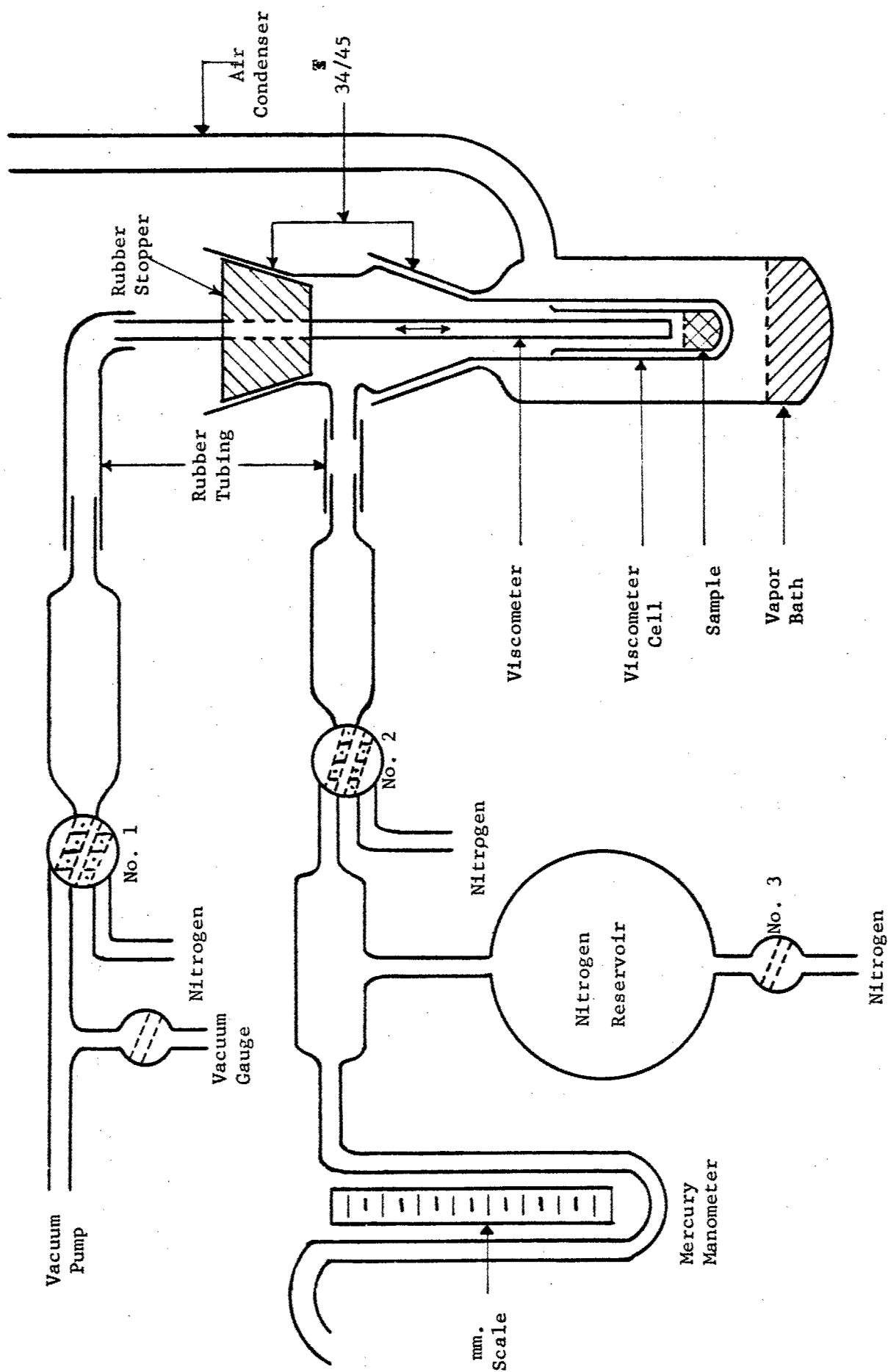
Figure 17 Schematic Diagram of the Apparatus Used to Measure Polymer Melt Viscosity.

Table IX

Viscometer Dimensions and Calibration Constants[1]

Capillary Bore (mm)	Capillary Length (cm)[2]	Capillary Constants (poise/min/cm Hg)		
		A[3]	B[3]	C[3]
Pipette Type				
0.5	5		0.01378	
0.5	10		0.01766	
1.0	15		0.1690	
1.0	7.5		0.3825	
Straight Capillary Type				
0.5	20.5	1.005	1.002	0.990
0.5	15.0	1.989	2.081	1.962
1.0	19.0	4.575	5.331	4.885
1.0	13.5	9.981	9.917	9.484
1.0	9.5	24.515	25.424	24.712
3.0	14.5	97.515	98.939	93.251
3.0	7.0	498.84	435.27	472.47
3.0	7.0	1052.6	1115.5	1033.4

(1) Determined by H. Nakayasu of this laboratory.

(2) Overall length of the uniform-bore capillary.

(3) Corresponding to the flow lengths between successive marks.

A brief description is given for the general procedure used in the measurement of the melt viscosity with occasional reference to Fig. 17.

The sample (ca. 2-3 grams) is placed in a 1 x 5 cm pyrex tube which is in turn placed in the sample holder. The appropriate viscometer is positioned just above the surface of the sample and the air replaced by nitrogen by successive addition of nitrogen and evacuation. Heat is then applied to the vapor bath and the sample is heated as far above its softening point as possible, without causing degradation. Stopcock #1 is then rotated until no more gas bubbles appear and a clear melt is obtained. This removes volatile impurities. The sample is now ready for the viscosity measurement.

The flow of nitrogen through Stopcock #1 is stopped and the lower end of the capillary is inserted into the clear melt. After a predetermined time to allow the system to reach thermal equilibrium, nitrogen pressure (2-25 cm Hg as required to give a reasonable flow time 2-3 minutes) is applied by opening Stopcock #2 which connects the pressure reservoir (ca. one liter) to the viscometer assembly. This forces the polymer up the capillary.

The flow time between successive marks is measured and the average pressure is read from the mercury manometer. This is corrected for mean difference in height between the polymer in the capillary and the surface of the melt. After the polymer reaches the fourth mark (or earlier), Stopcock #2 is closed and #3 is opened, releasing the pressure. A reverse pressure of nitrogen is applied through Stopcock #1, causing the polymer to flow slowly out of the viscometer.

The melt viscosity of the polymer is then calculated from the measured flow time and applied pressure (corrected) and from the capillary constant.

C. Results and Discussion

It is necessary that the polymer samples have a sufficiently low degree of polydispersity to allow reliable interpretation of the viscosity data. Therefore, it is also important that the characterized fractions do not undergo any changes prior to measurement of the viscosity which would affect the chain-length distribution. A thermal stability study was initiated to insure that this type polystyrene, prepared by anionic polymerization methods, could withstand the extreme temperatures to which it would eventually be subjected.

In the molecular weight range of $6-8 \times 10^4$, heating for one-two hours at 217°C is necessary to cause a two-gram sample to flow into a bubble-free mass suitable for capillary-viscosity measurements. For a sample having a molecular weight of 2×10^5, the required heating time increases to four-five hours. Some preliminary viscosity measurements on whole polymers indicated that the thermal stability of this type of polymer is relatively poor, a 15-20% decrease in η being observed in one hour at 217° under an atmosphere of nitrogen. Consequently, a comparative study was made of the effect on both the melt viscosity, η, and the intrinsic viscosity, $[\eta]$, of heating at 217°C under conditions corresponding to those during the measurement of the melt viscosity. The results, listed in Table X and shown in Fig. 18, clearly demonstrate that the stabilizer is required to prevent degradation during the lengthy heating period, leading to an increase in chain-length polydispersity.

Table X

Thermal Stability of Polystyrene Prepared

Via Anionic Polymerization Methods

| Heating Period at 217°C (Hours) | Unstabilized | | | Stabilized | |
	$[\eta]^{(1)}$	$\overline{M}_v^{(2)}$ x 10^{-3}	η x 10^{-3} (poises)	$[\eta]^{(1)}$	$\overline{M}_v^{(2)}$ x 10^{-3}
0.0	0.704	163		0.704	163
1.1	0.690	161			
1.2				0.700	162
2.2				0.696	162
2.5	0.634	143	12.0		
3.4				0.692	161
4.4	0.610	136	9.8		
5.3				0.686	160
6.1	0.590	130	8.0		
7.3				0.682	159
9.0	0.604	133	9.3		
9.3				0.654	151
11.3	0.610	136	9.5		
15.2	0.558	127			

(1) In Benzene at 30°C.

(2) Calculated from $\log \overline{M}_v = \dfrac{\log [\eta] + 4.013}{0.74}$

It is of interest to note that the increase in $[\eta]$ after seven hours of heating also shows up as an increase in η. This increase is probably due to a predominating crosslinking reaction because of the depletion of the scission agent (oxygen). The following decrease in $[\eta]$, after twelve hours indicates that, during the changing of the pipette, oxygen was introduced. Thus, extreme care needs to be taken during the changing of the pipette to insure that an atmosphere of nitrogen is maintained. However, it seems more significant that even the low concentration of stabilizer used was sufficient to prevent gross degradation during the extended heating period.

It is of interest to calculate the change in polydispersity during the apparent thermal degradation of both the unstabilized and stabilized polymer from the observed decrease in the intrinsic viscosity. The random scission of chains of uniform size has been treated by Bovey[15]. When the degradation is not far advanced, it was shown that
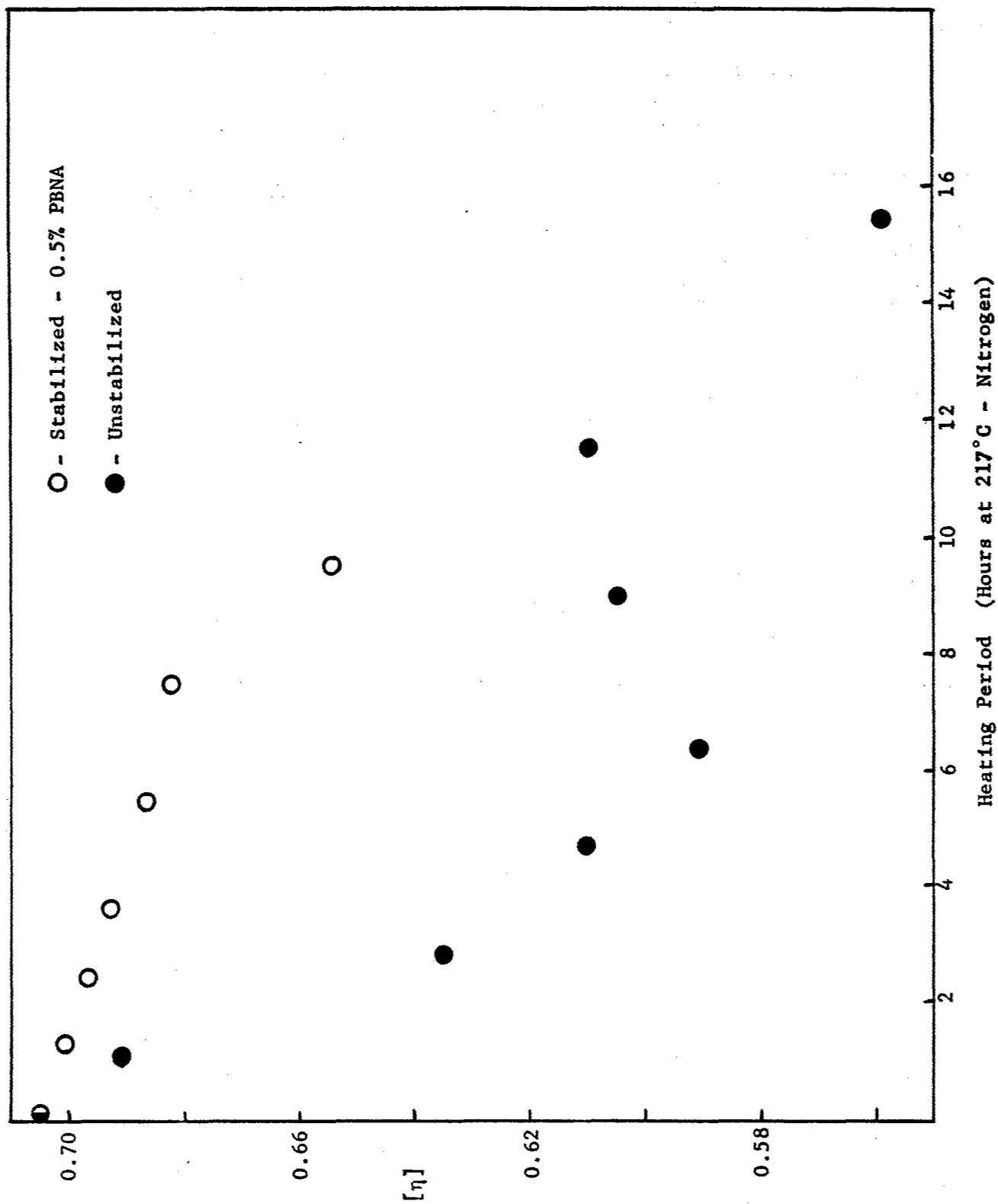
79

Figure 18 Thermal Stability of Polystyrene Prepared by Anionic Polymerization Methods.

$$P_w/P_o = (2/S^2)(e^{-S}+S-1) \qquad\qquad (46)$$

where P_w and P_o are the degree of polymerization of the degraded sample and the original sample, respectively, and S is the number of scissions per primary chain. Also, regardless of how far the degradation has proceeded, it was shown that

$$P_n/P_o = 1/(1+S) \qquad\qquad (47)$$

where P_n is number-average degree of polymerization of the degraded sample.

The number of chain scissions per primary chain was calculated using (3) and the molecular weights given in Table X. For this it was assumed that $M_v \approx M_w$.

Then the number-average degree of polymerization was calculated from (4) and the polydispersity M_w/M_n was determined. The results of these calculations are presented in Table XI. It is apparent from these values that stabilizer is necessary, particularly for the high molecular weight samples which require extended treatment at high temperatures in order to obtain a clear melt suitable for viscosity measurements. Further, it is clear from these calculations that every effort should be made to reduce the required heating period and to insure the exclusion of air from the sample during successive measurements.

Table XI

Polydispersity of Degraded Polystyrene[a]

Polymer	Stabilized[b]	Unstabilized
Heating Period (Hours at 217°C)	5.0	6.1
M_v (original)	160,000	160,000
M_v (degraded)	150,000	120,000
Scissions per chain	0.2	0.95
M_w/M_n	1.12	1.46

(a) Calculations based on treatment of Bovey[15].

(b) 0.5% phenyl-b-naphthylamine.

Based on the fairly low value of $M_w/M_n = 1.40$ for the unstabilized polymer, it would not be expected, according to theory[3], that the melt viscosity of the degraded samples would be appreciably different from that for the sharp fractions. That this is the case is shown graphically in Fig.19, wherein the η-M data of the degraded samples (open circles) are shown to be coincident with the η-M relation previously reported[7] (solid line).

The melt viscosity of five fractions, stabilized with 0.5% phenyl-b-naphthylamine, was measured at 217°C. The results are presented in Table XII and also in Fig.19 (solid circles). As with the degraded samples, the data are coincident with the reported[7] η-M relation, except for the lowest molecular weight fraction. The viscosity of this fraction is 50% higher than the reported value (or the molecular weight is 9% low). A recheck of both parameters is scheduled for this fraction.

The investigation of the effect of chain-length heterogeneity on macromolecular flow is being continued with particular emphasis on (a) the low molecular weight region and (b) the nature of the distribution. Also, the preliminary phase of an investigation of the viscosity-molecular weight relation of concentrated solutions of polystyrene in dibenzyl ether is in progress.

Table XII

Viscosities of Stabilized Fractions of Polystyrene

Sample	No. of Measurements[1]	Range of Pressure (corr.) (cm Hg)	Range of Flow Times (min)	$\bar{\eta}$ 217° (poises)
D-1-B	12	17-19	3.0-3.4	1,430 ± 25
D-3-B	6	13.9-14.5	2.9-3.2	15,650 ± 150
D-4-C	6	16.3-17.5	2.5-3.0	21,900 ± 500
D-5-B	3	15.0	2.8-3.0	46,800 ± 50
D-6-B	6	19.6-21.4	2.8-3.1	63,200 ± 800

(1) Assuming three measurements per capillary.
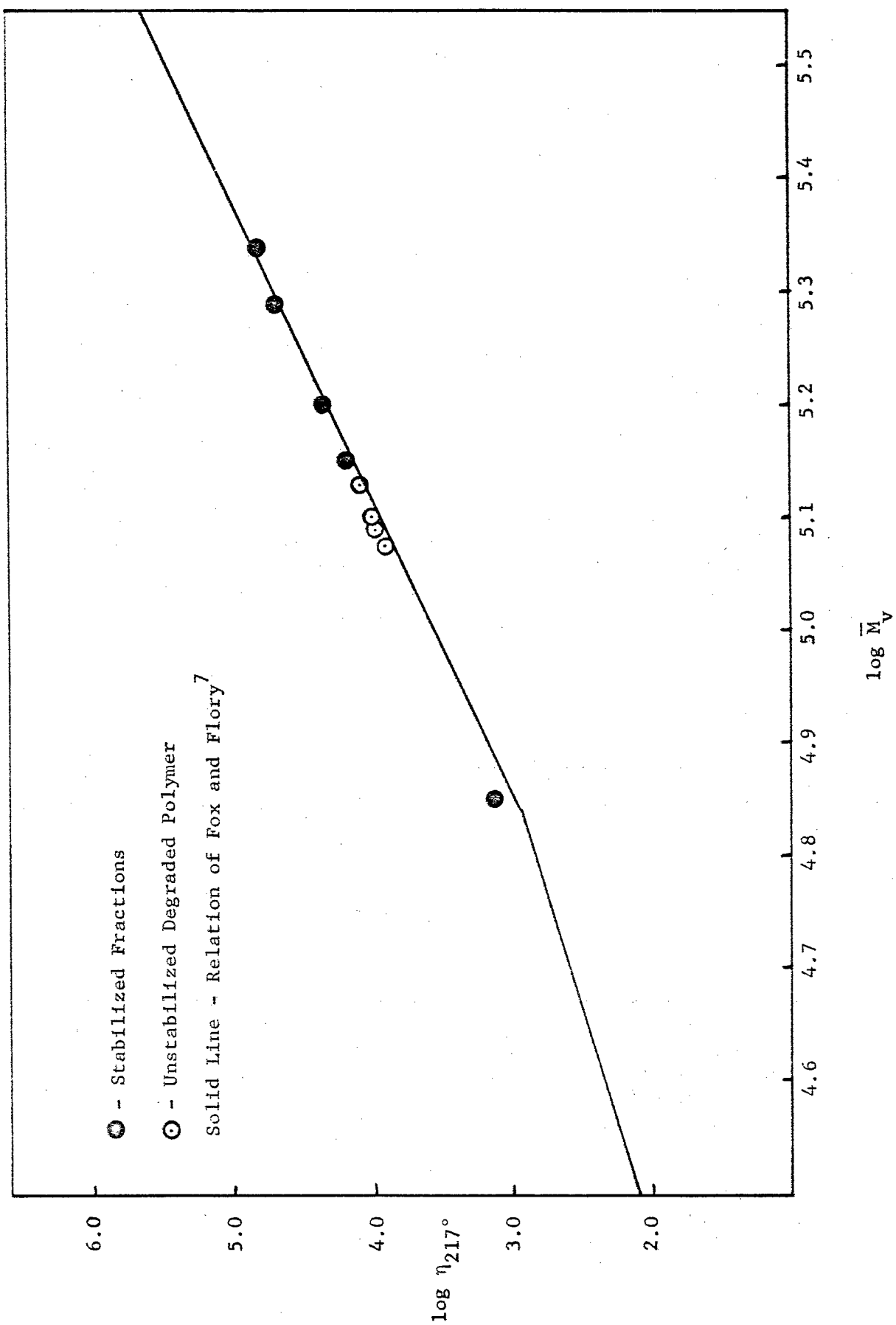
Figure 19 Viscosity-Molecular Weight Relation for Polystyrene at 217°C.

⊙ – Stabilized Fractions

⊙ – Unstabilized Degraded Polymer

Solid Line – Relation of Fox and Flory[7]

$\log \bar{M}_v$

$\log \eta_{217°}$

II. An attempted Stereospecific Emulsion Polymerization of Vinyl Acetate Employing Protein-Detergent Solubilizing Agents — V. R. Allen and T. G. Fox

A. Introduction

Breuer and Strauss, in an unpublished manuscript[16], have suggested recently the use of protein-detergent complexes in free-radical emulsion polymerizations to obtain stereoregular polymers. Because of the conveniences associated with polymerization in emulsion, it was considered of interest to prepare a vinyl polymer having a stereoregular structure employing this new technique. Such a polymer would be valuable in the study of the factors affecting flow in macromolecular systems.

We report here the results of this investigation of the application of the Breuer-Strauss technique to the polymerization of an emulsion of vinyl acetate stabilized by a bovine serum albumin-sodium dodecyl sulfate complex. A brief description is given of the experimental methods followed by the description of results to date. Although the preliminary present evidence suggests that crystalline products are obtained in some instances, the reproducibility is very poor. Hence, the results of this preliminary study, though quite striking, are not conclusive.***

B. Experimental Methods

1. <u>Polymerization conditions</u>. The polymers were prepared in an emulsion system according to the method reported by Breuer and Strauss[16]. The polymerization recipe, as given in Table XIII, was used, except as noted elsewhere.

*** Note added in proof (11-15-61): Originally in this manuscript we recorded observations on diffraction patterns and unique physical and chemical properties which suggested the presence of a crystalline component in six of the thirty-eight polymerization products. Subsequently, (cf. Quarterly Report #7, Nov. 15, 1961) we found that these samples were contaminated with sodium calcium silico aluminate introduced as an impurity in the sodium chloride used to coagulate the polymer in the early experiments; in addition, there were evidences of the presence of detergent in a crystalline form in a few samples. Since the original observations suggesting crystallinity were shown to be of no significance in this study, they have been deleted from this report.

Table XIII

Emulsion Recipe for Vinyl Acetate

Water (O_2-free)	100
Vinyl Acetate (dist.)	100
Bovine Serum Albumin (BSA)[1]	3.5
Sodium Dodecyl Sulfate (SDS)[2]	1.6
Potassium Persulfate[3]	0.3

     1. Nutritional Biochemicals Company - Crystalline Grade.
     2. Fisher Scientific Company - Reagent Grade.
     3. Eastman Company - Reagent Grade.

A typical polymerization may be described as follows:

     3.5 g. of albumin was dissolved in 100 ml of O_2-free water under nitrogen. The detergent and initiator were then added and allowed to dissolve. After solution, nitrogen was bubbled in for five minutes and the solution chilled in a refrigerator.

     100 g. of freshly-distilled vinyl acetate (chilled) was added through a self-sealing rubber stopper with a large syringe. The system was then flushed with nitrogen for five minutes and placed in the thermostatically controlled water bath.

     After a considerable induction period of one to thirty hours, the flask was removed from the bath after a given time and the latex poured (or spooned) into ca. three liters of concentrated NaCl solution. The polymer was filtered, washed with water, and dried in vacuo at 50°C. The conversion was calculated from the weight of dried polymer.

     2. Coagulation and solubility. Although mentioned in the typical experiment above, the method of coagulation of the polymer is described more fully. In the earliest runs, it was found that sufficient NaCl remained in the polymer after the washing to produce faint lines in the x-ray diffraction pattern. Consequently, in some of the later runs, the polymer was removed from the salt solution by filtration and redispersed in distilled water. After soaking 24 hours in successive portions of water, residual salt could not be detected by x-ray. The alternative method of coagulating in distilled water was also used although the soap made filtration difficult.

The solubility of the dried polymer was measured qualitatively by placing a small piece (0.1 g) in 2-3 ml of the desired solvent. The quantitative measurement of solubility (which is referred to in the description of results) was obtained by placing one-gram samples of the polymer in 100 ml of acetone with stirring. After 24 hours, the residue was allowed to settle (or centrifuged) and the solution decanted off. This procedure was repeated three times. The solubility was calculated from the weight of dried, soluble polymer.

3. <u>Hydrolysis</u> and <u>reacetylation</u>. The polymers to be hydrolyzed were in the form of thin strips cut from either cast or pressed films. The hydrolysis was carried out in small flasks, equipped with condensers, on a steam plate. Fifty milliliters (excess) of either 4M NaOH or 6M HCl were added to one gram of polymer and heated for 24 to 48 hours. The mixture was dialyzed against distilled water until neutral.

Reacetylation of these hydrolysates was according to the method of Melville and Sewell[17]. After 48 to 96 hours on the steam plate, the excess acid was neutralized with 1M NaOH and the product dialyzed.

4. <u>Infrared</u> <u>spectra</u>. The IR spectra of the various polymers were obtained using a Perkin-Elmer "Infracord". The samples were either in the form of cast films, pressed films, or KBr pellets.

C. Results

Poly-(vinyl acetate) PVAc, prepared in emulsion according to the recipe given in Table XIII without the BSA, hereinafter referred to as conventional polymer, is soluble in ketones, lower alcohols, and aromatics. It flows readily at slightly elevated temperatures ($T_g \sim 35\,°C$) and is rapidly (~ 2 hours) hydrolyzed by dilute acid or base at $100\,°C$ into a water-soluble product which can be easily crystallized. This poly-(vinyl alcohol) PVA can be reacetylated; the product having properties essentially identical to the original PVAc.

The x-ray diffraction pattern of this PVAc is typical of an amorphous polymer, having a strong absorption band at 7.0 Å and a slightly weaker band at 4.0 Å. Regardless of prior sample treatment, annealing, stretching, etc., this pattern persists.

The inclusion of the BSA in the emulsion recipe results in a product containing an insoluble phase (in acetone), even at low conversions, which contains tightly bound protein in quantities up to 20% by weight, as measured by nitrogen (Kjeldahl) analysis. The soluble phase, <u>in every case</u>, contains no protein. Numerous tests on the properties listed above for this soluble phase show that it is indistinguishable from the conventional polymer. Consequently, this phase need not be mentioned further, except occasionally for comparative purposes.

There is presented in Table XIV the experimental conditions
for thirteen of the thirty-eight polymerizations which were attempted.
Of the remaining, fourteen may be considered duplicates of one or more
of those listed, three were lost by frothing of the latex due to ex-
cessive heat build-up, and eight, which were modifications of the basic
system(Table XIII),either failed to polymerize or yielded the conventional
product.

1. Solubility and protein content. The solubility is one of
the more interesting properties of the polymers of vinyl acetate prepared
according to the Breuer-Strauss technique. There is presented in
Table XIV the results of solubility measurements of these polymers in
cold (30°) acetone, normally a good solvent for PVAc.

Table XIV

Polymerization Conditions and Polymer Properties

Polymer	Temp. (°C)	Induction[1] Period (Hours)	Polymerization[2] Period (Hours)	Con- version (%)	Insolubility in Acetone (%)	Bound Protein (%)
VC-1	30	9	9	88	0	0
VC-2	28	1	2	30	0	0
VT-1	30	9	9	80	100	3
VT-16	20	20	0.5	1.6	100	20.4
VT-20	35	2	2	19.3	90	13.7
VT-21	33	5	3	18.0	70	6.0
VT-23	33	21	3	30.0	50	11.1
VT-28	30	5	3	18.2	56	16.2
VT-29	30	5	3	18.3	65	19.7
VT-22	40	2	2	27	96	5.0
VT-15	28	1	3	35	52	7.4
VT-19	25	27	5	72	32	5.0
VT-11	30	8	4	30	0	0

[1]Time to appearance of blue fluorescense.

[2]Time after blue fluorescence.

The gels were swollen slightly and films could be formed on evaporation
of the solvent. Examination of these films in a polarizing microscope
revealed that considerable strain was present. When the strained portions
were heated to 70-80°, these strain patterns disappeared but appeared
again as the sample cooled to room temperature. These acetone-extracted
gels were resistant to other types of solvents, e.g. ethers, alcohols,
esters, and substituted benzenes, at various temperatures. They were
attacked by strongly basic amides and amines, e.g. dimethyl formamide
and triethylene tetraamine, resulting in partial solubility.

In every case, the insoluble polymer was found to contain
protein varying in concentration from 2-20% by weight. This protein
could not be extracted from the polymer by either boiling water, reflux-
ing alcohol-water mixtures, or aging in cold water.

The presence of the protein in the insoluble polymer was first
observed by infrared analysis (confirmed analytically with ninhydrin and
measured quantitatively by Kjeldahl analysis). The percentage of bound
protein is given in Table XV and typical infrared spectra presented in
Fig. 20.

2. <u>Glass transition temperature</u>. It was found that the glass
transition temperatures, Tg, for the insoluble gel and for the soluble
phase were essentially the same as for a sample of PVAc prepared by free-
radical polymerization in solution. Also, above Tg, the plots of the
change in specific volume with temperature were linear up to 140°C with
almost identical slopes, as listed in Table XV. Bubble formation was
observed above 150°C, indicating either volatile impurities in the sam-
ple or decomposition.

Table XV

<u>Dilatometric Comparison of Conventional and</u>

<u>Breuer-Strauss Poly-(vinyl acetate)</u>

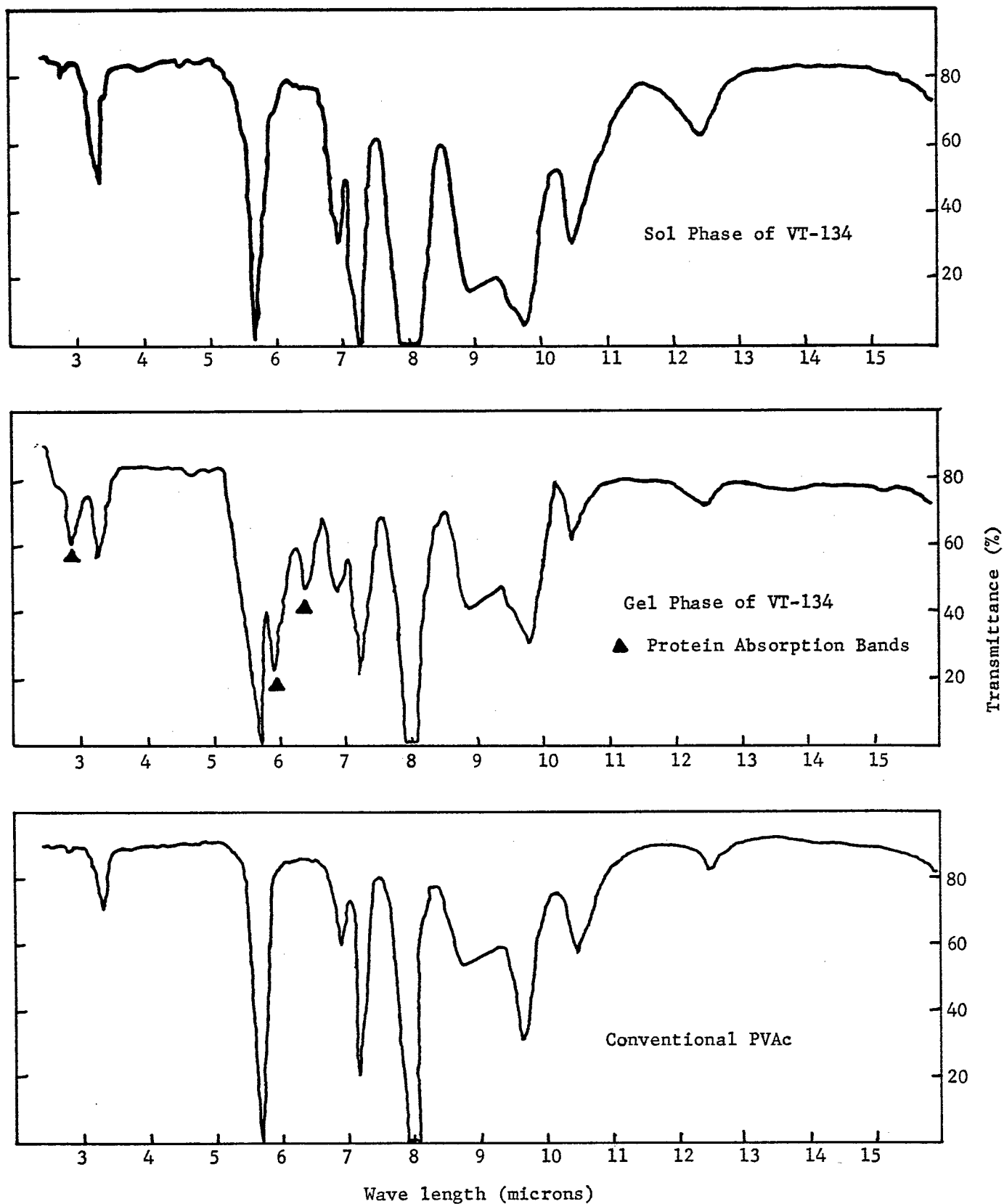| Sample Designation	Physical Characteristic	Tg (°C)	$(\partial \bar{v}p/\partial T) \times 10^4$ (above Tg)
VT-15	Soluble	30-32	4.70
VT-1	Insoluble	30-32	4.30
PD-2	Conventional	32-34	4.80

Figure 20. Infrared Spectra of Poly-(vinyl acetate).

3. Hydrolysis and reacetylation. Comparative hydrolysis studies of the insoluble gel, the soluble phase, and the conventional polymer revealed that the rate of solution of the insoluble gel in the hydrolysis media was lower by a factor of ten than that of the other two. Since conventional PVAc was also insoluble in these media prior to conversion into the alcohol, it is suggested that the lower rates observed for the insoluble, protein-containing gels may be due to the bound protein. Indeed, a physical mixture of 85/15 conventional PVAc/protein did exhibit a slightly lower rate (a factor of 2).

The properties of the hydrolysates of the Breuer-Strauss insoluble PVAc samples differ in certain respects from those of conventional polymer. Aside from the insolubility of the former in the hydrolysis media, it was observed that these insoluble hydrolysates were often crystalline without annealing. Further, sharply-oriented samples were obtained by pressing the water-insoluble hydrolysates at 150° with 10,000 psi ram pressure. Five series of sharp areas were observed in the diffraction patterns of some of these samples.

As with the hydrolysis study, a markedly lower rate of reacetylation (solution in the acetylating mixture) was observed in the case of the hydrolysates from the insoluble PVAc. Although these hydrolysates were free of protein, it was necessary to expose these samples to much longer heating periods (up to 48 hours) before solution as compared with 3-4 hours, for the hydrolysates of the conventional PVAc. In all cases, the reacetylated samples were amorphous.

4. Discussion. The polymerization of vinyl acetate in an emulsion stabilized by the BSA-SDS complex yields a polymer which is, for the soluble phase, indistinguishable from conventionally-prepared emulsion polyvinyl acetate, and, for the insoluble phase, strikingly different. The fact that there is present, in almost all the trials, an insoluble phase containing variable quantities of bound protein (up to 20%) indicates clearly that the protein plays an important role in the polymerization.

From the experimental facts reported above, a hypothesis can be formulated concerning the possible role of the protein or the protein-detergent complex in the polymerization. Let us assume that the protein-detergent complex is structurally composed of the extended protein molecule partially covered with adsorbed detergent. This appears reasonable since it has been reported by Harrap and Schulman[18] and confirmed by Strauss and Strauss[19] and by Blei[20] that denaturation of the protein (giving an extended molecule)[18] occurs rapidly when the detergent/protein mole ratio exceeds 35-40. (The mole ratio used in these polymerizations was 100.)

Let us now extend this speculative hypothesis to explain the formation of an insoluble phase which contains bound protein. Two specific facts directly related to this question are (a) the protein is not removed by extraction with boiling water or other polar-solvent

mixtures, and (b) some of the hydrolysis products still contain residual nitrogen corresponding to 2-4% protein. These facts strongly indicate that the protein is not simply trapped in a polymer matrix by powerful interchain forces, such as hydrogen bonding, but that there is a chemical bond between the two.

Thus, it would appear reasonable to suspect that the polymer initially formed on the surface of the protein-detergent complex is grafted onto the protein via chain transfer reaction with the sulfhydryl or other groups of the protein. After the surface of the protein is saturated with grafted polymer, the locus of the reaction changes, possibly to detergent-monomer micelles formed as polymer replaces soap on the protein surface, and the conventional type, acetone-soluble PVAc is formed, free of protein.

Examinations of Fig. 21 and 22 reveal that the polymers formed at low conversions (2-20%) are rich in protein and predominantly insoluble in acetone. Also, a very apparent change occurs in the polymerization medium at ca. 20% conversion; changing from a fluid latex to a very viscous psuedo-gel. Further, addition of only 0.3 part by weight of an efficient chain-transfer agent (n-dodecyl mercaptan) to the polymerization recipe resulted in a product (VT-11) which was amorphous, completely soluble in acetone, and free of protein.

Although not directly related to this question of how the polymer is bound to the protein, nevertheless, it may be significant that the viscosity-average molecular weights, Table XVI, of the soluble phases of VT-134 and VT-23 agreed within 14% of that of the conventional polymer, VC-1. This may be interpreted as signifying that the polymerization of the soluble phase does occur in a conventional monomer-detergent micelle, as suggested above. (This, of course, assumes that the other factors which affect molecular weight were constant.)

Table XVI

Molecular Weights of Poly-(vinyl acetate)

Polymer Designation	Per cent Soluble	$[\eta]$ Acetone at 30°C	M_V x 10^5 (1)	Remarks
VC-1	100	2.28	5.6	Conventional PVAc
VT-134	33	2.24	5.5	
VT-23	50	2.04	4.8	

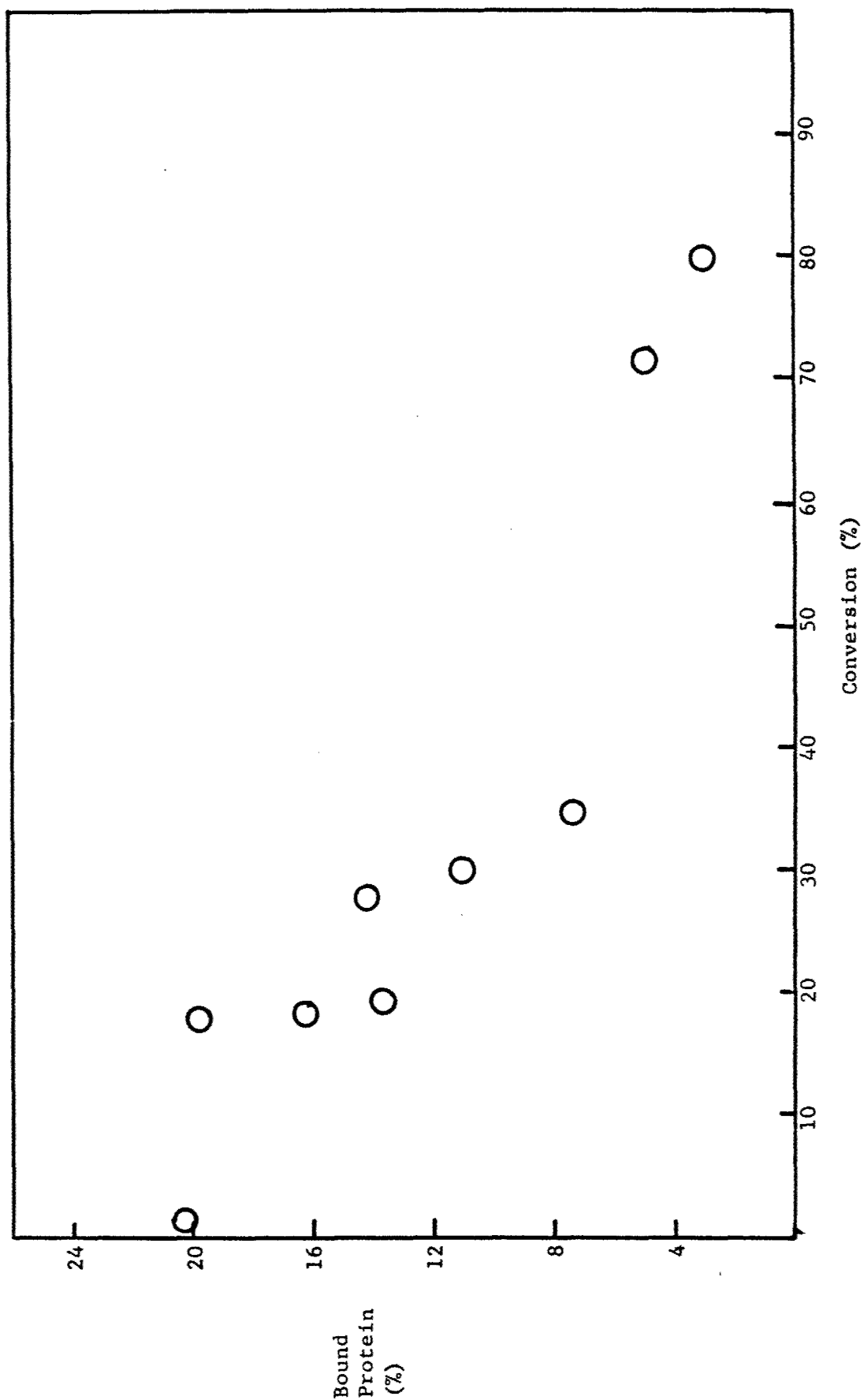(1) From $\log M_V = 1.39 \log [\eta] + 5.25$.

91

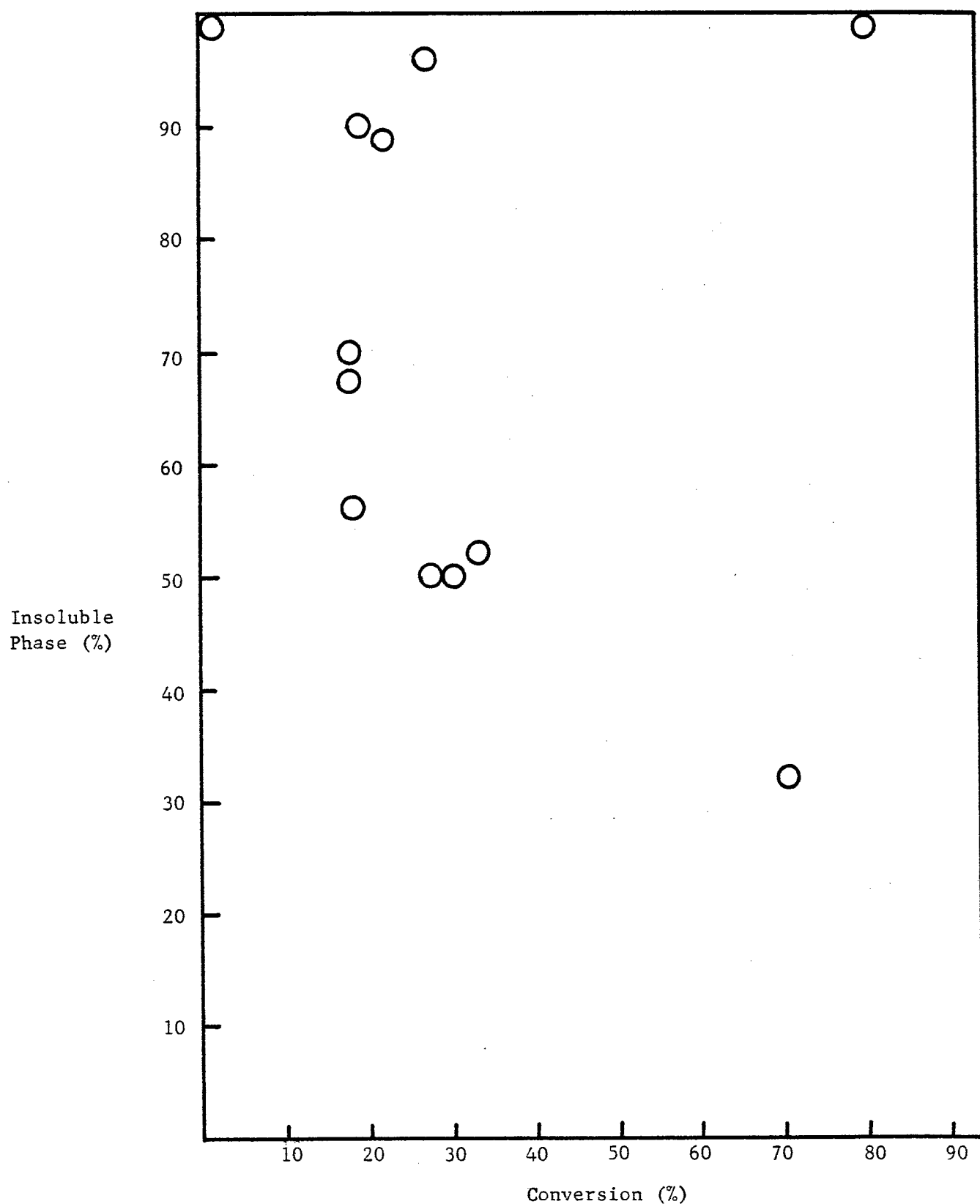Figure 21 Bound Protein versus Conversion for Poly-(vinyl acetate)

Figure 22 Dependence of the Solubility of Poly-(vinyl acetate) on the
Degree of Conversion

D. Summary

Application of the Breuer-Strauss technique of stereospecific polymerization to emulsions of vinyl acetate stabilized by a bovine serum albumin-sodium dodecyl sulfate complex yields a product which varies, depending on the extent of conversion, from an insoluble phase containing bound protein at low conversion to a mixture of the insoluble material and soluble, protein-free polymer at higher conversion. The soluble phase is similar in all respects to emulsion PVAc prepared without protein. The insoluble phase exhibits lower rates of hydrolysis and subsequent reacetylation than the conventional polymer.

BIBLIOGRAPHY

1. T. G Fox and S. Loshaek, J. Appl. Phys. $\underline{26}$, 1080 (1955).

2. F. Bueche, J. Chem. Phys. $\underline{20}$, 1959 (1952).

3. F. Bueche, J. Polymer Sci. $\underline{43}$, 527 (1960).

4. P. J. Flory, Principles of Polymer Chemistry, Cornell University Press, Ithaca, New York, 1953, p. 307.

5. P. J. Flory, J. Am. Chem. Soc., $\underline{62}$, 1057 (1940).

6. J. F. Rudd, J. Polymer Sci. $\underline{44}$, 459 (1960).

7. T. G Fox and P. J. Flory, J. Am. Chem. Soc. $\underline{70}$, 2384 (1948).

8. See Chapter 12, pp. 45204 of Rheology, Theory and Applications, Vol. I, F. R. Eirich, Ed., Academic Press, Inc., New York (1956).

9. F. Bueche, J. Polymer Sci. $\underline{45}$, 267 (1960).

10. cf. $\underline{8}$, p. 463-5.

11. cf. $\underline{4}$, p. 340.

12. R. H. Ewart and H. C. Tingey, Abstracts of papers presented at the 111th Meeting of the American Chemical Society, Atlantic City, New Jersey, April, 1947.

13. D. C. Pepper, Royal Dublin Soc. $\underline{25}$, 239 (1951).

14. cf. $\underline{8}$, p. 436-7.

15. F. A. Bovey, The Effects of Ionizing Radiation on Natural and Synthetic High Polymers, Interscience Publishers, N. Y., 1958, pp. 74-6.

16. M. Breuer and U. P. Strauss, Private Communication, April, 1960.

17. H. W. Melville and R. R. Sewell, Makromol. Chem., $\underline{32}$, 139 (1959).

18. B. S. Harrap and J. H. Schulman, Disc. for Soc. $\underline{13}$, 197 (1953).

19. G. Strauss and U. P. Strauss, J. Phys. Chem. $\underline{62}$, 1321 (1958).

20. I. Blei, J. Coll. Sci., $\underline{15}$, 370 (1960).

PART III - ELASTICITY OF POLYMERIC NETWORKS

I. Specific Diluent Effects on the Elastic Properties of Polymeric Networks
── C. A. J. Hoeve and M. O'Brien

A. Introduction

The thermoelastic properties of individual polymeric chains are at present rather well understood. Recent theoretical work[1,2] on the chain dimensions as a function of the hindrance to rotation around chain bonds has met with considerable success. For any given force the mean end-to-end distance of the chain may be calculated as a function of temperature. However, the thermoelastic properties of networks composed of such chains are much more difficult to comprehend. At first sight rather sweeping assumptions have to be made to enable the construction of idealized models, for which a theoretical treatment is feasible.

One basic assumption underlying all theories is that the chains in the unconstrained state are Gaussian. This assumption is not severely restrictive and appears to be a good approximation for networks of chains consisting of many links.

A second assumption is that interactions between chains are independent of deformation. This assumption has not yet been evaluated theoretically, although some recent experimental evidence[3] suggests that effects of this nature are not large.

A third assumption is that the unperturbed chain dimensions of the free uncrosslinked chains are independent of specific diluent effects. These diluent effects may be important in a study of the elastic properties of swollen networks. Contrary to the former two assumptions, the third one may be relaxed from a theoretical point of view. The consequences of this more general approach are investigated below.

Flory[4] has given the following equation for a network in the unswollen state

$$f = \nu k\, T(< \alpha >^2/L_{io})(\alpha - \alpha^{-2}). \qquad (48)$$

For a network at force zero in swelling equilibrium with a diluent, he obtained[4]

96

$$(\nu \, V_1/N_a V_0)[<\alpha>^2 \, v_2 - v_2/2] \;=\; -[\ln(1-v_2) + v_2 + \chi_1 \, v_2^2] \tag{49}$$

and for a force f,

$$(\nu \, V_1/N_a V_0) \, [<\alpha>^2 \, (v_2')^{2/3}(L_{io}/L) \; - v_2'/2] = -[\ln(1-v_2') + v_2' + \chi_1(v_2')^2], \tag{50}$$

combined with

$$f \;=\; \nu k \, T(<\alpha>^2/L_{io}^2) \, (v_2')^{2/3} L(1 - L_{io}^3/v_2'L^3). \tag{51}$$

ν is the number of chains in the sample; k and N_a are respectively Boltzmann's constant and Avogadro's number. T is the absolute temperature. L_{io} and L_i are the lengths of the isotropic sample in the unswollen and swollen state respectively, and L is the length corresponding to the force f, either for the swollen or unswollen sample. By definition $\alpha = L/L_{io}$. v_2 and v_2' are the volume fractions of polymer in the swollen sample in respectively the isotropic state and the deformed state, corresponding to f. χ_1 is the interaction parameter for diluent-polymer interaction. V_1 is the molar volume of the diluent and V_0 is the volume of the unswollen polymer. $<\alpha>^2 = <r_i^2>/<r_0^2>$, where $<r_i^2>$ is the mean square end-to-end distance of the polymer chains in the isotropic sample at the volume, corresponding to f, and $<r_0^2>$ is the mean square end-to-end distance for uncrosslinked chains.

Earlier theories have assumed that $<r_0^2>$ is constant, independent of temperature and specific diluent effects. However, it has recently[3,5] been shown that the temperature dependence of $<r_0^2>$ may be introduced in the rubber elasticity theory. In fact, at present, this theory is successfully used to evaluate d $\ln <r_0^2>/dT$ for various polymers.

We will now critically examine the implicit assumption that $<r_0^2>$ is independent of diluent effects. The relative probabilities of different conformations may conceivably depend on the diluent, as has been observed for 1,2 dichloroethane[6] in different solvents. If these effects also exist for polymeric chains, $<r_0^2>$ depends on the diluent. It follows then that $<\alpha>^2$, and through eq.(50) the force on an elongated swollen sample, is a function of the diluent.

B. Procedure

The procedure for obtaining the ratio R, defined as $<r_0^2>_{swollen}/<r_0^2>_{unswollen}$, was as follows. From the stress-strain curve in the

97

unswollen state $\nu <\alpha>^2$ was obtained through eq.(48). Substituting this value and the measured value of v_2 in eq.(49) we obtained χ_1. Subsequently v_2' corresponding to the length L was calculated with the aid of eq.(50) and with this value f was calculated according to eq.(51). During this procedure $<r_0^2>$ was assumed to be equal to $<r_0^2>_{unswollen}$. On comparing the calculated value of the force with that measured at the same L, we have that

$R = f_{calculated}/f_{measured}$.

C. Experimental

Linear polyethylene ("Super Dylan", low pressure polyethylene, obtained from the Koppers Company) was chosen as the polymer. The diluents chosen were paraffin, melting range 65-70°C, n-hexadecane, α-chloronaphthalene and di-2-ethylhexyl azelate. The latter three solvents were "Reagant Grade" and no attempt was made to purify them further.

Polyethylene films of a uniform thickness of 1-2 mm. were pressed at about 150°C and samples were cut at room temperature with a mold in the shape of a dumbbell. These samples are of uniform width of 3.1 mm. over a length of 25 mm. In order to crosslink the samples, they were irradiated at room temperature in evacuated glass containers by γ-radiation from a cylindrical Co^{60} source with a uniform dose rate of 0.61 megarep/hr. The samples investigated below received doses of 10 to 40 megarep. The dumbbell shape enabled the samples to be clamped in and stretched without breakage at the clamps. The clamps consisted of a pair of small metal plates, held together by screws. The lower clamp was fixed, while the upper clamp was suspended from a strain gauge which could be adjusted vertically. The strain gauge (Statham Instrument Company, Transducer Model G-1) had a capacity of 750 g. and a linear response of 0.05 mv. per g. under a supplied e.m.f. of 12 v. The output of the strain gauge was displayed on a Leeds and Northrup recorder, giving a full scale deflection of 10 mv. The instrument was calibrated by addition of known weights before and after each experiment.

The length of the sample was measured with a cathetometer. Two thin metal pins, perforating the uniform section 20 mm. apart, served as markers.

A stream of high purity nitrogen was passed through the sample chamber in order to prevent oxidative degradation. Samples were swollen by diluent in the sample chamber. After the stress-strain experiment, the polyethylene sample was extracted with boiling xylene and evaporated to dryness at 150°C in vacuum. The stress-strain curve in the unswollen state after this treatment was usually identical, within experimental error, to that before swelling; otherwise the experiment was discarded.

The liquid thermostat (containing Silicone Oil DC-550, Dow Corning Corporation) maintained a constant temperature of 150 ± 0.1°C.

Stress-strain curves were obtained by stretching the sample at intervals to an extension ratio of about 1.3 and decreasing the length in

similar intervals until the relaxed, isotropic state was reached. At each interval the length was kept constant for 15 minutes before the force was read.

D. Results and Discussion

Table XVII

Ratio $R = <r_o^2>_{swollen} / <r_o^2>_{unswollen}$

for Different Diluents

Solvent	α	$f_{unswollen}$ g.	$f_{swollen}$ g.	v_2'	calculated $f_{swollen}$ g.	R
DEHA	1.35	60.0	75.8	0.394	74.0	0.98
α-Cl. n.	1.275	55.5	95.5	0.217	81.3	0.86
α-Cl. n.	1.32	61.3	104.5	0.230	90.3	0.86
n-hexad.	1.35	63.5	103.0	0.221	89.8	0.87
n-hexad.	1.31	56.4	96.0	0.196	82.2	0.86

The results obtained are given in Table XVII. It is to be remarked, however, that the data are preliminary and need further confirmation. Eqs (48-51) are valid for measurements performed in equilibrium. It was apparent from the stress-strain curves for the unswollen samples, however, that the force was not constant after a period of 15 minutes. This results in hysteresis loops in the stress-strain curves. Attempts to increase this period showed that the time required would be impractically long. The results for the dry state are therefore open to doubt.

The measurements performed in the swollen state are more reliable, since hysteresis is small in this case. We are inclined to believe that the value of $<r_o^2>$ in n-hexadecane is close to that in polyethylene in the bulk, in view of the similarity of the molecules. If this is accepted, the value of $<r_o^2>$ in α-chloronaphthalene is the same as that in polyethylene in the bulk, but $<r_o^2>$ would be about 15 percent greater in di-2-ethylhexyl azelate.

We plan to perform stress-strain experiments in the swollen state only and compare the measurements for different diluents with those in paraffin. The hysteresis effects are greatly reduced by this procedure and more accurate results may be expected.

BIBLIOGRAPHY

1. C. A. J. Hoeve, J. Chem. Phys., $\underline{32}$, 888 (1960).

2. C. A. J. Hoeve, J. Chem. Phys., in press.

3. A. Ciferri, C. A. J. Hoeve and P. J. Flory, J. Am. Chem. Soc., $\underline{83}$, 1015 (1961).

4. P. J. Flory, J. Am. Chem. Soc., $\underline{78}$, 5222 (1956).

5. P. J. Flory, C. A. J. Hoeve and A. Ciferri, J. Polymer Sci., $\underline{34}$, 337 (1959).

6. M. V. Volkenstein and V. I. Brevdo, Zhur. Fiz. Khim. $\underline{28}$, 1313 (1954); Y. H. Inami, J. B. Ramsey, J. Chem. Phys. $\underline{31}$, 1297 (1959).

MELLON INSTITUTE, Pittsburgh, Pa. POLYMER
STRUCTURES AND PROPERTIES, by E. F. Casassa,
T. A. Orofino, J. W. Mickey, T. G Fox, G. C.
Berry, D. J. Plazek, R. E. Kerwin, H. Nakayasu,
V. R. Allen, C. A. J. Hoeve, and M. O'Brien,
100 p. incl. figs., tables and refs. (Project
0(7-7340); Task 73404)(ASD TR 61-22)(Contract
AF 33(616)-6968)   Unclassified report

Investigations relating to dilute solutions of
polymers have comprised: a theoretical treat-
ment of Rayleigh scattering to include both
intramolecular and intermolecular optical in-
terference effects; the temperature dependence
of the second virial coefficient for poly-
styrene in cyclohexane; the intrinsic viscosity-
molecular weight relation for poly-(vinyl ace-
tate) in butanone; and design and construction
of a precision light scattering photometer.

The melt viscosity-molecular weight relation
at 218° for monodisperse polystyrene prepared
anionically was found to be identical with
that for ordinary fractions.

Poly-(vinyl acetate), prepared by an emulsion
polymerization in the presence of a protein,
yielded an insoluble component containing
bound protein.

Preliminary stress-strain measurements on
cross-linked swollen polyethylene gave only
equivocal evidence for specific solvent
effects on the unperturbed random-flight
dimensions of the polymer chains.